Titre: Title:	Process Intensification and Scale-Up of Chinese Hamster Ovary Cell Cultures in Bioreactor for the Production of Recombinant Proteins
Auteur: Author:	Lucas Lemire
Date:	2025
Type:	Mémoire ou thèse / Dissertation or Thesis
Référence: Citation:	Lemire, L. (2025). Process Intensification and Scale-Up of Chinese Hamster Ovary Cell Cultures in Bioreactor for the Production of Recombinant Proteins [Thèse de doctorat, Polytechnique Montréal]. PolyPublie. https://publications.polymtl.ca/65772/

POLYTECHNIQUE MONTRÉAL

affiliée à l'Université de Montréal

Process Intensification and Scale-Up of Chinese Hamster Ovary Cell Cultures in Bioreactor for the Production of Recombinant Proteins

LUCAS LEMIRE

Département de génie chimique

Thèse présentée en vue de l'obtention du diplôme de *Philosophiæ Doctor*

Génie chimique

Mai 2025

POLYTECHNIQUE MONTRÉAL

affiliée à l'Université de Montréal

Cette thèse intitulée :

Process Intensification and Scale-Up of Chinese Hamster Ovary Cell Cultures in Bioreactor for the Production of Recombinant Proteins

présentée par **Lucas LEMIRE**

en vue de l'obtention du diplôme de *Philosophiæ Doctor*

a été dûment acceptée par le jury d'examen constitué de :

Mario JOLICOEUR, président
Olivier HENRY, membre et directeur de recherche
Yves DUROCHER, membre et codirecteur de recherche
Moncef CHIOUA, membre
Bruno GAILLET, membre externe

DEDICATION

"No weapon formed against me shall prosper,

My will is stronger."

-To my parents for their unwavering and unconditional support

ACKNOWLEDGEMENTS

Foremost, I would like to thank my supervisor, professor Olivier Henry, for his guidance and the trust he has placed in me, but most of all, for pushing me into believing in myself and my knowledge. I equally thank Yves Durocher and Phuong Lan Pham for welcoming me to the Process Intensification team at National Research Council of Canada Royalmount. Lan's passion for research and attention to detail without a doubt elevated both my knowledge and the quality of my work. My thanks further extend to everyone at NRC Royalmount for making me feel welcome to the team and being there to help solve any, of the many, issues I encountered throughout my journey. Particularly, I am grateful for Larissa who showed me how to operate the bioreactors as well as Helene and Brian for their assistance in solving problems I encountered with said bioreactors. I also thank the friends I made through common dreads along the way; especially to Camila and Zalma who have been there for me in each their own way. To Sebastian, I am thankful not only for the countless hours of discussion, for your assistance in the analysis of results, or for your help in planning a cell culture, but also for having a friend to walk this path with me. I sincerely hope our lives will intersect again someday. To all my loved ones, who have believed in me and supported me in this endeavour from close or far, I deeply thank you for the much-needed emotional support. And last of all, but most certainly not least, I am eternally grateful to my parents for their unyielding supporting in whatever I desire. If I am here today, and made it this far, it is because of their love; they have been with me from reading my first dinosaur book until reading my doctoral thesis.

RÉSUMÉ

Les cellules ovariennes de hamster chinois (CHO) constituent la principale plateforme pour la production industrielle de protéines recombinantes. Elles sont généralement cultivées dans des bioréacteurs à grande échelle en mode cuvée alimentée. Le processus de mise à l'échelle, passant des flacons aux bioréacteurs de production pouvant atteindre 20 000 litres, est essentiel dans le développement des procédés biopharmaceutiques. Étant donné qu'il est impossible de maintenir constants tous les paramètres opérationnels lors de la mise à l'échelle, les stratégies se concentrent sur un paramètre clé, tel que la puissance volumétrique (P/V), le transfert d'oxygène, le débit gazeux volumétrique (vvm), ou la vitesse en bout de pale de l'agitateur. Parmi ces paramètres, l'aération et le mélange sont critiques pour améliorer la productivité des cultures cellulaires. L'aération est réalisée par bullage, utilisant des diffuseurs poreux (microsparger) ou à trous percés (macrosparger), qui a des impacts sur les taux de transfert d'oxygène, l'élimination du dioxyde de carbone et le cisaillement des cellules. Cependant, les effets du type de bulleurs et des stratégies d'aération sur la croissance cellulaire et la production de protéines recombinantes en mode cuvée alimentée n'ont pas été fréquemment étudiés dans les bioréacteurs de paillasse. De plus, le transfert de gaz dans les flacons agités, influencé par la vitesse d'agitation et le volume de remplissage, est crucial pour optimiser la croissance cellulaire, en particulier dans les cultures à haute densité. Cette thèse vise à explorer l'équilibre entre un apport suffisant en oxygène et une réduction du stress de cisaillement dans les cultures de cellules CHO afin d'intensifier les procédés cuvés alimentés par l'optimisation du transfert de gaz et des stratégies d'aération.

Les indicateurs de performance clés, notamment l'intégrale de la concentration cellulaire (IVCC), la viabilité cellulaire, et le titre du produit, ont été évalués pour diverses configurations de bulleurs et stratégies d'aération. Les configurations de microspargers ont atteint les IVCC les plus élevées, dépassant significativement les configurations de macrospargers. Par ailleurs, les cultures munies de deux types de diffuseur ont présenté une meilleure viabilité à 14 jours post-induction (DPI) et les titres de produits les plus élevés. L'analyse statistique a montré une augmentation significative du titre pour les configurations avec l'aération par cascade. De plus, une corrélation négative a été observée entre les niveaux maximums en lactate et le titre du produit, soulignant l'effet néfaste de l'accumulation de ce métabolite sur la productivité. Une analyse en composantes principales (PCA) a révélé une forte association entre des résultats de culture favorables et l'utilisation de diffuseurs

micro/macro ou les systèmes de microsparger avec débit d'air limité. En revanche, les configurations de macrosparger ont été associées à une production accrue de lactate. Ces résultats mettent en évidence le rôle crucial du mode d'aération dans l'optimisation des cultures de cellules CHO.

L'optimisation des cultures de cellules CHO dans des bioréacteurs de paillasse a été effectuée en se concentrant sur les paramètres critiques d'aération et de mélange. L'application d'un faible régime d'alimentation par bolus a diminué les pics d'osmolalité, entraînant une augmentation de 25% du titre volumétrique et une amélioration de la croissance cellulaire par rapport à un régime d'alimentation par bolus à débit plus élevé. L'utilisation d'une aération en cascade avec des débits d'air croissants a démontré l'importance de l'optimisation du bullage. Des débits d'air maximums plus élevés ont résulté en des densités cellulaires viables (VCD) plus faibles et une baisse plus rapide de la viabilité cellulaire, probablement en raison de stress de cisaillement causé par des débits gazeux élevés. Un débit d'air maximum de 2 mL/min a conduit à la meilleure performance. Le procédé établi a ensuite été validé avec deux lignées cellulaires différentes, atteignant 90 à 109 % des titres obtenus en flacons agités, démontrant ainsi la robustesse du procédé. Pour l'évaluation de la capacité de mise à l'échelle, le procédé a été transféré d'un bioréacteur de 1 L à un bioréacteur de 10 L en utilisant une stratégie de P/V et vvm constants; des VCDs, des viabilités, et des productivités comparables ont été obtenus.

Toujours dans l'objectif d'améliorer le rendement des cultures, une méthode de perfusion transitoire semi-continue dans des flacons agités a été développée, permettant l'ensemencement des bioréacteurs de paillasse à des densités cellulaires ultra-élevées (UHSD) sans nécessité d'équipement de perfusion spécialisé. En utilisant l'UHSD, le temps de culture a été réduit de 50 % par rapport aux densités d'ensemencement standard (SSD), atteignant 87 % du titre volumétrique SSD et résultant en une augmentation de 49,3 % du rendement espace-temps. Un échange quotidien de milieu était essentiel pour prévenir les limitations en nutriments et garantir une densité cellulaire viable maximale. La mesure du taux de transfert d'oxygène (OTR) a révélé que la densité cellulaire maximale était limitée par la disponibilité en oxygène dans les flacons.

En conclusion, ce travail offre des informations précieuses sur la gestion du transfert de gaz, les stratégies d'aération, et les régimes d'alimentation, contribuant ainsi à l'optimisation des proccédés de culture cellulaire CHO pour la production de biothérapeutiques. Ces résultats ouvrent la voie à

des avancées futures en génie des bioprocédés, améliorant la robustesse des processus, réduisant les coûts de production et proposant des solutions adaptées aux besoins de l'industrie biomanufacturière.

ABSTRACT

Chinese Hamster Ovary (CHO) cells are the primary platform for industrial production of recombinant biotherapeutic proteins, typically cultivated in large-scale fed-batch bioreactors. The scale-up process, transitioning from flasks to production bioreactors of up to 20,000 liters, is critical in biopharmaceutical process development. Since maintaining all operating parameters constant across scales is impossible, scale-up strategies typically focus on a single key parameter, such as volumetric power input (P/V), oxygen mass transfer, volumetric gas flowrate (vvm), or impeller tip speed. Among these parameters, aeration and mixing are vital for enhancing cell culture productivity. Aeration is achieved through sparging, using frit or drilled hole spargers, which affect oxygen transfer rates, carbon dioxide stripping, and shear stress on the cells. However, the effects of sparger type and aeration strategies on CHO cell growth and recombinant protein production in fed-batch cultures have not been thoroughly investigated in benchtop bioreactors. Additionally, gas transfer in shake flasks, influenced by agitation rate and fill volume, is crucial for optimizing cell growth, especially in high-density perfusion cultures. This study aims to explore the balance between sufficient oxygen supply and reduced shear stress in CHO cell cultures to intensify fed-batch processes through improved gas transfer and aeration strategies.

Key performance indicators, including integral viable cell density (IVCC), cell viability, and product titer, were assessed for a variety of sparger configurations and aeration strategies. The microsparger configurations achieved the highest IVCCs, significantly surpassing the macrosparger setups. Meanwhile, dual sparger cultures demonstrated superior viability at 14 days post-induction (DPI) and achieved the highest product titers. Statistical analysis revealed a significant increase in titer for configurations with air caps compared to those without. Furthermore, product titer showed a negative correlation with maximum lactate levels, highlighting the detrimental effect of lactate accumulation on productivity. Principal component analysis (PCA) revealed a strong association between the dual sparger and the microsparger with air cap systems and favorable culture outcomes. In contrast, macrosparger setups were linked to increased lactate production. These findings emphasize the critical role of sparger configuration in optimizing CHO cell cultures.

CHO cell cultures in benchtop bioreactors were also studied by focusing on critical aeration and mixing parameters for scale-up. Implementing a lower bolus feeding regimen reduced osmolality

spikes, resulting in a 25% increase in volumetric titer and improved cell growth compared to a high bolus feeding regimen. The use of cascade aeration with increasing air caps demonstrated the importance of optimizing gas sparging. Higher air caps resulted in lower viable cell densities (VCD) and more rapid declines in cell viability, likely due to shear stress from elevated gas sparging rates. The best performance was achieved with an air cap of 2 mL/min. The process was then validated using two different cell lines, achieving 90-109% of the shake flask titer, demonstrating its robustness. For scalability assessment, the process was successfully transferred from a 1-L to a 10-L bioreactor using a constant P/V and vvm strategy, allowing to maintain comparable VCD, viability, and productivity. This study highlighted the delicate balance between mixing efficiency, gas transfer, and cell stress, providing valuable insights for optimizing scalable CHO cell cultures.

In an effort to further enhanced process yields, a semi-continuous transient perfusion method in shake flasks was successfully developed, enabling the seeding of benchtop bioreactors at ultra-high cell densities (UHSD) without the need for specialized perfusion equipment. By utilizing UHSD, culture time was reduced by 50% compared to standard seeding densities (SSD), achieving 87% of the SSD volumetric product titer and resulting in a 49.3% increase in space-time yield. Daily media exchange was essential to prevent nutrient limitations, ensuring maximum viable cell density. Measurements of the oxygen transfer rate (OTR) identified oxygen limitation as a critical factor in determining maximum cell density. Increasing the agitation from 200 RPM to 300 RPM improved OTR and VCD in 500-mL flasks; however, it led to early cell death in 1000-mL flasks due to shear stress. The developed UHSD process enables cost-effective, and flexible bioreactor operation, improving asset turnover by shortening production bioreactor usage.

Overall, this work offers valuable insights into gas transfer management, aeration strategies, and feeding regimens, which contribute to optimizing CHO cell culture processes for biotherapeutic production. These findings pave the way for further advancements in bioprocess engineering, enhancing process robustness, cost-effective biotherapeutic manufacturing, and providing scalable solutions for future biopharmaceutical needs.

TABLE OF CONTENTS

DEDICATION iii

ACKNOWLEDGEMENTS iv

RÉSUMÉ v

ABSTRACT viii

TABLE OF CONTENTS x

LIST OF TABLES xv

LIST OF FIGURES xvi

LISTE OF SYMBOLS AND ABBREVIATIONS xix

LIST OF APPENDICES xxiii

CHAPTER 1 INTRODUCTION 1

1.1 Research Problem 1

1.2 Hypothesis and Objectives 2

1.3 Thesis Structure 2

CHAPTER 2 LITERATURE REVIEW 4

2.1 Chapter Presentation 4

2.2 Introduction 4

2.2.1 CHO cells: The Workhorse of Industrial Protein Production 6

2.2.2 Scale-up, Scale-out, and Scale-down in Process Development 7

2.2.3 The Scale-up Challenge 9

2.3 Cultivation Systems for CHO cells 10

2.3.1 Uninstrumented Systems 10

2.3.2 Stirred-tank Bioreactors (Glass and Stainless-steel) 12

2.3.3 Single-use Bioreactors 12

2.3.4 Micro- and Mini-bioreactors 13
2.4 Key Process Conditions Impacted by Scale-up 15
2.4.1 Aeration 15
2.4.2 Oxygen 17
2.4.3 Carbon Dioxide 18
2.4.4 Mixing 19
2.4.5 Hydrodynamic Shear Stress 21
2.5 Basic principles for Bioreactor Scale-up 22
2.5.1 Geometrical Similarity 24
2.5.2 Dynamic Similarity and Scale-up Criteria 24
2.6 Common Scale-Up Strategies 26
2.6.1 Constant Volumetric Power Input 26
2.6.2 Constant Oxygen Mass Transfer 27
2.6.3 Constant Volumetric Gas Flowrate 28
2.6.4 Constant Impeller Tip Speed 30
2.7 Tools to Assist Culture Scale-Up 33
2.7.1 Computational Fluid Dynamics (CFD) 33
2.7.2 Scale-Down Models 36
2.8 Process Intensification and Scale-Up 37
2.9 Conclusion 38
CHAPTER 3 EXPLORATION OF THE IMPACT OF SPARGER TYPE AND AERATION STRATEGY ON CELL GROWTH AND PRODUCTIVITY 40
3.1 Chapter Presentation 40
3.2 Importance of Aeration and Mixing 40

3.3 Materials & Methods 41
3.3.1 Benchtop Bioreactor Cell culture 41
3.3.2 Aeration Strategies 42
3.3.3 Analytical 42
3.4 Impact of Sparger Type, Configuration, and Aeration Strategy 43
CHAPTER 4 ARTICLE 1: SCALE-UP OF A MONOCLONAL ANTIBODY CHO FED-BATCH PRODUCTION IN STIRRED TANK BIOREACTORS: EFFECT OF HYDRODYNAMIC CONDITIONS AND FEEDING REGIMEN 49
4.1 Article Presentation 49
4.2 Abstract 49
4.3 Introduction 50
4.4 Materials and Methods 53
4.4.1 Small-Scale Cell Culture Maintenance and Pre-Culture 53
4.4.2 Bioreactor Cell Culture and Operating Conditions 54
4.4.3 Sampling and Handling of Samples 59
4.5 Results and Discussion 62
4.5.1 Effect of Feeding Strategy 62
4.5.2 Effect of Impeller Number and Aeration Strategy 65
4.5.3 Scale-up from 1-L to 10-L Bioreactor 68
4.5.4 Process Transfer to a Different Product 69
4.5.5 Effect of Culture Hydrodynamic Conditions on Productivity 71
4.6 Conclusion 74
4.7 Author Contributions 75
4.8 Acknowledgements 75
4.9 Conflict of Interest Statement 75

CHAPTER 5 ARTICLE 2: N-1 SEMI-CONTINUOUS TRANSIENT PERFUSION IN SHAKE FLASK FOR ULTRA-HIGH DENSITY SEEDING OF CHO CELL CULTURES IN BENCHTOP BIOREACTORS 76

5.1 Article Presentation 76

5.2 Abstract 76

5.3 Introduction 77

5.4 Materials And Methods 80

5.4.1 Cell Culture Maintenance 80

5.4.2 Semi-Continuous Transient Perfusion 80

5.4.3 Bioreactor Cell Culture 81

5.4.4 Gas Transfer Rates and Shear Stress Estimations in Shake Flasks 82

5.4.5 Sample Handling 83

5.5 Results and Discussion 83

5.5.1 Time-of-Action Study 83

5.5.2 Effect of Media Exchange Frequency 86

5.5.3 Effect of Flask Size on Semi-Continuous Transient Perfusion 90

5.5.4 Effect of Orbital Agitation Speed on Cell Growth and OTR 95

5.5.5 Effect of Semi-Continuous Transient Perfusion on Cell Doubling Time and Productivity 98

5.5.6 Improvement of Increased Seeding Density 100

5.6 Conclusion 101

5.7 Author Contributions 103

5.8 Acknowledgments 103

5.9 Conflict of Interest Statement 103

CHAPTER 6 GENERAL DISCUSSION 104

CHAPTER 7 CONCLUSION AND RECOMMENDATIONS 109

7.1 Conclusion 109

7.2 Recommendations and Future Work 111

REFERENCES 113

APPENDICES 130

LIST OF TABLES

Table 2.1 FDA approved monoclonal antibody therapeutics. 5

Table 2.2 Automated micro and mini-bioreactor systems available for batch or fed-batch mammalian cell culture 14

Table 2.3 Common aeration strategies in mammalian cell cultures 16

Table 2.4 Scale-independent and dependent variables 23

Table 2.5 Typical values of scale-dependant parameters: mixing time, mixing speed, impeller tip speed, and Reynolds number. 24

Table 2.6 Interdependence of scale-up parameters for geometrically similar bioreactors with diameters increased by a factor of 5. 25

Table 2.7 Overview of recent scale-up criteria used from benchtop bioreactors to industrial scales 31

Table 2.8 Recent uses for CFD in cell cultures 35

Table 3.1 Aeration Conditions 42

Table 4.1 Bioreactor operating conditions 56

Table 4.2: Low- and high-volume bolus BalanCD CHO Feed4 addition regimens described as a percentage of initial culture volume. 57

Table 5.1 Maximum observed viable cell densities and oxygen transfer rates of semi-continuous transient perfusion cell cultures with daily media exchange in 125-mL, 250-mL, 500-mL, and 1000-mL shake flasks at a fill volume of 20% and an agitation rate of 200 RPM. 91

Table 5.2 Maximum oxygen transfer rates observed in biological systems and measured in sulfite systems (cell-free) for 125-mL, 250-mL, 500-mL, and 1000-mL unbaffled shake flasks at 20% fill volume agitated at 200 RPM. 93

Table 5.3 Reynolds numbers (Re), average ($\varepsilon_{\emptyset}$) and maximum ($\varepsilon_{\max}$) energy dissipation rates, and Kolmogorov lengths (λK) in 500-mL and 1000-mL shake flasks at 20% fill volume and different agitation rates. 96

LIST OF FIGURES

Figure 2.1 Biopharmaceutical production process scale-up and scale down. 9

Figure 3.1 The effect of sparger configuration and use of cascade aeration on cell culture performance. 44

Figure 3.2 Impact of aeration strategy on key process indicators. 46

Figure 4.1 Measurements and mixing configuration of the A) 2-impeller and B) 1-impeller bioreactor. 58

Figure 4.2 The effect of feeding strategy on the A) viable cell density, B) cell viability, C) volumetric titer, D) cell specific titer, and E) cumulative cell culture volume of 1-L benchtop bioreactor cell cultures. 62

Figure 4.3 Effect of impeller number and aeration strategy on A) viable cell density, B) cell viability, C) volumetric titer, D) cell specific titer, E) lactate concentration, and F) total cumulative oxygen sparged from air and pure oxygen for low (1 mL/min, red), mid (2 mL/min, blue), and high (12.3 mL/min, green) air caps; 1-impeller configuration (full dots) and 2-impeller configuration (empty dots). 65

Figure 4.4 Scale-up of 1-L benchtop bioreactor to 10-L bioreactor using constant P/V and vvm as criterion and their measured A) viable cell density, B) cell viability, C) volumetric titer, and D) cell specific titer obtained in 1-L benchtop bioreactor with high AC aeration (-●-) and 10-L benchtop bioreactor with high AC aeration (-○-). Error bars represent measurement errors for viable cell density (A) and volumetric titers (C). 68

Figure 4.5 Benchtop 1-L bioreactor cell culture performance of clone 1 (-■-), and clone 2 (-▲-) for the production of Product B operating at mid AC with single impeller and LFS A) viable cell density, B) cell viability, C) volumetric titer, D) cell specific titer, E) lactate concentration, and F) osmolality. Error bars represent measurement errors for viable cell density (A) and volumetric titers (C). 69

Figure 4.6 Comparison of final volumetric product titer of product A, product B from clone 1, and product B from clone 2 in 1-L bioreactor (green) and shake flask (blue). Error bars of replicates represent standard deviations. 71

Figure 4.7 Effect of constant volumetric gas flowrate (vvm) at air cap, constant volumetric power input (P/V), and constant volume on A) viable cell density, B) cell viability, C) volumetric titer, D) cell specific titer, E) space-time yield 72

Figure 5.1 Time-of-action study for determination of beginning of media replacement for semi-continuous transient perfusion in shake flasks. 85

Figure 5.2 Effect of Media Exchange Frequency performed in shake flasks. 87

Figure 5.3 L-Glutamine and L-Asparagine kinetic profile in 250- and 1000-mL shake flask. 89

Figure 5.4 Effect of flask size on cell growth and OTR profile. 92

Figure 5.5 Effect of orbital shaking speed on cell growth and OTR**.** 95

Figure 5.6 Effect of daily medium replacement on shake flask cell growth performance..... 98

Figure 5.7 Effect of daily medium replacement cell expansion on shake flask fed-batch production. 99

Figure 5.8 Effect of Ultra High Seeding Density (UHSD) on fed-batch bioreactor production performance**.** 101

Supplemental Figure A.1: The effect of feeding strategy on the A) residual glucose, B) specific glucose consumption, C) measured lactate, D) specific lactate production E) ammonia concentration, and F) specific ammonia production of 1-L benchtop bioreactor cell cultures. Low feeding strategy (-●- LFS); High feeding strategy (-●- HFS). 130

Supplemental Figure A.2: Online sparging data A) air, B) pure oxygen, and C) carbon dioxide for low air cap with 1-impeller (red), mid air cap with 1-impeller (blue), and high air cap with 1-impeller (green) operating parameters. 131

Supplemental Figure B.1: Amino acids measured throughout semi-continuous transient perfusion in shake flasks for daily media exchange (DME) and daily media exchange daily except for days 1 and 2 (DME_D3) media exchange frequency. 132

Supplemental Figure B.2: Oxygen transfer rate of semi-continuous transient perfusion cultures in 250-mL and 1000-mL shake flasks with daily media exchange except day 1 and 2 (DME_D3) agitated at 200 RPM. 133

Supplemental Figure B.3: Maximum oxygen transfer rate measured using the sulfite system in 125-mL, 250-mL, 500-mL, and 1000-mL flasks at 20% fill volume agitated at 200 RPM. 133

LISTE OF SYMBOLS AND ABBREVIATIONS

ϕ_G	Gas fraction
ε	Energy dissipation rate
[Glu]	Glucose concentration
[Lac]	Lactate concentration
[NH_3]	Ammonia concentration
a	Specific area
AC	Air cap flowrate
A_c	Cross sectional area
ATF	Alternating tangential flow filtration
CER	Carbon evolution rate
CFD	Computational fluid dynamics
CHO	Chinese Hamster Ovary
CR5	Cumate promoter
CSPR	Cell specific perfusion rates
CTR	Carbon transfer rate
CuO	Operator sites
CymR	Cymene repressor
d_0	Orbital shaking diameter
DHFR	Dihydrofolate reductase
DHS	Drilled hole sparger
D_i	Impeller diameter
D_L	Oxygen diffusivity
DME	Daily media exchange
DME_D3	Daily media exchange from day 3
DMSO	Dimethylsufoxide

DO	Dissolved oxygen
DPI	Days post induction
D_T	Vessel diameter
F_{air}	Air flowrate
F_{O2}	Oxygen flowrate
GEV	Gas entrance velocities
GMP	Good Manufacturing Practice
GOI	Gene of interest
GS	Glutamine synthetase
HFS	High-volume feeding strategy
H_i	Impeller height
IME	Intermittent media exchanges
IVCC	Integral viable cell density
k_La	Oxygen mass transfer coefficient
LDH	Lactate dehydrogenase
LFS	Low-volume feeding strategy
mAbs	Monoclonal antibodies
MCT	Monocarboxylate transporter
MSX	L-methionine sulfoximine
MTX	Methotrexate
N	Mixing speed
Ne’	Modified Newton number
N_f	Flow number
N_p	Power number
OMLZM	Omalizumab
OTF	Oxygen transfer flux
OTR	Oxygen transfer rate

OUR	Oxygen uptake rate
P	Mixing power input
P/V	Volumetric power input
PC	Principal components
PCA	Principal component analysis
pCO_2	Carbon dioxide partial pressure
P_i	Product concentration at time i
PLVZM	Palivizumab
p_R	Operating pressure
Q_g	Gas flowrate
qGlu	Specific glucose consumption rate
qLac	Specific lactate production rate
qNH_3	Specific ammonia production rate
qO_2	Specific oxygen consumption
qP	Specific titer production rate
rcTA	Cumate reverse transactivator
Re	Reynolds number
ROS	Reactive oxygen species
RQ	Respiration quotient
SCE	Standard cell expansion
SSD	Standard seeding density
STP	Semi-continuous transient perfusion
STY	Space time yield
SUB	Single-use bioreactors
t	Time
TCO	Total cumulative oxygen sparged

t_d	Doubling time
TFF	Tangential flow filtration
t_m	Mixing time
TMFC	Thermal mass flow controllers
t_r	Gas residence time
UHSD	Ultra-high seeding density
V	Volume
VCD	Viable cell density
v_s	Superficial gas velocity
V_t	Impeller tip speed
VVD	Vessel volume per day
vvm	Volumetric gas flowrate
y_{O2}	Oxygen molar fraction
$\varepsilon_{\emptyset}$	Average energy dissipation rate
λ_K	Kolmogorov length
μ	Dynamic viscosity
ν	Kinetic viscosity
ρ	Density

LIST OF APPENDICES

Appendix A - Effect of Hydrodynamic Conditions and Feeding Regimens on the Performance of a Monoclonal Antibody for Scale-Up of CHO Fed-Batch Cell Culture Production 130

Appendix B - N-1 Semi-Continuous Transient Perfusion in Shake Flask for Ultra-High Density Seeding of CHO Cell Cultures in Benchtop Bioreactors 132

CHAPTER 1 INTRODUCTION

1.1 Research Problem

Mammalian cells, more specifically Chinese Hamster Ovary (CHO) cells, are the primary platform used for the industrial production of biotherapeutic recombinant proteins such as monoclonal antibodies. Large-scale production is most often done in fed-batch bioreactor cell cultures of volumes of up to 20,000 L. Before reaching these production volumes, the processes are optimized stepwise from flasks, to benchtop bioreactors, to pilot scale, before finally reaching the final desired volumes. As such, bioreactor scale-up is an important part of biopharmaceutical production process development. Since it is not possible to maintain all operating parameters constant throughout scale-up, the predominant strategy is to maintain a single parameter constant across scales. The most used scale-up criteria revolve around mixing and aeration: constant volumetric power input (P/V), constant oxygen mass transfer, constant volumetric gas flowrate (vvm), and impeller tip speed. It is then obvious that the optimization of parameters pertaining to aeration and mixing is necessary to improve cell culture productivity. Aeration in bioreactors is mainly accomplished by sparging the desired gas through two main types of spargers: microsparger, also named frit sparger, and macrosparger, also named drilled hole sparger (DHS). The difference between these two types of spargers is the size of bubbles produced which has known impacts on oxygen transfer rates, carbon dioxide stripping, and shear stress applied to cells. However, the impact of the use of different sparger configurations and associated aeration strategies on cell growth and productivity in the context of a fed-batch cell culture to produce recombinant protein has seldom been explored. In a similar manner to bioreactors, gas transfer in shake flasks is key to optimized performance in cell growth and productivity. In shake flasks, aeration comes from the formation of a thin film on the wall of the flask such that the fill volume and agitation rate play a major role on gas transfer rate, both of which have impact on the shear stress applied to cells. This concept is important when high cell densities are achieved such as in semi-continuous perfusion cultures performed in shake flasks. This study aims to explore the delicate balance involved between delivering sufficient oxygen supply and minimizing shear stress imposed on cells from agitation and aeration.

1.2 Hypothesis and Objectives

The overall goal of this thesis is the process intensification of CHO cell fed-batch cultures to produce recombinant protein with a focus on gas transfer and aeration strategies. The hypothesis being that the use of different aeration strategies, such as the type of equipment used for sparging and the minimum gas flowrate, have a significant impact on the cell growth and final product concentration. The specific objectives to achieve this were:

1. Explore the effect of sparger type (drilled hole sparger and frit sparger) and configuration on cell culture growth and production.
2. Establish process conditions resulting in enhanced growth and productivity of cell culture processes using feed regimen selection and parameters most relevant to process scale-up (mixing and aeration).
3. Develop a semi-continuous transient perfusion process in shake flasks for the seeding of ultra-high density seeding cell cultures in bioreactors.

The main connecting theme among these objectives is the impact of gas transfer and the strategies used to supply oxygen to cells during cell culture. Objective #1 will identify the sparger configuration better suited for benchtop cell cultures. Objective #2 will investigate the effects of the amplitude of sparged air flowrate as well as the number of impellers used for mixing, both of which influence gas transfer in bioreactors. Objective #3 aims to develop a preculture process capable of seeding benchtop bioreactors at ultra-high cell densities with a focus on oxygen transfer and limitations in shake flask.

1.3 Thesis Structure

Chapter one of this thesis outlines the problem being addressed as well as the general objective of the project and how it was separated into various specific objectives. The second chapter gives an in-dept literature review of the cells most used in biopharmaceutical production, how these cells are developed, the equipment used in biopharmaceutical production, key process parameters and concepts of scale-up, and the predominant successful scale-up strategies. The third chapter presents a study on the use of different micro and macro spargers and their effects of cell growth and productivity. Chapter four details the process development efforts through feeding regimens, mixing, and aeration strategies in the objective to scale-up the process from 1-L to 10-L cultures.

This work has been submitted to *Biotechnology Progress* as a research article entitled “Scale-Up of a Monoclonal Antibody CHO Fed-Batch Production in Stirred Tank Bioreactor: Effect of Hydrodynamic Conditions and Feeding Regimen”. In the fifth chapter, the 1-L fed-batch cell culture process is further intensified by seeding at ultra-high cell densities (15 million cell/mL rather than 0.3 million cell/mL). However, to have the capability to seed at such high cell densities, a semi-continuous transient perfusion process is developed in shake flasks while demonstrating the occurrence of gas transfer limitations determining the maximal cell densities achievable in such culture systems. The development of this process is the subject of a research article published in *Biotechnology Progress* entitled “N-1 Semi-Continuous Transient Perfusion in Shake Flask for Ultra-High Density Seeding of Benchtop Bioreactors”. Chapter six is a general discussion that describes how the three previously mentioned studies relate to each other and also details some of the challenges encountered during this research project. Finally, chapter seven concludes this thesis and gives an overview of its accomplishments and provide recommendations for future work.

CHAPTER 2 LITERATURE REVIEW

2.1 Chapter Presentation

This chapter serves as a literature review for this thesis which highlights the importance of the use of CHO in biomanufacturing, the different cultivation systems, the important parameters related to cell culture scale-up, how cell culture scale up is done and typical scale-up criterion, as well as different tools which may be useful in this endeavor. From which, conclusions can be made as to efficient scale-up techniques as well as the impact of the choice of equipment such as gas spargers.

2.2 Introduction

It is expected that the biopharmaceutical market, which includes monoclonal antibodies (mAbs), vaccines, interferons, hormones and growth factors, will have a compound annual growth rate of 13.8% between the years 2018 and 2025 allowing markets to increase from $186 billion in 2017 to $526 billion in 2025. Monoclonal antibodies accounted for nearly 20% of the biopharmaceutical market in 2017 [1]. In 2018, six monoclonal antibody products (adalimumab, nivolumab, pembrolizumab, trastuzumab, bevacizumab, and rituximab) had sales exceeding 6 billion USD [2]. Furthermore, new drugs are continually being approved by the FDA, with 18 new mAb products approved in the US in 2018-2019 [2]. These monoclonal antibodies have been used to treat osteoporosis (Romosozumab), complications in sickle-cell anemia (Crizanlizumab), cancer (Polatuzumab), and many other medical conditions [2]. More recently, novel monoclonal antibodies have been discovered which could be used to block SARS-CoV-2 infections (human 47D11 mAb) [3]. Many antibodies which could potentially be used for treatment of SARS-CoV-2 have entered clinical trials, including Regeneron's REGN-COV2 dual-antibody cocktail [4], AstraZeneca's AZD7442 dual-antibody cocktail [5], and Eli Lily, Amgen, and AbCellera's bamlanivimab (LY-CoV-555) entering clinical trials phase 3 in July, phase 1 August, and phase 3 in August of 2020 respectively. The expiration of blockbuster biotherapeutics is also spurring the emergence of biosimilars, which will continue to drive the demand for product development and manufacturing capacity.

Table 2.1 FDA approved monoclonal antibody therapeutics.

Monoclonal Antibody	**Brand Name**	**Developer**	**Targeted Disease**	**US Approval Year**
Crizanlizumab	Adakveo	Novartis Pharmaceutical Corp.	Sickle cell disease	2019
Brolucizumab	Beovu	Novartis Pharmaceutical Corp.	Macular degeneration	2019
Polatuzumab vedotin	Polivy	Roche, F. Hoffmann-La Roche, Ltd.	Diffuse large B-cell lymphoma	2019
Risankizumab	Skyrizi	Boehringer Ingelheim Pharmaceuticals/ AbbVie Inc.	Plaque psoriasis	2019
Romosozumab	Evenity	Amgen/UCB	Osteoporosis in postmenopausal women at increased risk of fracture	2019
Caplacizumab	Cablivi	Ablynx	Acquired thrombotic thrombocytopenic purpura	2019
Rvulizumab	Ultomiris	Alexion Pharmaceuticals Inc.	Paroxysmal nocturnal hemoglobinuria	2018
Moxetumomab pasudodox	Lumoxiti	MedImmune/AstraZeneca	Hairy cell leukemia	2018
Ibalizumab	Trogarzo	Taimed Biologics Inc./ Theratechnologies Inc.	HIV infection	2018
Fremanezumab	Ajovy	Teva Pharmaceutical Industries, Ltd.	Migraine prevention	2018
Emapalumab	Gamifant	NovImmmune	Primary hemophagocytic lymphohistiocytosis	2018
Cemiplimab	Libtayo	Regeneron Pharmaceuticals Inc.	Cutaneous squamous cell carcinoma	2018
Tildrakizumab	Ilumaya	Merck & Co. Inc./Sun Pharmaceutical Industries, Ltd.	Plaque psoriasis	2018
Galcanezumab	Emgality	Eli Lilly	Migraine prevention	2018
Erenumab	Aimovig	Novartis	Migraine prevention	2018

Mogamulizumab	Poteligeo	Kyowa Hakko Kirin	Mycosis fungoides or Sézary syndrome	2018
Lanadelumab	Takhzyro	Dyax Corp.	Hereditary angioedema attacks	2018
Burosumab	Crysvita	Kyowa Hakko Kirin/Ultragenyx Pharmaceutical Inc.	X-linked hypophosphatemia	2018

Table adapted from Lu *et al.* [2]

2.2.1 CHO cells: The Workhorse of Industrial Protein Production

Various expression systems can be used to produce recombinant proteins: bacteria, yeast, microalgae, filamentous fungi, insect cells, and mammalian cells. However, mammalian cell cultures, more specifically Chinese Hamster Ovary (CHO) cells, are typically used for the large-scale production of recombinant proteins used in clinical applications. Mammalian cells are favored over other expression systems mainly for their ability to produce gram quantities of biologics with human-like post-translational modifications [6,7]. CHO cell cultures have been extensively optimized and can now routinely achieve yields of ~3 g/L [8] and sometimes up to 10 g/L [9,10].

For CHO cell line development, two selection systems are prevalently employed: GS (glutamine synthetase) and DHFR (dihydrofolate reductase). In the former, the GS gene is used as a selectable marker and is introduced alongside the gene of interest. Therefore, cells which lack the desired recombinant product gene cannot survive in a glutamine-free medium containing L-methionine sulfoximine (MSX), which inhibits GS activity. Transfected cells having integrated the exogenous gene for GS found in a transcriptionally active locus have the ability to synthesize glutamine. Alternatively, CHO cells can be transfected with the dihydrofolate reductase (DHFR) gene alongside the recombinant protein gene. Cells without DHFR cannot synthesize glycine or thymidine [11]. Methotrexate (MTX), which inhibits DHFR activity, is added to media in order to select the highest producing cells [12,13]. Cells are typically subjected to several rounds of MTX selection for stepwise gene amplification, unlike for the GS-base system which requires only a single round of MSX selection [14].

Another factor contributing to the popularity of CHO cells is their ability to grow well in suspension, which allows better control of the culture environment. Proper mixing to obtain homogeneous culture conditions is of importance to maintain a desirable (i.e. productive) metabolic state. However, cell culture homogeneity cannot always be achieved by increasing mixing speed alone due to concerns related to cell damage. The lack of cell walls makes animal cells much more sensitive to shear stress than their microbial counterparts.

CHO cell lines have also been adapted to be cultivated in serum-free environments [15]. Although the presence of serum was shown to protect cells from mechanical damage, its supplementation is a potential source of contamination by virus or prions, leads to lot variability, increases contaminant protein content resulting in a more difficult purification, and increases operating costs [16]. The use of serum-free media has been shown to have no impact on recombinant protein production [17] and quality [16]. In large-scale bioreactors, contamination remains one of the predominant cause of failure [18]. Due to the large loss of time and product, it is important to eliminate all sources of batch failure.

Some CHO expression systems have also been engineered to be inducible with the most common regulatory systems being tetracycline-induced [19-21], ecdysone-induced [22,23], and cumate gene-switch [24-26]. With inducible cell lines, some of the critical operating parameters in scale-up such as mixing, aeration, and shear stress can be optimized for both the growth and production phases across scales.

2.2.2 Scale-up, Scale-out, and Scale-down in Process Development

In cell line development, CHO cells are transfected with the desired gene to form a stable transfected cell pool. Individual cells are isolated from the stable cell pool from which a production clone is selected based on its growth, productivity, and quality attributes. These clone screening steps have traditionally been performed in shake flasks, static flasks, microtiter plates or deep-well plates at a volume typically lower than 20 ml. However, fully instrumented mini-bioreactors have emerged on the market and have recently gained in popularity such that plates and flasks are rapidly being replaced in upstream development [27]. Once a suitable candidate production clone is selected, process development from lab- to industrial-scale productions is typically done stepwise. The cell culture process is first transferred to benchtop bioreactors (1L - 10L) for optimization of the process conditions. Benchtop bioreactors are used as a process prototype to further optimize

pH, temperature, dissolved oxygen tension (DO), media, feeding strategies, culture additives such as antifoam and surfactants, agitation, and aeration strategy. The cell culture process is then transferred to pilot-scale bioreactors (50L – 200L) before finally being scaled-up to commercial-scale stainless-steel bioreactors (250L – 30,000L) or single-use bioreactors (250L – 2,000L) for mass production. Process scale-up is a crucial non-trivial step, due to the many issues that may be encountered at manufacturing-scale, including culture environment heterogeneity, dissolved CO_2 accumulation, as well as detrimental impacts related to aeration and mixing conditions. Most of these problems must be addressed and resolved at the pilot-scale before translating to commercial-scale production. Pilot-scale bioreactors are also typically used to supply materials for pre-clinical and clinical trials. Through-out bioreactor scale-up, bioreactor scale-down and scale-down models, typically 2L – 5L benchtop reactors or mini or micro-bioreactors, are used for troubleshooting and process understanding and optimization.

Another method of increasing production in lieu of scale-up is the scale-out approach. Scale-out consists of using multiple bioreactors rather than increasing the bioreactor volume (e.g. using five 2,000L bioreactors for a 10,000L production rather than a single 10,000L bioreactor). Scale-out reduces risk associated with process scale-up and its impacts on product quality and quantity as well as provides greater flexibility to cope with changes in product demand. However, the use of multiple culture vessels inherently introduces a large source of variability which is not found in scale-up thus impacting product consistency [28].

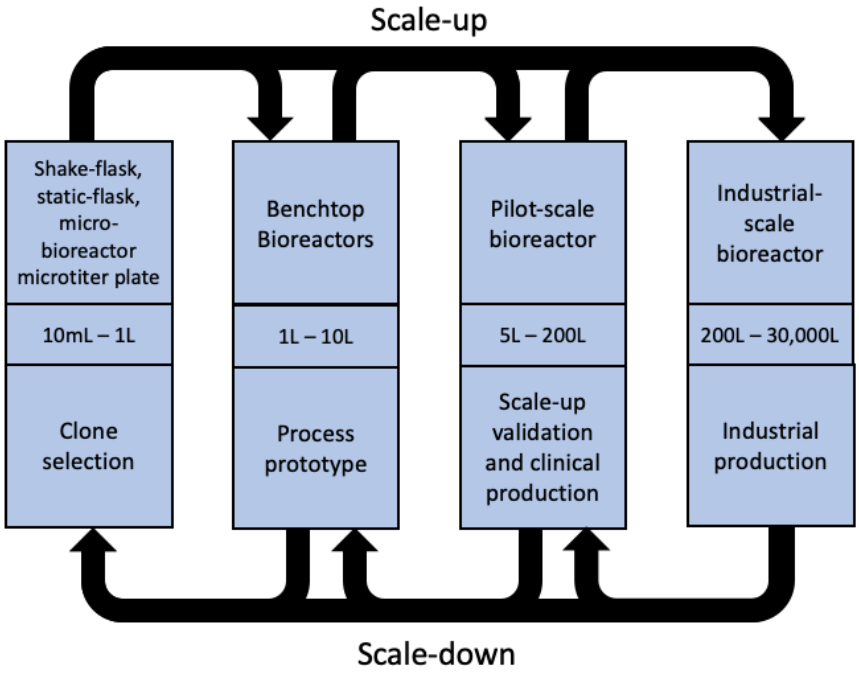

Figure 2.1 Biopharmaceutical production process scale-up and scale down.

2.2.3 The Scale-up Challenge

Although benchtop bioreactors and mini-bioreactors are abundantly used in upstream process development, cell culture behavior and performance (cell density and viability, final titer and product quality, cellular metabolism) may not always be predictive of large-scale processes probably due to key differences in shear stress levels, presence of concentration gradients of nutrients, gases, and pH, and gas transfer capabilities. In bioreactor process design, operating parameters may be divided into two distinct groups: scale-independent and scale-dependent. Scale-independent parameters include temperature, dissolved oxygen setpoint, pH, and feed regimens. In principle, these parameters can be matched across different production scales. On the other hand, scale-dependent parameters may vary considerably with bioreactor size. These include impeller tip speed (V_t), mass transfer coefficient (k_La), the surface area to volume aspect ratio, gas residence time (t_r), mixing time (t_m), mixing power input (P), Reynolds number (Re), and superficial gas velocity (v_s). Bioreactor scale-up consists in keeping all scale-independent parameters constant, while prioritizing which scale-dependent parameters to maintain constant. Due to their interdependence, keeping all scale-dependent parameters constant throughout scale-up is virtually impossible. For instance, if agitation speeds were to be kept unchanged throughout

scales in an attempt to maintain mixing times, impeller tip speeds would increase with size, potentially causing cell damage due to high levels of shear stress in the impeller region. On the other hand, if impeller tip speed is kept constant across scales, large bioreactor vessels will have drastically decreased agitation speed and thus increased mixing times. In addition to differences in mixing during scale-up, gas transfer characteristics will also be significantly impacted. With an increase in culture size, the ratio of surface area to volume decreases, thereby reducing the contribution of the headspace on the overall gas transfer. A decrease in gas transfer in the headspace implies greater sparged gas flowrates to meet the oxygen demand, which may also result in cell damage due to shear stress caused by bubbles. Thus, there is no obvious method to perform the scale-up of bioreactors, as critical trade-offs must be made. This is further complicated by the fact that the best scale-up practices used in industry are often kept secret. As such, scale-up remains an art that still relies on trial and error to determine optimal operating parameters and strategies.

In this review, we will focus on CHO high-density fed-batch cultivation systems, process parameters, scale-up strategies, and tools that can be used to tackle the challenge of cell culture process scale-up. More specifically, the most common CHO cell cultivation systems, from uninstrumented flasks and micro-bioreactors to large-scale stirred-tanks and their role in the scaling-up of biopharmaceutical production will be first described. Second, key process parameters during bioreactor scale-up and their impact on cell culture will be identified. Third, basic scale-up principles and recent strategies employed in scale-up across scales will be described. Finally, useful tools in scale-up such as computational fluid dynamics (CFD) and scale-down models will be discussed.

2.3 Cultivation Systems for CHO cells

2.3.1 Uninstrumented Systems

Many different uninstrumented cell cultivation systems are available for mammalian cell culture such as Erlenmeyer shake flasks, static flasks, roller bottles, multi-well plates, TubeSpin, and spinner flasks. Uninstrumented systems are mainly used for their ease of use, low costs, and high throughput capabilities. Their major downside lies in the inability to measure and control culture conditions such as pH and dissolved oxygen levels, although new sensor technologies adaptable for these cultivations systems are increasingly available as discussed below.

Shake flasks, the most widely used uninstrumented cultivation system, come in sizes typically ranging from 25mL to 5L. Smaller flasks can be used for clone selection and seed train and larger flasks of up to 5L are routinely used for rapid productions. These containers can be made of glass or plastic and can be with or without baffles to improve aerating and mixing. They can be agitated through orbital or linear movements and are usually kept in a temperature and CO_2 controlled environment. Operating parameters such as vessel size, fill volume, material of construction, geometry of baffles, cap and its filter, shaker orbit, and agitation speed can all potentially impact cell culture performance due to their relevance in mixing and gas transfer [29,30]. Their major limitation is the reliance on surface aeration, leading to reduced oxygen transfer rates when compared to stirred-tank bioreactors. They have thus a limited capacity to support high cell density cultures. The presence of baffles increases oxygen transfer, however high mixing speeds may cause excess splashing resulting in blocking the gas-permeable plug in the cap of the flask. Spinner flasks, which resemble shake flasks but are agitated with a magnetic stirring impeller are easier to scale-up due to their geometry which more closely resembles bioreactors.

Plates with numbers of wells ranging from 4 (25 mL / well) to 3456 (1-2.2 µL / well) may also be used for cell culture. This allows for high and even ultra-high throughput miniaturized cultures particularly useful for screening purposes. These plates can be employed for fluorescence and phosphorescence measurements and allow for stacking which reduces space used in incubators. Comparable growth rates, viability, and protein production between 24 deep well plates and shake flasks were noted [31].

Static flasks and roller bottles function similarly to shake flasks, however they provide a surface onto which adherent cells may stick to. Roller bottles allow for increased surface area in order to increase cell density. Expanded surface roller bottles have the same dimensions as standard bottles, but further increase the surface area available for cells by the addition of a pleated design inside the bottle. Roller bottles are advantageous over static flasks not only for their higher surface area, but also enhanced gas transfer capabilities and increased homogeneity of the culture media. Roller bottles can be stacked and incorporated within a fully automated system for seeding, feeding and harvest (e.g. RollerCELL).

In order to allow for closer cell culture monitoring and parameter control, new sensor technologies compatible with small culture devices have been developed. The SFR shake flask reader by

PreSens can monitor pH, dissolved oxygen levels, and oxygen uptake rate (OUR) allowing for control of dissolved oxygen by adjustment of the shaking speed. Additionally, modern incubators may have tri-gas (carbon dioxide, oxygen, and nitrogen) control such that cell culture may be performed under hypoxia or hyperoxia conditions. RAMOS® (Respiration Activity Monitoring System) and TOM® (Transfer-Rate Online Measurement) by Kuhner allow to measure dissolved oxygen and carbon dioxide levels in the headspace. This can provide real-time measurements of oxygen uptake rate (OUR), carbon evolution rate (CER), and the respiration quotient (RQ). Until recently, these parameters could only be reliably measured within a stirred-tank bioreactor. While uninstrumented flasks used to be abundantly employed for upstream process development, they are being steadily replaced with mini-bioreactors that better mimic large-scale conditions.

2.3.2 Stirred-tank Bioreactors (Glass and Stainless-steel)

The use of stirred-tank bioreactors is the favored method of producing recombinant proteins in the biopharmaceutical industry [32]. For cell culture applications, glass and stainless-steel bioreactors are available in sizes ranging from 1L benchtop to 20,000L industrial bioreactors. Stirred-tank bioreactors are used to control the temperature, pH, mixing, and dissolved gas levels in cell cultures, as they all can have a significant impact on cell growth and productivity. Typically, bioreactors are equipped with dissolved oxygen and pH probes and temperature sensors. Oxygen levels are controlled by sparging air, pure oxygen and sometimes nitrogen; pH setpoints are controlled by base addition and carbon dioxide sparging; temperature is controlled either with a heating blanket and cooling coil combination or jacketed wall. Mixing is achieved through the rotation of an impeller attached to a shaft. Rotation is powered by a mechanical or magnetic motor found at either the top or the bottom of the stirred-tank.

2.3.3 Single-use Bioreactors

Single-use bioreactors (SUBs) are a valuable alternative to reusable glass or stainless-steel bioreactors and are increasingly adopted by the biomanufacturing industry due do their numerous advantages. SUBs allow for faster facility set-up, reduction of down-time, reduced risk of contamination, easier to follow Good Manufacturing Practice (GMP) guidelines, and simplified validation as SUBs are pre-sterilized, reduced handle, and lower initial capital costs when compared to reusable bioreactors. Single-use bioreactor performances have been shown to be comparable to those of reusable bioreactors at various scales [33,34]. However, due to being single

use equipment, the costs of consumables are higher than that of reusable bioreactors. Two main types of SUBs are available: stirred-tank and Wave bioreactors. Stirred-tank SUBs consist of plastic bags placed inside a more permanent bioreactor vessel or rigid plastic vessels containing an integrated stirrer. A driver is connected to the stirrer mechanically or magnetically. Stirred SUBs can achieve power inputs of up to 20 W/m^3 and oxygen mass transfer coefficients of 3-8 h^{-1} with drilled hole spargers [35], which are values comparable to those typically seen in reusable bioreactors. Wave SUBs are bags placed on a rocking agitator and thus do not contain stirrers. They are often used in perfusion mode during seed train expansion of large-scale productions [36,37]. Wave SUBs have more uniform energy dissipation and reduced foam formation, and were also shown to yield comparable cell culture performance as stirred SUB [38]. Single-use bioreactors range in size from 15mL (ex: Ambr® 15) up to 2,000L for stirred-tank and 50mL to 500L for Wave. All sensors and control loops present in reusable bioreactors can be found in stirred-tank SUBs and come in the form of *in-situ* disposable sensors or non-invasive optical sensors or ultra-sonic sensors [39].

2.3.4 Micro- and Mini-bioreactors

Miniature bioreactor systems provide a powerful tool for the optimization of cell culture parameters (e.g. pH, DO, temperature, nutrient concentration, pre-culture age, seeding density, aeration, mixing, etc.). Miniature bioreactor systems allow for high-throughput cell cultures while still monitoring and controlling DO, pH, agitation, and gas sparging. Owing to ease of set-up and short turn-around times, such systems are ideal for design of experiments (DoE) resulting in a higher resolution and accurate definition of design space as well as shorten clone selection timelines and accelerate process development. Many different micro- and mini-bioreactor systems are commercially available and can be operated in either batch or fed-batch modes, as shown in Table 2.2. These micro and mini-bioreactor systems ranging in volume from 10mL to 1L with 1 to 48 cultures run in parallel (depending on manufacturer) all have pH, DO, and temperature control. Additionally, some mini-bioreactor systems are designed for perfusion cell cultures (e.g. CellBRx). Two of the most frequently used micro- and parallel mini-bioreactor systems are the Ambr® 15 and the Ambr® 250. The latter has temperature and mixing capabilities for individual units and can be operated in both fed-batch and perfusion modes, while temperature and agitation control in the former is limited to a block of 12 units.

Table 2.2 Automated micro and mini-bioreactor systems available for batch or fed-batch mammalian cell culture

System	Manufacturer	Volume	Units
Ambr® 15	Sartorius	10mL - 15mL	24 or 48
Ambr® 250	Sartorius	100mL - 250mL	12 or 24
Biostat® Qplus	Sartorius	500mL - 1000mL	12
DASbox®	Eppendorf	60mL - 250mL	Up to 24*
DASGIP®	Eppendorf	200mL - 3.8L	Up to 12*
MiniBio	Applikon®	250mL, 500mL, 1000mL	1
MicroMatrix	Applikon®	1mL - 7mL	24
Multifors 2	Infors HT	300mL - 750mL	Up to 6**
Micro24	Pall Life Sciences	7mL	24
Medicel cultivation unit	Medicel Oy	100mL - 200mL 200mL - 500mL	15
Clone screen	Biospectra	400mL	32
Biopod f800	Fogale Biotech	80mL	8
CellStation	Fluorometrix	35mL	12

*In modules of 4

**In modules of 2

Micro and mini-bioreactor systems are invaluable tools not only for use as a scale-down model but also for clone selection. Cell culture performances (cell density, viability, cellular metabolism, and product yield and quality) in Ambr® 15 was shown to more closely resemble that of bench-scale

or larger bioreactors compared to shake flasks [40]. For example, a 26% and 33% decrease in titer and peak viable cell density respectively from shake flask to 2L bioreactor cell cultures have been observed. Meanwhile, cell viability, viable cell concentration, and titer were comparable between Ambr® 15, 2L bioreactor, and 5L bioreactor [41,42]. Similarly, cell cultures performed in Ambr® 250 bioreactors have been shown to have comparable final titer, metabolite (glutamine, glutamate, glucose, lactate and ammonia) profiles, and product quality to those of a 5 L bioreactor [12].

2.4 Key Process Conditions Impacted by Scale-up

2.4.1 Aeration

In bioreactors for mammalian cells, aeration is a critical component, particularly when operating at high cell density, as sufficient oxygen needs to be supplied to the cells, while carbon dioxide must be stripped to prevent its accumulation in the culture broth. This is usually achieved using a combination of gas spargers and headspace aeration. In bioreactors, particularly at large scales, oxygen is supplied by being dispersed close to the bottom of the vessel using a gas sparger. Gas diffusers employed in bioreactors can be either porous-frit spargers (made of ceramic, Teflon, or stainless steel) or drilled hole spargers (DHS). The former creates smaller bubbles, thereby increasing both the interfacial surface area and gas hold-up but is also more prone to foaming and not as effective for CO_2 stripping. Hence, dual-sparger designs are frequently encountered. Table 2.3 presents an overview of the different design and aeration configurations employed. In most cases, oxygen and carbon dioxide are sparged on demand in order to control dissolved oxygen levels and pH, while air is continuously sparged and often also supplied to the headspace.

Table 2.3 Common aeration strategies in mammalian cell cultures

Reference Source	Bioreactor type & scale	Gas sparging			Headspace gas	Mixing
		Type	On demand	Continuous		
[43]	Ambr® 250mL	Open pipe	O_2 & CO_2	Air	No gas	2-PB
	500L SUB	0.4 mm DHS for air Frit for O_2 & CO_2	O_2 & CO_2	Air	Air	1-PB
	2,000L SUB	2 mm DHS for air Frit for O_2 & CO_2	O_2 & CO_2	Air	Air	1-PB
[12]	Ambr® 250mL	Open pipe	O_2 & CO_2	Air	No gas	2-PB
	5L benchtop	DHS	O_2 & CO_2	Air	Air	2-PB
	250L SUB	DHS and Frit	O_2 & CO_2	Air	Air	1-PB
[44]	Ambr® 250mL	Open pipe	O_2 & CO_2	N/A	No gas	2-PB
	3L benchtop	0.5 mm DHS **OR** 20µm Frit	O_2 & CO_2	Air	Air	Marine
	2,000L SUB	2 mm DHS Air/N_2 20µm Frit O_2 & CO_2	O_2 & CO_2	Air **OR** N_2	Air	1-PB
[45]	5L (glass)	15µm Frit	O_2 & CO_2	Air	Air	Marine
	20L (glass)	15µm Frit	O_2 & CO_2	Air	Air	Marine
	5,000L (Stainless Steel)	1.8mm DHS	O_2 & CO_2	Air	Air	Marine
[46]	Ambr® 250mL	Open pipe	O_2 & CO_2	Air	No gas	2-PB
	200L	1 mm DHS Air 20µm Frit O_2 & CO_2	O_2 & CO_2	Air	Air	1-PB
[47]	2L benchtop	N/A	O_2 & CO_2	Air	Air	Marine
	1,500L	N/A	O_2 & CO_2	Air	Air	N/A
[48]	5,000L	N/A	O_2 & CO_2	Air	N/A	3-Marine
	25,000L	N/A	O_2 & CO_2	Air	N/A	2-HF

DHS: Drilled hole sparger
Frit: Frit sparger
PB: Pitched blade
HF: Hydrofoil

2.4.2 Oxygen

In CHO cell cultures, dissolved oxygen (DO) levels are typically maintained between 10% and 80% of air saturation [41]. Excessive oxygen concentrations result in the undesired accumulation of reactive oxygen species (ROS), which can cause alterations in the mitochondrial respiratory chain and intracellular redox, ultimately leading to cell growth inhibition and decreased specific productivity [49,50]. On the other hand, hypoxic conditions have also been known to induce ROS accumulation [51]. Although specific oxygen consumption (qO_2) is comparable to higher DO set-point, a prolonged exposure of 10 days at 20% DO has been shown to illicit the same hypoxic response typically observed after 1-3 days exposure at 0.5% - 5% DO. Hypoxia results in an increase ROS accumulation, reduced oxygen uptake, and increased lactate production [50]. Furthermore, ROS accumulation has been shown to be a significant cause for decrease in productivity at large scale (5,000L), while such problem was not encountered at small scale (20L) [51]. Considerations of optimal DO set-point are particularly important during scale-up. Due to hydrostatic pressure, if DO set-points are chosen to be identical at both small and large-scale, the corresponding oxygen concentrations will be higher in larger scales. Thus, DO set-points should be adjusted accordingly during scale-up in order to keep oxygen concentrations constant across scales [50].

Although surface aeration reduces shear stress caused by bubbles, its impact on mass transfer becomes negligible at larger scales [52]. In order to reduce shear stress caused by bubbles bursting at the gas-liquid interface [53], surfactants such as Pluronic F-68 (or Kolliphor® P188) are added to the cell culture broth. Pluronic concentrations in the range of 1 g/L (and up to 5 g/L) are typically used to confer shear protection [52,54].

The oxygen mass transfer coefficient (k_La) is used as a measure of a system's oxygen transfer capabilities. For a given system, k_La is mainly correlated to the volumetric power input (P/V) and to the superficial gas velocity (v_s) as shown in Equation 2.1 where parameters α and β are empirically fitted parameters of approximately 0.4 and 0.5 respectively [55] and K is an empirically fitted proportionality coefficient.

$$k_L a = K \left(\frac{P}{V}\right)^{\alpha} v_s^{\beta} \qquad 2.1$$

Process parameters such as gas bubble size, mixing speed, gas flowrate, volume and bioreactor geometry all impact the k_La. Various medium components, including salts, antifoam and surfactants, have also been shown to influence the mass transfer coefficient. Particularly, antifoam was found to significantly decrease k_La [42,56]. Pluronic F-68 also decreases k_La but to a lesser extent [42], and the addition of salts increases k_La [40,42]. Another factor found to influence the k_La is the number of impellers. The use of single impellers was demonstrated to increase k_La when compared to a 3-impeller configuration when keeping volumetric power and gassing flowrate constant in coalescence-repressing media, such as most culture broths. This indicates that concentrating the power input where bubbles are formed increases the overall mass transfer [32].

Generally speaking, an increase in bioreactor scale of similar geometry will result in an increase of the k_La, as noted in both conventional stirred-tank [57,58] and single-use bioreactors [12,59]. The increase in liquid height results in longer gas residence time allowing for more efficient gas transfer.

2.4.3 Carbon Dioxide

In mammalian cell cultures, carbon dioxide partial pressure (pCO_2) levels are typically maintained at 4-10% CO_2 saturation (30 – 70 mmHg) [60,61]. High levels of dissolved carbon dioxide (150-200mmHg) were found to have detrimental effects on cell growth and productivity for many types of mammalian cells including CHO cells. In CHO cell cultures, high pCO_2 levels were shown to inhibit cell growth [61-64], cell productivity [61,64], and alter product quality [65]. Dissolved carbon dioxide in water causes acidification by reacting with water to form carbonate which dissociates into carbonic acid. The acidification of the culture broth causes base addition in pH-controlled cultures, which leads to an increase in osmolarity. Elevated levels of osmolarity (460 – 500 mOsm/kg) have been shown to reduce viable cell density and viability [63] when compared to normal levels (260 – 320 mOsm/kg) [66]. Thus, it is suggested to operate at large pH dead band as this reduces the need for base addition which affects osmolarity. In addition to base addition, feeding of concentrated nutrients, such as what is done in fed-batch operations, increases osmolarity up to 540 mOsm/kg [67]. Although carbon dioxide may have detrimental effects on cell culture, it is needed in metabolic synthesis of nucleic acids so its concentration must not fall too low, hence becoming a limiting factor [32,68]. Ultra-low pCO_2 levels (12.5 – 24.5 mmHg) were found to decrease viable cell density (VCD) and cell viability after 6 days of cell culture compared to normal pCO_2

levels (28-54 mmHg). However, ultra-low CO_2 levels (12.5 – 24.5 mmHg) were shown to have a positive effect on mAb galactosylation [69].

Large-scale animal cell cultures are faced with the issue of withdrawing (or stripping) carbon dioxide produced by cells at roughly the same molar rate as oxygen is consumed. At larger scales, headspace aeration was not found to be efficient for carbon dioxide removal [45,56,57]. The gassing and aeration strategy may require increase in sparge flowrates or agitation speeds to increase carbon dioxide removal when comparing large-scale and small-scale bioreactors [45]. Additionally, carbon dioxide stripping was shown to be independent of gas mass transfer coefficients in large scale bioreactors. Instead, carbon dioxide accumulates in the culture media due to long gas-residence time relative to gas bubble saturation time; gas bubbles become saturated in carbon dioxide before leaving the culture media such that mass transfer is no longer limiting carbon dioxide stripping [48].

2.4.4 Mixing

Mixing serves not only in ensuring homogeneous conditions but also plays an important role in improving mass transfer, which is important for supplying oxygen to the cells and stripping carbon dioxide. Mixing in large-scale mammalian cell cultures is typically provided by axially pumping impellers such as pitched blade or hydrofoil impellers. Axial flow impellers allow for decreased mixing times, when compared to radial flow impellers such as Rushton impellers. Moreover, axial flow impellers result in lower shear stress applied to cells, which are more fragile compared to their microbial counterparts [32]. In large-scale bioreactors, baffles are typically used around the circumference of the tank in order to induce turbulence. Without baffles present, the circular energy provided by the impeller does not sufficiently contribute to the turbulent motion required for proper mixing. The absence of baffles allows for the formation of a central vortex which may result in uncontrolled gas transfers between the headspace and culture broth. Another strategy which may be employed to increase flow turbulence is the use of eccentrically introduced impeller shaft. This is mainly used in situations where baffles are inconvenient, such as in the case of single use bioreactors. However, the use of eccentrically introduced impeller shaft is known to require roughly double the power input in order to achieve the same mixing times as concentric impeller shafts [32].

Mixing is related to aeration through volumetric power input (P/V), as seen in Equation 2.1. Volumetric power input is an important engineering parameter often used in scale-up in order to ensure comparable culture homogeneity mixing environment. The volumetric power input can be measured or calculated using Equation 2.2, where N_p is the dimensionless power number, N is the mixing speed, D_i is the impeller diameter, and V is the volume. Depending on the type of impeller used, various correlations are available to evaluate the power number for agitated vessels, typically as a function of the flow regime (i.e. Reynolds number) and aspect ratios. When the flow is turbulent, the power number becomes independent of the Reynolds (Re) number in baffled vessels.

$$\frac{P}{V} = \frac{N_p N^3 D_i^5}{V} \qquad 2.2$$

In CHO cell culture bioreactor operation, mixing speeds are typically adjusted in order to obtain a P/V in the range of 10-80 W/m^3 [12,43,70]. Another factor that must be taken into account when setting the mixing conditions is the impeller tip speed. As high impeller tip speeds (V_t) create zones of high shear stress, it is favourable to minimize V_t.

Under increased air or oxygen sparged flowrates, lower mixing speeds are required in order to maintain the gas mass transfer coefficient (k_La) constant. This in turn increases the mixing time (t_m) which may create heterogeneities in the culture broth [53], including the presence of significant dissolved oxygen gradients resulting from different localized gas mass transfer coefficients [71]. This can be further exacerbated by the fact that mixing times are already significantly longer at larger scales. For instance, mixing times were found to increase from ~10s for benchtop 3L bioreactors to ~120s for industrial-scale bioreactor [72]. An increase in mixing time results in pH, dissolved oxygen and carbon dioxide, and nutrient concentration gradients. These gradients are important since cells may pass through a region of non-optimal operating conditions (the so-called micro-environment) resulting in an overall reduced culture performance. In particular, glycosylation patterns have been found to be impacted by varying dissolved oxygen levels [73] and viable cell densities, and thus product titers, are decreased due to pH inhomogeneities [74]. A higher gas mass transfer coefficient is found at the bottom near the impeller due to mixing and increased hydrostatic pressure. In order to improve mixing, Xing *et al.* [45] suggest minimizing culture volumes and performing alkali additions near the impeller to minimize pH peaks.

2.4.5 Hydrodynamic Shear Stress

Gas sparging is recognized as being a significant source of cell damage by shear stress. The damage to the cells can occur at the formation of bubbles, at the sparger, at impeller-bubble interactions, when bubbles rise, and during the bursting of bubbles at the liquid surface. The later was found to be the predominant source of cell damage [53]. In addition, smaller bubbles cause more cell damage due to higher specific energy dissipation rates when bursting at the surface [75]. The higher energy dissipation rates are a result of an increase in excess pressure, as shown in Equation 2.3, such that the recoil speed of bursting bubbles of smaller size is larger [53].

$$\Delta p = 4\sigma/d_p \qquad 2.3$$

where Δp is the Laplace pressure, σ is the surface tension, and $d_p$is the bubble diameter. Due to the fact that mammalian cells are sensitive to shear forces, mixing and aeration speeds must be maintained below certain thresholds to reduce cell damage. The most important consideration when reducing mixing and aeration speeds is meeting the oxygen demands of the cells. Hence, pure oxygen can be used in order to reach the cell's oxygen requirement at lower gas flowrates, although care has to be taken since the principal carbon dioxide removal strategy is through stripping by the sparged gas. Shear stress may have impacts on cell metabolism at sublytic levels. Elevated sublytic shear stress of 0.8 N/m^2 (60,000 W/m^3) was found to decrease specific productivity, decrease glucose intake, and decrease lactate production when compared to lower levels of shear stress of 0.005 N/m^2 (2 W/m^3) [76].

However, volume average hydrodynamic stress caused by mixing was shown, through computation fluid dynamic simulation, to be independent of scale for the same volumetric power input. Rather, hydrodynamic stress is influenced by bioreactor configuration (number of baffles and impellers). Meanwhile, variations such as small differences in vessel aspect ratios and large changes in impeller shaft angle do not have a significant impact on volume average hydrodynamic stress [77]. In most bioreactors, the average energy dissipation rate is typically in the range of 10-80 W/m^3, while the maximum energy dissipation rate is approximately 100-fold greater. CHO cells in suspension may support energy dissipations rates of up to 10^7 W/m^3 [78]. Product quality was shown to be affected at lower mixing rates than those resulting in cell damage, suggesting that shear damage due to mixing had previously been overestimated [32]. Furthermore, a decrease in antibody production has been observed with increase hydrodynamic stress as a result of mixing [79].

In an effort to minimize cell damage and death, protecting agents such as Pluronic® F-68, a surfactant, can be added to culture media [45,53,80]. Pluronic® F-68 reduces surface tension which reduces the excess pressure in a bubble, as seen in Equation 2.3, which in turn decreases the specific energy dissipation associated with a bubble, of size d_p, bursting at the liquid interface [53]. Cells incorporate Pluronic® F-68 in their membrane [81] which increases the membrane strength [82]. Additionally, high concentration of Pluronic® F-68 in intracellular vesicles stiffen the cell's mechanical properties which may also contribute to its shear stress sensitivity [83]. But the largest contribution of Pluronic® F-68 to reduced cell death might be due to the fact that it reduces the hydrophobicity of the membrane, resulting in less cells attaching to bubbles and experiencing the highly localised energy dissipation generated during bursting [53].

2.5 Basic principles for Bioreactor Scale-up

The purpose of bioreactor scale-up is to increase the production volume while keeping similar product yield and quality. This implies that comparable cell specific productivity, cell density and viability, and cell metabolism must be preserved across scales. In order to accomplish this, as many operating parameters as possible must be kept constant. Volume independent variables such as temperature, pH, dissolved oxygen setpoints, and nutrient feed strategy can easily be kept constant during process scale-up. However, scale-dependent parameters, such as agitation, impeller tip speed (V_t), mixing time (t_m), the Reynolds number (Re), and aeration flowrates, cannot all be simultaneously kept constant throughout scale-up. Scale-dependent parameters have varying dependencies on mixing speed (N), impeller diameter (D_i), and vessel diameter (D_T), as seen in Table 2.4. These parameters impact cell damage, operating costs, foaming, heterogeneity, and gas transfer. In essence, bioreactor scale-up involves trade-offs and compromises.

Table 2.4 Scale-independent and dependent variables

	Culture Parameter	
Scale-dependent	Impeller tip speed (V_t)	$V_t = \pi N D_i$
	Mass transfer coefficient (k_La)	$k_L a = K\left(\frac{P}{V}\right)^{\alpha}(v_s)^{\beta}$
	Surface area to volume ratio (A_c/V)	$\left(\frac{A_c}{V}\right) = \frac{\pi(D_T/2)^2}{V}$
	Gas residence time (t_r)	$t_r = \frac{V\phi_G}{Q_g(1-\phi_G)}$
	Mixing time (t_m)	$t_m = \frac{V}{N_f N D_t^3}$
	Mixing power input (P)	$P = N_p N^3 D_i^5$
	Reynolds number (Re)	$Re = \frac{N{D_i}^2\rho}{\mu}$
	Superficial gas velocity (v_s)	$v_s = Q_g/A_c$
Scale-independent	Temperature (T)	
	pH	
	Feed regimen	
	Dissolved Oxygen (DO)	

Although volumetric power is typically maintained within the range of 20-80 W/m^3 across scales, other factors, namely mixing speed, mixing time, impeller tip speed, and Reynolds number, are generally not maintained constant with changing volumes. As seen in Table 2.5, mixing speeds decrease with an increase in scale. However, impeller tip speed and Reynolds numbers follow the opposite trends due to increased impeller size. Finally, mixing times also increase with vessel volume due to the increase in vessel diameter.

Table 2.5 Typical values of scale-dependant parameters: mixing time, mixing speed, impeller tip speed, and Reynolds number.

Parameter	Micro and Mini-Bioreactor (<1L)	Benchtop (1-10L)	Pilot-Scale (10-200L)	Industrial-Scale (>200L)
Mixing time (s)	<10 [72]	10 [72]	20 [59,84]	50-200 [45,51,59,72,84]
Mixing Speed (RPM)	400-1,400 [12,41,43,44,46,85-87]	200-300 [10,12,41,44,47,52,58,70,85,88,89]	100-150 [46,58,59,87,90-92]	50-100 [44,45,58,79,87,91,92]
Impeller tip speed (m/s)	<1 [85]	0.75-1 [58,70,85]	1-2 [57-59,70,84,90,92]	1.5-2.5 [43,56,58,70,79]
Reynolds Number	2,000-15,000 [85,87]	20,000-50,000 [70,85,87]	50,000-150,000 [59,70,87,90]	>150,000 [70,87]

2.5.1 Geometrical Similarity

Geometric similarity is typically the first criterion applied for scaling-up bioreactors. If tank diameter is increased, all other lengths (tank height, impeller diameter, and impeller width) are increased by the same factor. Generally, bioreactor vessels used for cell culture maintain a height to diameter ratio (H/D) of 1-2 for benchtop bioreactors and 2-3 for pilot and industrial scale bioreactors [93,94]. However, preserving H/D impacts factors related to surface and volume such as heat transfer, gas transfer and mixing. Heat transfer per unit volume decreases as volume increases, due to heat exchange occurring at the walls of the vessel. A constant H/D aspect ratio will also significantly decrease the surface area to volume ratio (A_c/V), resulting in a decreased contribution of surface aeration for oxygenation and carbon dioxide stripping [57]. This is critical for shear sensitive cells, because of the importance of gas transfer rates and restrictions on mixing speeds and gas sparging flowrates.

2.5.2 Dynamic Similarity and Scale-up Criteria

During scale-up, a criterion is selected based on which parameters have the highest impact on cell culture performance (i.e. product titer and quality). Due to the interdependencies, when one critical parameter is held constant, other factors may exhibit a significant variation following an increase

in volume, potentially leading to problems that were not encountered at smaller scale. For instance, a constant volumetric power input during scale-up results in a decreased mixing speed. In turn, a decrease in mixing speed results in increased mixing time allowing for the formation of heterogeneities. Constant impeller tip speed or constant Reynolds number (i.e. similar hydrodynamic regime) during scale-up also implies decreased mixing speed. A large decrease in mixing speed reduces volumetric power input and increases mixing time. These interdependent variations can be observed in Table 2.6 for the most common scale-up criteria employed. For example, if volumetric power input is kept constant for the scale-up of a small-scale bioreactor to a bioreactor with volumes 125-fold greater, mixing speed, impeller tip speed, Reynolds number, and mixing time would be affected by a factor of 0.34, 1.7, 8.5, and 2.92 respectively.

Table 2.6 Interdependence of scale-up parameters for geometrically similar bioreactors with diameters increased by a factor of 5.

Parameter	**Small-Scale (1L)**	**Large-scale (125L) Scale-up Criterion**			
		Volumetric power input (P/V)	**Impeller tip speed (V_t)**	**Reynolds number (Re)**	**Mixing time (t_m)**
Power Input	1	125	25	0.2	3125
Volumetric Power Input	1	1	0.2	0.0016	25
Mixing speed	1	0.34	0.2	0.04	1
Impeller diameter	1	5	5	5	5
Impeller tip speed	1	1.7	1	0.2	5
Reynolds number	1	8.5	5	1	25
Mixing time	1	2.92	5	25	1

Impeller tip speed may be used in shear sensitive cell cultures; however, the decrease in volumetric power requires high gas flowrates in order to maintain acceptable oxygen transfer rates, which is also a major source of cell damage [53]. Additionally, the lower mixing speeds used to keep impeller tip speeds constant results in poorer mixing in large scales. Thus, impeller tip speed may not be a

suitable scale-up criterion for large differences in scale. A constant mixing time used as a scale-up criterion results in an increase in impeller tip speed which may cause cell damage.

More recently, oxygen transfer [95,96], bulk mixing [97], and proper CO_2 stripping [43,47,56,58,98] are recognized as important factors during bioreactor scale-up. Hence, scale-up criteria which minimize the impacts on gas transfer and mixing are most often selected for CHO bioreactor cell cultures.

2.6 Common Scale-Up Strategies

In this section, the most common scale-up strategies employed for scaling-up CHO cell cultures in bioreactor will be reviewed and their implications will be discussed.

2.6.1 Constant Volumetric Power Input

Using a constant impeller power input per liquid volume (P/V) is one of the most commonly used scale-up criteria for agitated and aerated vessels, where mechanical power from the impeller impacts both gas transfer characteristics and culture mixing. The P/V ratio can be set by adapting the impeller type, size and speed to the different working volumes. This scale-up criterion is either used alone or in combination with other factors (e.g. constant normalized gas flowrate) as shown in Table 2.7.

Constant P/V has been used to successfully transfer from benchtop Ambr®250 mini-bioreactor system to 200L pilot-scale single-used bioreactor to demonstrate the scalability of a new pH control strategy [46]. Applying the same criterion resulted in comparable final viability and normalized antibody titer for scale-down from 500L pilot-scale bioreactor to 3L benchtop bioreactor [99], scale-down from 18,000L industrial scale bioreactor to Ambr®250 [86], as well as for scale-up from Ambr®250 to 3L benchtop bioreactor and to 50L pilot-scale [100]. Comparable cell culture performances at 200L and 2,000L scales were also reported using constant P/V as a scale-up criterion, although pCO_2 levels were found to be higher in the large-scale bioreactor [84].

Using constant P/V as a scale-up criterion may translate into significant difference between small and large-scale k_La values if the same volumetric gas flowrate per volume of liquid (vvm) is employed. In order to compensate for the decrease in oxygen transfer at smaller scales, an increased gas flowrate is required for maintaining the desired dissolved oxygen levels [43,96]. This is particularly true when upstream process development steps are done using miniature bioreactors

(e.g. Ambr®15 and Ambr®250 systems). However, the required flowrate adjustments may have detrimental impacts on culture performance, as exemplified by the study of Tescione *et al.* [96]; when scaling-down from 2,000L industrial-scale vessels to 3L lab-scale bioreactors using P/V as the sole criterion, significantly reduced viable cell densities and final product titers were observed. The normalized gas volumetric flowrate (vvm) was three-fold higher in the small-scale bioreactor, resulting in increased bubble-associated cell damage. An approach combining constant P/V, with reduced gas flowrates in Ambr®15 compared to 2L bioreactors, has been successfully implemented to scale-up Ambr®15 bioreactor system to 2L benchtop bioreactors, resulting in matching pCO_2 gas evolution profiles, as well as comparable viable cell density, cell viability and less than 8% difference in product titer [41].

Scale-up from miniature bioreactor Ambr®15 to 10L bioreactor using either constant impeller tip speed or constant P/V were compared and evaluated by transcriptome analysis to assess the impact on gene expression. Comparable cell growth and specific productivity were obtained for both scale-up criteria used, but a decrease in pCO_2 levels throughout the culture was observed in the Ambr®15 compared to the 10L bioreactor, due to the larger oxygen flowrate required in the micro-bioreactor resulting in an increased CO_2 stripping. The transcriptome analysis revealed only minor differences (below 6 %) over time in gene expression between both scales. Although 2455 and 1601 genes were uniquely regulated in the Ambr®15 and 10L bioreactor respectively, no functional correlation was made to scale or cellular behaviour [85].

2.6.2 Constant Oxygen Mass Transfer

Maintaining proper oxygen transfer is an important factor in CHO cell cultures, particularly when bioreactors are operated at high cell densities. Thus, keeping a constant k_La as scale-up criterion is used to ensure proper oxygen supply to the cells. Constant oxygen transfer rate has successfully been employed as a criterion when using Ambr®250 as a scale-down model for 5L lab-scale and 250L SUB systems. A k_La of 2-3 h^{-1} satisfied oxygen requirements in the scale-down model and led to comparable growth, productivity, and final titer for 11 out of 13 GS-CHO and DG44-CHO cell lines [12]. Maintaining a constant k_La (7.9 h^{-1}) via gas flowrate and stir speed adjustments was also shown to yield similar growth profiles in single-used bioreactors ranging from 50L to 2,000L [91]. However, a change of production scale may require the use of different types of gas sparger further complicating the attainment of similar process conditions. To scale-down from 2,000L to

3L bioreactor using a constant k_La, Tescione *et al.* [96] had to resort to a frit sparger in order to avoid excessive mixing speeds or high gas flowrates, which had been shown to be detrimental to culture performance. The use of a frit sparger nonetheless resulted in a decrease of viable cell density.

To attain proper oxygen transfer, He et al. (2019) developed a mathematical mass-transfer model to describe the gas exchange within a bioreactor. Mass balance equations involving both cell respiration rates (qO_2, qCO_2) and mass-transfer characteristics (k_La_{O2}, k_La_{CO2}) were used to calculate the gas flowrates required to meet the oxygen demand and predict pCO_2 levels. This scale-up method resulted in matching viable cell density and antibody production at 2L and 1,500L. Similarly, a scale-down model of a 3L lab-scale bioreactor made use of the maximum oxygen transfer rate (OTR) as the main criterion [96]. Assuming the same oxygen demand as that measured in a 2,000L bioreactor, the required k_La (function of P/V and gas flowrate) and oxygen enrichment levels required in the 3L scale-down model were determined. This allowed to set appropriate sparge rates that resulted in comparable cell culture performances with no impact on protein quality.

In a similar vein, Gimenez et al. [88] have suggested to keep similar overall oxygen transfer flux (OTF) during scale-up, a parameter based on the k_La and the oxygen enrichment in the gas mix:

$$OTF = k_La \times \left(\%O_{2,gas\ mix}/\%O_{2,air}\right) \qquad 2.4$$

A cell culture process first developed in 2L and 10L lab-scale bioreactors was successfully scaled-up to 80L by selecting the maximum OTF (~$6x10^{-3}$ s^{-1}) as the primary scaling parameter. Selection of appropriate P/V and gas flowrate for k_La and oxygen ratio in gas mix led to comparable cell culture performances across the scales [88].

2.6.3 Constant Volumetric Gas Flowrate

Dissolved CO_2 accumulation being a major concern during scale-up of CHO cell cultures in bioreactors, normalized total gas flowrate (vvm) is often used as a scale-up criterion to ensure sufficient CO_2 stripping, while adjusting mixing speeds to provide proper oxygenation.

The miniature bioreactor Ambr®15 was used to develop a scale-down model of industrial and benchtop scale bioreactors using total sparge gas flowrate as a primary scale-down parameter (vvm of 0.01 to 0.02). This scale-down method allowed for adequate CO_2 stripping and kept CO_2 evolution profiles constant across scales. Optimal operating conditions identified by DoE (growth

temperature, production temperature, and pH) were shown to be consistent for Ambr®15 and 5L bioreactor [98].

A different study attempted to use constant sparged gas flowrate per volume to generate a representative scale-down model for a 500L and 2,000L SUB using the Ambr®250 platform [43]. However, surface gas transfer generally accounts for a significant portion of CO_2 stripping at small-scale while generally deemed negligible in large-scale bioreactors. Hence, a lower normalized aeration rate was required in the mini-bioreactor system to match the pCO_2 gas evolution profiles between scales.

In a different process where pCO_2 had been identified as having a major impact on culture performance, constant vvm was used as a criterion in order to match pCO_2 profiles between industrial scale process and Ambr®250. This scale-up method resulted in comparable viable cell density and product titer across scales, emphasizing that proper scale-up criteria should be selected based on the needs of the process [86].

Minimum air sparge vvm and constant P/V have been used in combination as scale-up criteria to ensure that cell growth, gas transfer, and mAb productivity were all matched across scales in 3L, 500L, and 2,000L SUB [58]. The constant air flowrate was selected to ensure proper stripping of CO_2 produced from respiration during the initial growth phase. This strategy led to CO_2 levels maintained below 50 mmHg during the initial growth phase across scales. Due to lower k_La at smaller scales, higher oxygen flowrates were required to maintain dissolved oxygen levels. Thus, higher total gas flowrates were observed in small-scale bioreactors. The disparity in total gas flowrates resulted in ~10 mmHg lower pCO_2 levels in 3L benchtop bioreactors compared to the large-scale counterparts. The authors suggest an improvement to this strategy by the addition of an online pCO_2 probe with feedback control on gas sparge rate. In a different study, the use of constant P/V and vvm as criteria to create a scale-down model using the Ambr®250 resulted in low DO levels (<5%) due to lower k_La (< 2-3 h^{-1}) [12]. A decrease in k_La with decrease in scale, at constant P/V and vvm, can be explained by an increase in gas residence time with an increase in scale. As a consequence of hypoxic conditions, titer was lower in the Ambr®250 compared to the 5L and 250L bioreactors. A constant k_La criteria was used for further development of the scale-down model.

Another important factor to take into account during scale-up is the impact of the gas entrance velocity. This is particularly a concern in industrial-scale bioreactors where higher gas flowrates are required for oxygen supply and to ensure proper CO_2 stripping. A high gas entrance velocity (>60 m/s) is considered detrimental for culture performance, due to the sharp increase in turbulent energy transfer in the sparger region [101]. Additionally, a high sparge rate has been shown to trigger an oxidative stress response and was also associated with an increase in amino acid consumption to restore redox balance [102]. Entrance velocities of less than 20 m/s [101], and in some cases up to 50 m/s [58], were shown to not cause significant cell damage in small to large-scale bioreactors.

2.6.4 Constant Impeller Tip Speed

In order to maintain shear stress levels comparable at different production scales, impeller tip speed may be used as a scale-up criterion. For instance, the use of this scale-up method has resulted in comparable viable cell densities and final product titers between Ambr® bioreactor systems and benchtop bioreactors when using tip speed of 0.7-0.8 m/s [42,85]. However, maintaining a constant tip speed may result in a drastic change in power input, particularly if the difference in scale is important (see Table 2.6). As a result of changes in volumetric power input, higher dissolved oxygen levels are maintained due to higher oxygen mass transfer rates in a study by Hsu *et al.* (2012) [41]. Despite differences in dissolved oxygen levels, impeller tip speed as a criterion allowed for comparable viable cell density, viability, and product titer between Ambr®15 and 2L benchtop bioreactors.

Although impeller tip speeds greater than 1.5 m/s were originally suspected to cause cell damage [103], impeller tip speeds of up to 3.5 m/s have been shown to have no detrimental effect on cell cultures [70]. As such, CHO cells may be more resistant to shear stress than previously thought. This is further accentuated by the use of surfactants such as Pluronic F-68. Furthermore, when scale-up is done between large differences in volume, the use of constant impeller tip speeds causes low oxygen mass transfer rates as the volumetric power is significantly reduced. This highlights why impeller tip speed as a scale-up criterion is impractical and leads to incomplete mixing at large volumes [45,70]. For these reasons, impeller tip speed may not be as important of a scale-up criterion when compared to volumetric power input, oxygen mass transfer coefficients, and volumetric gas flowrate which are parameters related to mixed and gas transfer rather than shear stress.

Table 2.7 Overview of recent scale-up criteria used from benchtop bioreactors to industrial scales

Reference	Scale-up Criteria	Scales	Results
85	Impeller tip speed or P/V	10L to Ambr®15	• Comparable cell viability and specific productivity for both criteria. • Lower pCO_2 in Ambr®15 when using P/V scale-up.
84	P/V or k_La ratio $k_La_{CO_2}/k_La_{O_2}$	200L SS, 200L SUB, 1,000L SUB, and 2,000L SS	• P/V: Comparable VCD, viability, and titer. Higher CO_2 levels in 2,000L SS. • k_La ratio: Comparable VCD, viability, titer and CO_2 levels.
88	Oxygen transfer flux $OTF=k_La*(\%O_{2,gas\_mix}/\%O_{2,air})$	2L / 10L to 80L	• Cell viability and final titer are comparable throughout scales. • Differences in VCD are observed
47	Gas mass balance (OTR=OUR and CER=CTR)	2L to 1,500L	• Consistent VCD, titer, and glycosylation.
46	P/V	Ambr®250 to 200L SUB	• Comparable viability, volumetric productivity, and antibody quality attributes. • Decrease of 10% in peak VCD in the 200L SUB.
41	P/V or Impeller tip speed	Ambr®15 to 2L	• Comparable cell viability, VCD, and titer for both scale-up criteria.
98	vvm	Ambr®15, 5L, and 15,000L	• Comparable CO_2 evolution profiles are obtained.

Table 2.7 Overview of recent scale-up criteria used from benchtop bioreactors to industrial scales (Continued)

Reference	Scale-up Criteria	Scales	Results
86	P/V or vvm	Ambr®250 and 18,000L	• Scale-up strategy selected based on process requirements. • Both P/V and vvm based scale-up result in comparable VCD, viability, and titer.
91	k_La	50L, 200L, 500L, 1,000L, and 2,000L	• Comparable VCD.
100	P/V	30-50mL SF, Ambr®250, 2L, 50L	• Comparable specific growth rate and mAb production.
99	P/V	3L and 500L	• Comparable titer, integrated VCD, and viability
42	Impeller tip speed	Ambr®250 and 5L	• Comparable VCD and titer
96	P/V or k_La or OTR	2,000L to 3L	• P/V and kLa: Significantly higher VCD and thus final titers in the 2,000L bioreactor. • OTR: Comparable cell culture performances and protein quality.
12	P/V and vvm or k_La	Ambr®250, 5L, and 250L SUB	• P/V and vvm: Comparable VCD and viability profiles. Titer was lower in the Ambr®250 due to insufficient aeration. • k_La: Comparable growth, productivity, and final titer.

Table 2.7 Overview of recent scale-up criteria used from benchtop bioreactors to industrial scales (Continued)

Reference	Scale-up Criteria	Scales	Results
[58]	P/V and minimum air sparge vvm	3L, 500L, and 2,000L SUB	• Comparable VCD, cell viability, and titer.
[43]	vvm	Ambr®250, 500L SUB, 2,000L SUB	• Comparable peak VCD, final viability, normalized titer, and product quality.

2.7 Tools to Assist Culture Scale-Up

2.7.1 Computational Fluid Dynamics (CFD)

Computational fluid dynamics (CFD) is a powerful numerical tool that is widely used for the analysis of fluid flow and can be an invaluable tool to assist with bioreactor scale-up. Many commercial or open-source CFD packages are available to characterize the flow in bioreactors based on the vessel geometry and operating conditions. On an existing vessel, CFD offers a way to optimize process conditions without conducting extensive and costly experimentation at large-scale. For the design and scale-up of bioreactors, CFD simulations can be employed to predict the behaviour in a large vessel. Of particular interest, the volumetric oxygen mass transfer coefficient (k_La) can be derived from the CFD simulation outputs. Most often, this is accomplished based on Higbie's penetration theory [104-108]. In this model, the film mass transfer coefficient (k_L) is expressed as a function of the eddy dissipation rate (ε), the oxygen diffusivity (D_L) and the fluid properties (kinetic viscosity, ν) [109].

$$k_L = \frac{2}{\sqrt{\pi}}\sqrt{D_L\sqrt{\frac{\varepsilon}{\nu}}} \qquad 2.5$$

The k_La can then be estimated by multiplying the mass transfer coefficient by the specific area (a), given by:

$$a = \frac{6\alpha_G}{d_b} \quad 2.6$$

where α_G is the gas volume fraction and d_b is the average bubble diameter. Other expressions for the mass transfer coefficients have also been shown to give consistent estimations of k_La, some of which also explicitly include the superficial velocity of the gas phase, as reviewed in Maltby *et al.* [109].

Computational fluid dynamics has been used to characterize and improve cell culture systems ranging from microtiter plates to industrial scale bioreactors. Average k_La estimations using CFD are particularly useful for cell culture systems for which this experimental measurement is not readily accessible, such as in 96-deep well and 6-deepwell microtiter plates [105]. With CFD, it is possible to generate contour plots of k_La values [108], which allow to conveniently visualize mass transfer rate gradients within a bioreactor vessel at various production scales, geometries, and operating conditions. This can provide invaluable information to optimize the conditions so as to minimize oxygen gradients within the cell culture environment. For instance, Villiger et al. have observed no significant dissolved oxygen horizontal variation, while vertical variations were in the order of 6% in a 15,000L bioreactor maintained at 50% air saturation [107]. In the same vein, CFD has also been employed to generate fluid velocity and energy dissipation contour plots [104,106,110-114]. Such data can help identify the presence of mixing dead zones, as well as differences in mixing patterns between bioreactor systems. Another useful application of CFD for bioreactors is to determine hydrodynamic stress during cell culture [105,107,108,111-114]. Determination of hydrodynamic stress can assist in establishing culture conditions that reduce shear damage to cells.

A 2,000L process was successfully transferred to the 5,000L scale with the aid of CFD to determine proper operating conditions based on k_La and fluid velocity contour plots [108]. First, mixing speeds providing adequate mixing times were determined, then flowrates resulting in minimal k_La were established. Other key variables, such as gas entrance velocity and shear rate, were also optimized trough CFD. Table 2.8 presents an overview of bioreactor studies based on computational fluid dynamics.

Table 2.8 Recent uses for CFD in cell cultures

Reference	What CFD is Used For
104	• k_La estimation • Fluid velocity, kinetic energy dissipation rate, and bubble size distribution contours plots
105	• k_La estimation • Hydrodynamic stress simulations
106	• k_La estimation • Fluid velocity flow field simulation • Bubble and turbulent energy dissipation rate distribution simulation
107	• k_La estimation • Hydrodynamic stress, gas volume fraction, bubble size, and k_La contour plot • Simulation of hydrodynamic stress applied to a massless tracker over time • Mixing time simulations • Oxygen gradient simulation
110	• k_La estimation • Fluid velocity contour and vector plots • Gas volume fraction and bubble size contour plot
108	• Gas exit velocity, mean shear rate near impeller, mean bubble residence time, gas hold-up, mean bubble rise velocity, mean bubble diameter, and k_La surface plots at various agitation and gas flowrates • k_La contour plots within bioreactor vessel
111	• Fluid velocity contour plot • Impeller, bulk zone, average, and maximum shear strain rate (SSR) estimation
112	• Radial, tangential, and axial fluid velocity, shear stress, and turbulent intensity contour plots

Table 2.8 Recent uses for CFD in cell cultures (Continued)

Reference	What CFD is Used For
[114]	• k_La estimation • Fluid velocity contour and vector plot • Shear stress contour plot and distribution within the volume of liquid
[113]	• Average eddy size estimation • Velocity, shear stress, and energy dissipation rate contour plots

2.7.2 Scale-Down Models

Scale-down models attempt to reproduce large-scale cell culture performances and operating conditions in smaller cultivation devices. Reduced size models offer the opportunity to optimize operating parameters in smaller units, often in parallel, which reduces costs and time needed for optimization. Micro- or mini-bioreactor systems, such as Ambr®15 and Ambr®250, are being extensively used as reduced size scale-down models. These cell cultivation platforms are favoured over plates and flasks as they have been shown to more accurately represent cell culture performances [12,40-42,86]. The small scale of mini-bioreactors allows for high-throughput cell cultures at low volumes. Reduced size scale-down models employ the same criteria as scale-up: constant k_La, P/V, vvm, and combinations of these.

Scale-down models can also be specifically designed to generate and study the impact of undesired or extreme conditions that can prevail in large-scale vessels (i.e. “worst-case” scenarios), such as poor mixing or pH heterogeneities. A recent study was done at various agitations rates in benchtop bioreactors in order to mimic the impact of hydrodynamic stress encountered in various regions of large-scale bioreactors [79]. This allowed to assess the extent of hydrodynamic stress CHO cells can tolerate before exhibiting a reduced specific productivity. Other studies have aimed at reproducing heterogeneities found in large-scale bioreactors. A small-scale 2-compartment bioreactor system was employed to reproduce impact of pH heterogeneities encountered at large scales [74,115]. Such heterogeneities were found to affect cell growth, particularly towards the beginning of the cell

culture and differences in pH as small as 0.4 units have been found to significantly impact viable cell density.

2.8 Process Intensification and Scale-Up

Process intensification aims to increase process production efficiency by increasing volumetric productivity, lowering manufacturing costs, and reducing physical footprint. Volumetric productivity is largely dependent on the cell density achieved in bioreactor. Therefore, the highest values are obtained in highly optimized fed-batch, perfusion, and concentrated fed-batch processes [89]. A recently popular approach to enhancing volumetric productivity in fed-batch bioreactors is to increase inoculation viable cell density in the production vessel (N stage bioreactor) from ~0.5x10^6 cells/mL to 2-10x10^6 cells/mL through the use of a perfusion bioreactor (N-1 stage).

High-seeding fed-batch bioreactors were found to have almost double final titers when compared with conventional fed-batch [116]. Seeding cell density in the range of 10 – 20x10^6 cells/mL was also shown to translate into significant improvements of productivity and the strategy was successfully scaled-up at the 500L scale [117]. An alternate method to increase the seeding density using batch or fed-batch cultures with concentrated media at the N-1 stage resulted in comparable final titers and protein quality. This approach has the advantage of being simpler than perfusion N-1 and the required associated equipment (retention device and storage vessels) [118].

Process intensification through continuous process operation is largely applied in the chemical industry. However, the biopharmaceutical industry is still largely dominated by fed-batch bioprocessing for recombinant protein production. Since higher productivity can be achieved with a perfusion mode, it is an interesting avenue for process intensification. In perfusion cell cultures, alternative tangential flow filtration (ATF) and tangential flow filtration (TFF) are the preferred methods of cell retention when compared to internal and external spin filters. ATF filtration benefits of reduced filter fouling and higher cell densities as a result of a self-cleaning effect [119,120]. Perfusion cell cultures using ATF cell retention was shown to be economically viable over fed-batch when cell concentration in perfusion culture are at least 3-fold greater [119].

Economically, integrated continuous processes utilising perfusion cell cultures are most feasible when market demands are high. Economic benefits are mostly driven by capital costs while media usage increased operating costs; thus, indicating that perfusion cell cultures require media

optimization to maximize volumetric productivity [120]. The concept of integrated continuous production is gaining increased interest for cost-effective biomanufacturing. A proof of concept for integrated continuous processes has been done using perfusion cell culture and semicontinuous chromatography purification [121]. Representative scale-down models will have to be developed for the rational optimization of these processes.

Process intensification has many impacts on scale-up considerations. Increasing production efficiency and volumetric productivity through process intensification naturally reduces the volume required for increases in production volume. Thus, intensified processes benefit from reduced risk associated to scale-up. However, extremely high cell density (up to $100x10^6$ cells/mL) [122] results in increased oxygen transfer and carbon dioxide stripping demands. These requirements are achieved through increased sparged gas flowrates and mixing speeds. This may potentially accentuate issues with mixing and mass transfer limitations which are of high importance in conventional bioreactor scale-up. Furthermore, additional considerations must be taken into account when performing scale-up of intensified processes. For example, in perfusion cell cultures, a successful scale-up is highly dependent on cell retention efficiency, fouling prevention efficiency, and the similarity of perfusion equipment using between scales [123].

2.9 Conclusion

Predictable scale-up of biologics production is critical due to high costs associated with manufacturing down-time and failure. For example, a biologic product operation with expected annual sales of $1 billion would cost $80 million for every month loss during start-up, technology transfer, or scale-up [124]. However, there exists no single method of performing scale-up and as such scale-up remains an art. Nevertheless, gas transfer and mixing are recognized as the limiting factors in cell culture bioreactor scale-up. Therefore, the predominant scale-up criteria are constant impeller tip speed (V_t), volumetric power input (P/V), mass transfer coefficient (k_La), normalized gas flowrate (vvm), and a combination of P/V and vvm or P/V and k_La.

In light of this review, the following considerations should be taken into account for the scale-up of CHO cell culture:

- Constant P/V may be best suited for scale-up between small differences in volumes. For larger jumps in volume, methods such as constant oxygen transfer rate and mass transfer

balance may be better suited. Additionally, different cell culture processes may have specific prioritised requirements (oxygen mass transfer, CO_2 accumulation, mixing, etc.) such that scale-up criteria should be selected based on the needs of particular processes.

- Although micro-bioreactor systems are increasingly being used for high-throughput process optimization, they may not always constitute a representative scale-down model due to mass transfer limitations. Mini-bioreactors or benchtop bioreactors, which have more flexibility in terms of mixing and sparging conditions, may more closely resemble large-scale bioreactors in their operation.
- During small-scale process optimization, it is of high importance to evaluate the impact of additives such as surfactants (e.g. Pluronic F-68 or Kolliphor® P188) or anti-foaming agents. Such additives may have impacts on gas transfer in cell cultures which is an important factor during process scale-up.
- Different equipment, such as gas sparger, may be required when changing scales. Such change may greatly impact cell culture performance and gas evolution profiles. In most cases, process adjustments must be made in order to obtain comparable cell culture performances both at the same scale and across scales.
- Computation fluid dynamics (CFD) can be a powerful aid to predict process factors such as oxygen mass transfer coefficient and hydrodynamic stress, as well as to study the effect of operating parameters in large-scale while avoiding costly experiments.
- Scale-down models are a valuable tool to assist in process optimization and study the effects of non-optimal conditions encountered at large-scales. The small scales used allow for reduced costs by reducing consumables required as well as having a higher throughput by running experiments in parallel.

CHAPTER 3 EXPLORATION OF THE IMPACT OF SPARGER TYPE AND AERATION STRATEGY ON CELL GROWTH AND PRODUCTIVITY

3.1 Chapter Presentation

This chapter presents a study entitled "Exploration of the Impact of Sparger Type and Aeration Strategy on Cell Growth and Productivity" covering objective 1 of this thesis. The two predominant sparger types (frit microspargers and drilled hole macrospargers) along with two gassing strategies (with or without aeration cascade) comprise 5 aeration configurations that were investigated: dual sparger with air cap and micro and macrospargers with and without air caps. The optimal aeration configuration, dual sparger with air cap or microsparger with air cap, is described, and principal component analysis (PCA) is used to analyse the effects of the aeration on the cell culture. The presence of an air cap allows for lower lactate production and thus a higher product titer.

3.2 Importance of Aeration and Mixing

Due to lengthy cell line development times, additional issues may arise when there is a need to produce urgently, such as, generating representative material necessary for process design during preclinical and clinical trials, or in response to a public health crisis, such as the acute respiratory syndrome of COVID-19 caused by SARS-CoV-2. In such case, cell pools are a viable consideration to produce biopharmaceuticals while eliminating the several months required for clone screening. Stable production pools have the inherent disadvantages of heterogeneity and instability with ageing, which may result in production instability. However, stable production pools have been shown to successfully produce gram quantities of monoclonal antibodies at 200-L and 2,000-L volumes with no significant impact on protein quality [125-127].

At bubble formation, sustained gas entrance velocities (GEV) greater than 60m/s causes irreparable harm to CHO cells and GEVs less than 20m/s are recommended [101]. At the same total gas flowrate, spargers with a greater total hole size will have a lower GEV. However, since lower total gas flowrates are required to maintain dissolved oxygen setpoints using microspargers, a lower GEV would be expected when compared to a macrosparger having the same total hole size. The hydrodynamic stress associated with gas entrance is significantly higher than the stress applied

to the cells by the fully developed flow of the rising bubbles [128]. After the bubble's journey through the media, it reaches the surface of the liquid, bursts, releasing energy and applying hydrodynamic stress to the cells surrounding the bubble. The amplitude of the stress applied is increased for smaller bubbles [53,75,129,130]. The greatest source of stress applied to cells from sparging occurs when bubbles burst at the surface.

Although many effects of bubble size have in a cell culture are known, the impact of changing between micro and macro spargers has seldom been studied. Furthermore, there is no consensus as to which type of sparger is best used in benchtop bioreactor cell culture and sparger types are often interchanged (Table 2.3). In this chapter, the impact of micro and macro spargers and aeration strategies on the performance (integral viable cell density, viability, and product titer) of CHO cell cultures to produce SARS-CoV2-2 trimeric spike recombinant protein was explored.

3.3 Materials & Methods

3.3.1 Benchtop Bioreactor Cell culture

An inducible CHO-GS cell pool with cumate gene switch producing SARS-CoV-2 trimeric spike protein, which was developed by our research team as previously described [131], was used for production in 1-L BioFlo120 (Eppendorf, Germany). The cells were cultured in BalanCD CHO Growth A media (Fujifilm Irvine Scientific, USA) supplemented with 0.1% (w/v) Kolliphor P118 (BASF, Germany) and 50µM L-methionine sulfoximine, MSX (Sigma-Aldrich, USA) under fed-batch mode using 0.8X BalanCD CHO Feed4 (Fujifilm Irvine Scientific, USA) as a feeding solution. Cell cultures were sampled for cell count, metabolite measurements, and titer measurements at -3, -2, -1, 0, 3, 5, 7, 10, 12, and 14 days post induction (DPI) and fed at all sampling points starting at 0 DPI. At feeding, glucose is supplemented as needed to maintain glucose concentration above 17mM. Cell cultures were stopped at 14 DPI due to a stop in product formation even at high viable cell densities (VCD) and viabilities (data not shown). The inducible cell pool system, previously described by our research team [26], allows for two distinct phases during the cell culture: growth and production. During the growth phase, from -3 to 0 DPI, temperature is maintained at 37°C after which temperature is decreased to 32°C for the production phase, from 0 to 14 DPI. At -1 DPI, pH is shifted from 7.05±0.05 to 6.95±0.05. At 0 DPI, the culture is induced with 0.2 µg/mL of cumate, 4-Isopropylbenzoic acid (Ark Pharm, USA) and 75µM MSX. The 1-L benchtop bioreactor was operated at a mixing volumetric power input of 35

W/m^3 (180 RPM), an initial volume of 650 mL (65% of the maximum fill volume), and initial viable cell density of $0.4x10^6$ cell/mL.

3.3.2 Aeration Strategies

The aeration strategies studied varied sparger types, including microsparger (frit sparger with 10-15µm pore size) and macrosparger (drilled hole sparger with 1mm hole size) as well as the use of an aeration cascade operating mode. In aeration cascade mode, air is first sparged through the designated sparger until the air cap flowrate is reached, after which sparging is supplement with pure oxygen to maintain the DO setpoint. For all conditions, surface air flowrate is maintained at 0.038 vvm, carbon dioxide is sparged for pH control, and air and oxygen are sparged through the appropriate sparger for oxygen control at a setpoint of 40%. The aeration strategies studied are described in Table 3.1.

Table 3.1 Aeration Conditions

Condition	Sparger	
	Microsparger	Macrosparger
Microsparger	CO_2, O_2	
Macrosparger		CO_2, Air
Dual Sparger	O_2, CO_2	Air
Microsparger Air Cap	CO_2, O_2, Air	
Macrosparger Air Cap		CO_2, O_2, Air

3.3.3 Analytical

A Cedex MS20C Automated Cell Counter (Innovatis, Germany) counted viable cell density (VCD) and viability. A Vitros350 (Ortho-Clinical Diagnostics, USA) measured glucose, lactate, and ammonia concentrations by colorimetric assays. SDS-PAGE TGX gels separated proteins and the Image Lab Software (Bio-Rad, USA) quantified product titer by band intensity analysis. The

integral viable cell density (IVCC) was calculated from Equation 3.1 where ΔIVCC is the change in integral viable cell density, V is the liquid culture volume, and t is the sampling time with subscripts 1 and 2 referring to the previous and the current sampling times. Principal component analysis was done using GraphPad Prism 10 software with the following variables: endpoint viability, endpoint lactate, endpoint ammonia, endpoint IVCC, endpoint pH, endpoint titer, total base addition, total CO_2 sparge, total O_2 sparge, total glucose consumed and maximum lactate.

$$IVCC_2 = IVCC_1 + \Delta IVCC = IVCC_1 + \frac{(VCD_2 \times V_2) + (VCD_1 \times V_1)}{2} * \frac{(t_2 - t_1)}{V_2} \qquad 3.1$$

3.4 Impact of Sparger Type, Configuration, and Aeration Strategy

Cell cultures were performed in 1-L benchtop bioreactors utilizing five different operating parameters relating to sparger configurations and aeration strategies: microsparger with air cap, microsparger without air cap, macrosparger with air cap, macrosparger without air cap, and dual sparger (both micro and macrospargers) with air cap. In the case of single sparger conditions, all gasses are sparged from the same sparger. In the case of the dual sparger condition, air is sparged by the macrosparger while oxygen and carbon dioxide are sparged by the microsparger. This gassing strategy aims to mimic gassing in large-scale bioreactors where air is typically sparged through a macrosparger to achieve more efficient CO_2 stripping while O_2 is sparged through a microsparger to maximize its gas transfer efficiency. Although CO_2 accumulation is not usually an issue in benchtop bioreactors, this configuration is explored for its impact on the hydrodynamic environment of the cell culture.

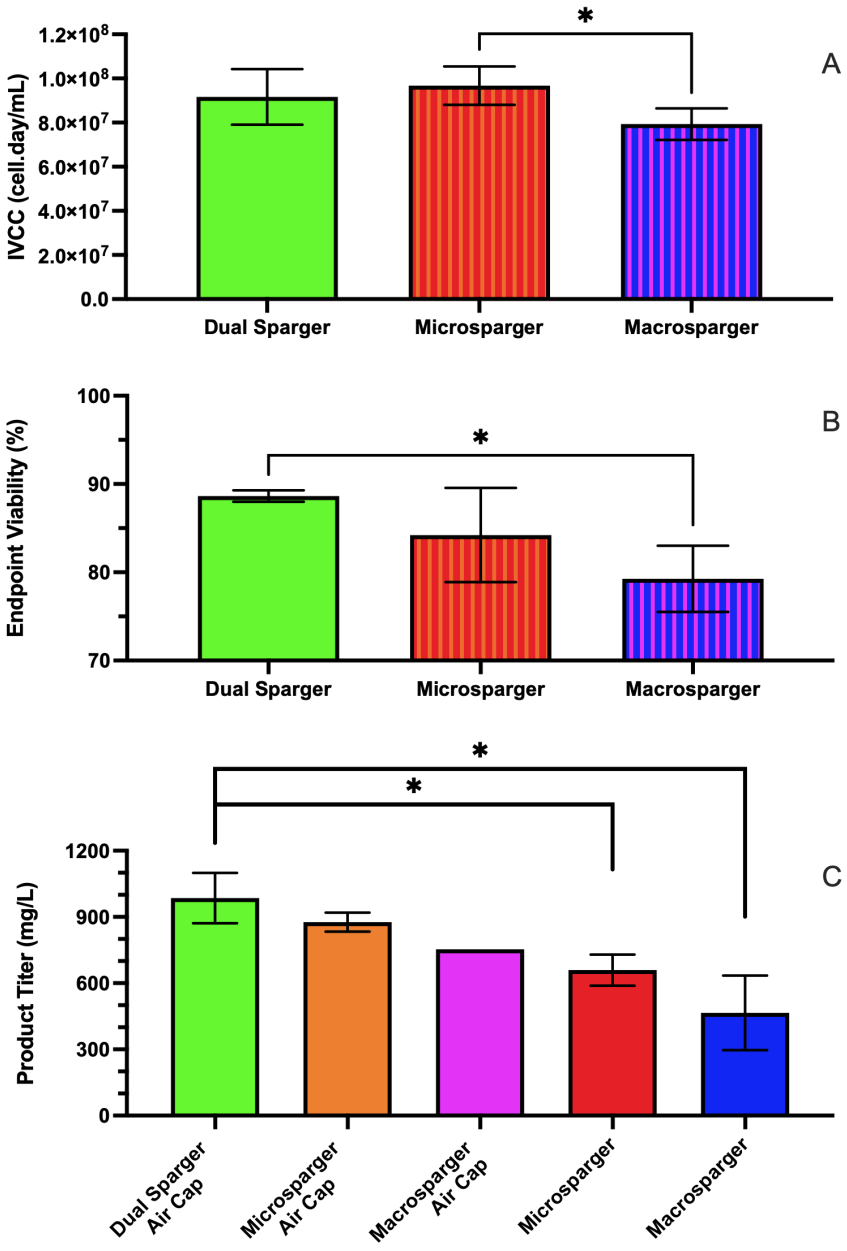

Figure 3.1 The effect of sparger configuration and use of cascade aeration on cell culture performance. A) Integral viable cell density (IVCC) of dual sparger with air cap (green) [n=3], microsparger with and without air cap (red and orange) [n=4], and macrosparger with and without air cap (blue and magenta) [n=3]. B) Cell viability at 14 DPI of dual sparger with air cap (green) [n=3], microsparger with and without air cap (red and orange) [n=4], and macrosparger with and without air cap (blue and magenta) [n=3]. C) Volumetric product titer at 14 DPI of dual sparger with air cap (green) [n=3], microsparger with air cap (orange) [n=2], macrosparger with air cap (magenta) [n=1], microsparger without air cap (red) [n=2], macrosparger without air cap (blue) [n=2]. Error bars represent standard deviations of replicates. Asterisks (*) indicate statistically significance between conditions ($p < 0.05$, t-test).

The integral viable cell density (IVCC), cell viability and volumetric product titer under the five different operating parameters were analyzed to evaluate the performance of the CHO cell cultures (Figure 3.1). When comparing sparger configurations, without considering the different aeration strategies (with or without air caps), microsparger cell cultures resulted in the highest endpoint IVCC compared to the use of dual sparger and macrosparger (Figure 3.1A). The cell cultures with a microsparger configuration had statistically significantly higher IVCCs than when a macrosparger was used ($p < 0.05$). As for endpoint viability at 14 DPI, cultures with the dual sparger gassing configuration maintained the highest viability (Figure 3.1B), whereas viability was lowest in the macrosparger configuration ($p < 0.05$). Product titer at 14 DPI was highest in cultures using the dual sparger with an air cap, which is consistent with the IVCC and viability trends (Figure 3.1C). This configuration had a significantly higher volumetric product titer than both sparger setups without air caps ($p < 0.05$). The microsparger with air cap configuration had the second highest average product titer due to high attained IVCCs. In small-scale bioreactor cultures, a microsparger with air cap aeration performs nearly as well as a dual sparger, since the high surface area to volume ratio allows for sufficient CO_2 stripping at the liquid surface, preventing accumulation. However, the dual sparger configuration may still outperform the microsparger air cap strategy due to the more efficient carbon dioxide stripping associated with the presence of larger bubbles.

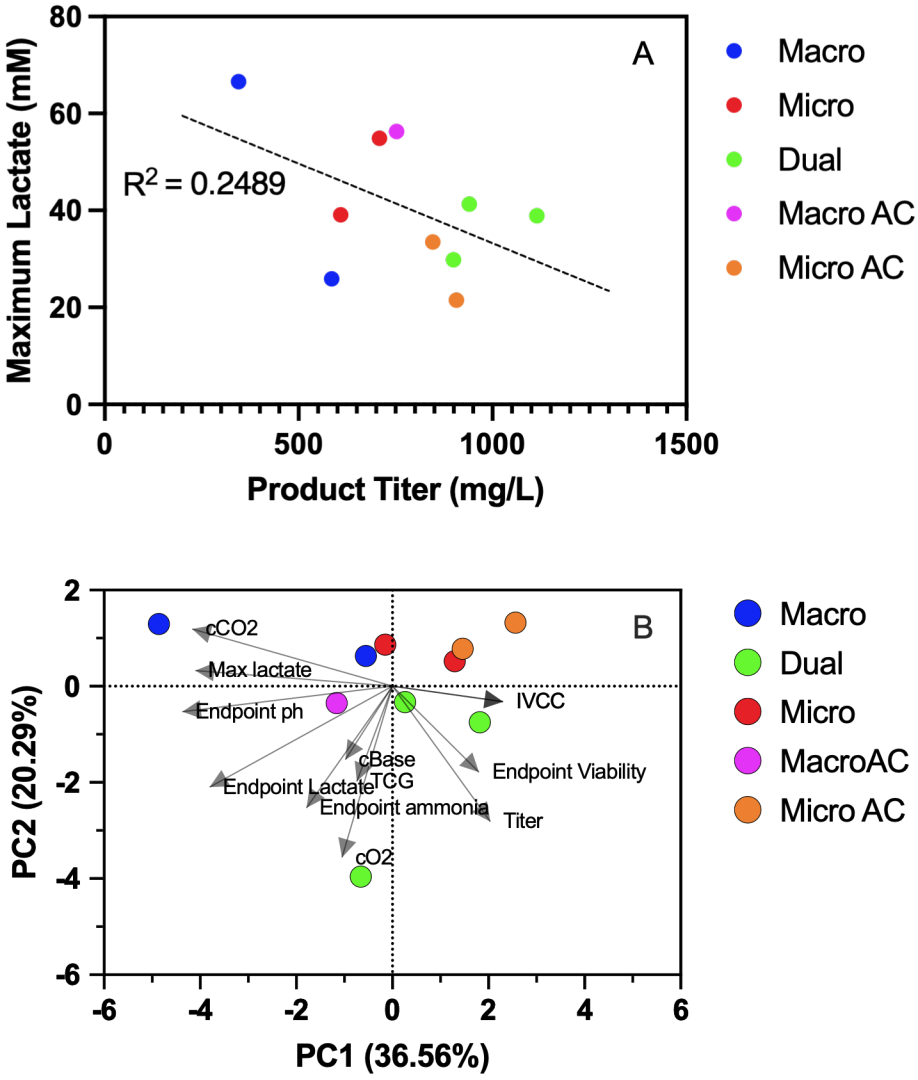

Figure 3.2 Impact of aeration strategy on key process indicators. A) Correlation of peak lactate achieved with product titer (R^2=0.2489) and B) principal component (PC) scatter plot of PC1 (x-axis) which accounts for 18.39% of variance and PC2 (y-axis) which accounts for 34.71% of variace for dual sparger with air cap (green), microsparger with air cap (orange), macrosparger with air cap (magenta), microsparger without air cap (red), macrosparger without air cap (blue).

The product titer was found to be negatively correlated with the maximum observed lactate of cell cultures utilizing the five different aeration strategies presented (Figure 3.2A). This is expected as it is well known in the literature that high lactate production will result in lower titer.[132] Although the correlation between titer and maximum lactate is too weak for accurate prediction of culture outcomes, their relationship provides insight into the effects of aeration strategies. The highest

producing cell cultures are those utilizing an air cap through cascade aeration. This aeration mode allows for greater sparging and thus greater CO_2 removal. A lower level is known to produce less lactate.[133] This was demonstrated by Hoshan et al. (2019) when they replaced base addition with air sparging for pH control resulting in lower peak lactate levels.[46] The low correlation observed between peak lactate and maximum titer in Figure 3.2A is likely due to the fact that lactate is not the sole indicator of performance in bioreactor cell cultures. The aeration strategy also has impacts on cell growth, as seen in Figure 3.1A, cell viability, as seen in Figure 3.1B, and substrate consumption. Furthermore, the low correlation between lactate and titer may be caused by the inherent variability of cell pools.[134] Despite their variability, cell pools remain a valuable tool to achieve short cell line development times and similar product quality to clones.[135,136] As shown here and in the literature, with proper process parameters, pools can produce sufficient recombinant protein material useful for clinical trials and toxicology research.[125-127]

The principal component analysis (PCA) of these cultures further demonstrates the link between the aeration strategies and lactate production (Figure 3.2B). In PCA, multiple variables are transformed into a low-dimensional space as principal components (PC). PCs are ranked such that the first one explains the most variance of the dataset. This information can be useful for process development and scale-up.[127] The loading vectors, represented by arrows on the PCA plot, represent the contribution of each original variable. Loading vectors are positively correlated when pointing in the same direction, negatively correlated when pointing in the opposite direction, and not correlated when perpendicular. The PCA analysis was done on 10 cell cultures using different gas sparger configurations and aeration strategies (dual sparger [n=3], microsparger AC [n=2], macrosparger AC [n=1], microsparger [n=2], macrosparger [n=2]). The variables used in this analysis were: cumulative sparged CO_2 (cCO_2), maximum lactate, endpoint pH, endpoint lactate, cumulative base added (cBase), total consumed glucose (TCG), endpoint ammonia, cumulative oxygen sparged (cO_2), product titer, endpoint viability, and IVCC. The PC1, which accounts for 36.56% of the variability of this dataset, illustrates that IVCC, endpoint viability, and titer are positively correlated in the positive PC1 direction with the dual sparger and microsparger with air cap positioned furthest in this direction. On the other hand, maximum lactate, total carbon dioxide sparging, and endpoint pH are positively correlated in the negative PC1 direction with macrosparger (with and without air cap) and microsparger without air cap positioned in this direction (Figure 3.2B). This indicates the large role that sparger configuration plays in lactate

production. In this case, total CO_2 sparged is a negative indicator since cultures with the highest maximum lactate also have the highest lactate re-consumption. Lactate consumption increases the pH of the media which requires CO_2 sparging to maintain pH withing dead-band setpoint.

Overall, these results emphasize the critical role of sparger configuration and aeration strategy in optimizing CHO cell culture performance. The findings provide valuable insights for process development and scale-up, supporting the implementation of dual sparger systems to achieve enhanced bioreactor productivity in both small- and large-scale operations. Further investigations into fine-tuning gas flow rates and additional process parameters may optimize culture performance and product yield.

CHAPTER 4 ARTICLE 1: SCALE-UP OF A MONOCLONAL ANTIBODY CHO FED-BATCH PRODUCTION IN STIRRED TANK BIOREACTORS: EFFECT OF HYDRODYNAMIC CONDITIONS AND FEEDING REGIMEN

4.1 Article Presentation

The article titled "Scale-Up of a Monoclonal Antibody CHO Fed-Batch Production in Stirred Tank Bioreactor: Effect of Hydrodynamic Conditions and Feeding Regimen" was submitted to *Biotechnology Progress* on March 26, 2025. This article covers objective 2 of this thesis by describing the optimization of a benchtop bioreactor cell culture through feeding regimens, number of impellers, and gassing strategies. The optimized process was then successfully scaled-up from 1-L to 10-L using a constant volumetric power input and gas flowrate criterion. Further investigation in hydrodynamic conditions revealed the importance of maintaining mixing and aeration constant throughout the cell culture. For this article I have done conceptualization, methodology, data curation, investigation, validation, and writing – original draft.

Lucas Lemire[1,2], Sebastian-Juan Reyes[1,2], Yves Durocher[2], Robert Voyer[2], Olivier Henry[1*], Phuong Lan Pham[2*]

[1] Department of Chemical Engineering, Polytechnique Montreal, Montreal, QC H3T 1J4, Canada

[2] Human Health Therapeutics Research Centre, National Research Council Canada, 6100 Royalmount Avenue, Montréal, QC H4P 2R2, Canada

*Correspondence:

Phuong Lan Pham: phuonglan.pham@nrc-cnrc.gc.ca

Olivier Henry: olivier.henry@polymtl.ca

4.2 Abstract

Key hydrodynamic-related parameters such as volumetric power input (P/V), impeller configuration, aeration strategy, and maximum gas sparge rate, as well as an appropriate feeding strategy, must be carefully selected to improve production yields in bioreactor. In this study, the

feeding regimen was found to have an important impact on cell growth and productivity of a cumate-inducible CHO fed-batch cell culture. A low-volume feeding regimen avoided a rapid increase in osmolality, allowing for prolonged cell viability and a 33% increase in volumetric titer compared to the high-volume feeding regimen. Both sparged air and oxygen were used for dissolved oxygen (DO) control, utilizing three levels of airflow rates. An optimum airflow rate of 2 mL/min was found to improve cell growth, longevity, and thus final titer. A larger air cap required increased gas flowrates, which led to an earlier cell mortality. Scale-up from 1-L to 10-L bioreactor using constant P/V and air cap volumetric gas flowrate (vvm) allowed for comparable cell growth and productivity. Further investigation of the effect of mixing and aeration was done by maintaining P/V and vvm constant throughout the cell culture which further improved product titers at 11 days after induction. Our study also demonstrates that keeping a constant volume by removing a culture amount equal to the feed volume added at each sampling event can significantly improve the final volumetric titer. This finding shows the benefit of developing a concentrated feed to reduce the volume increase, which in turn could greatly ease the scale-up task.

Keywords: CHO Fed-batch, Monoclonal antibody, Bioreactor production, Aeration strategy, Feeding regimen, Scale-up

4.3 Introduction

Chinese Hamster Ovary (CHO) cells are the established workhorse for producing recombinant therapeutic proteins such as monoclonal antibodies (mAb) due to their ability to produce human-like proteins. In order to satisfy the ever-increasing demand for these biologics, there have been major improvements in cell engineering[137,138], media composition[139], and cellular micro-environments such as shear stress[105], pH levels[74], and carbon dioxide levels[48,140]. However, the scale-up of these cell cultures in bioreactors, which is necessary to supply market needs, remains a non-trivial task. Bioreactor scale-up challenges are due to differences in shear stress levels, gas transfer capabilities, and the formation of undesired concentration gradients (e.g., nutrients, gases, and pH) in larger vessels. Operating parameters in bioreactor design can be divided into scale-independent (e.g., temperature, pH, dissolved oxygen, and feed regimens) and scale-dependent variables (e.g., impeller tip speed, mass transfer coefficient k_La, gas residence time, and mixing time).[141] While scale-independent parameters can generally be matched across scales, scale-dependent variables are interdependent, making it impossible to maintain all of them constant

during scale-up. For instance, maintaining constant mixing times across scales increases impeller tip speeds, potentially damaging cells. Alternatively, maintaining impeller tip speeds constant reduces agitation, potentially leading to poor mixing. Similarly, as bioreactors increase in size, the reduced surface area-to-volume ratio impacts surface gas transfer, necessitating higher sparged gas flow rates, which may also cause cell damage due to bubble shear stress. Many different strategies, most notably constant mass transfer coefficient, constant volumetric power input, and constant volumetric gas flowrate, have been applied for scaling-up of CHO cell culture processes. However, given the trade-offs mentioned, there is no universally applicable method for bioreactor scale-up such that the optimal scale-up approach is dependent on the needs of the process[141]. As illustrated by the most prevalent scale-up criteria, some of the most important parameters in scale-up relate to mixing and gassing. As such, it is important to optimize these parameters in small-scale bioreactor vessels before large-scale production.

In fed-batch, which is the most prevalent mode of cell culture due to its simplicity and efficacy, a highly concentrated nutrient solution is added throughout the cell culture. An unoptimized feeding strategy may result in a lack of nutrients required for cell growth and protein production, an accumulation of intermediate metabolites, and a sharp rise in osmolality. Glucose depletion (below 2mM) has been linked to a drastic reduction of intracellular ATP and certain intracellular amino acids[142], which in turns leads to a decrease in specific productivity and deficient glycosylation of the recombinant proteins.[143] Asparagine and aspartic acid depletions have been linked to an arrest in cell growth and antibody production, which only restarts after these nutrients are added back to the media.[144,145] Alanine was found to negatively affect biomass production by serving as a signal indicating that TCA cycle intermediates, such as α-ketoglutarate,[146,147] are in abundance.[148] On the other hand, accumulation of certain amino acids (glycine, leucine, methionine, phenylalanine, serine, tryptophan, and tyrosine) is known to inhibit cell growth.[149] Higher ammonia accumulation has also been observed in high-volume feeding regimens[150] which is known to negatively impact growth, production, and glycosylation of the recombinant protein.[151] When a concentrated feed is added to the cell culture, this creates a spike in osmolality. Osmolality levels of 460-500 mOsm/kg have been shown to reduce viable cell density and viability.[63]

Mixing of CHO cell culture across all scales is primarily done through a pitched-blade impeller.[141] To optimize cell culture mixing, the main parameters that can be changed are: the mixing speed,

the number of impellers, the liquid fill volume, and the pumping direction of the impeller. Up-pumping impellers lose less power while down-pumping impellers have flow instabilities as well as torque and power fluctuations such that up-pumping impellers are generally favoured.[152] A reduction of the fill volume can allow for a higher P/V at the same impeller tip speed such that better mixing is achieved without an increase in shear stress applied to the cells. Furthermore, low fill volumes lead to an improvement in oxygen transfer rates.[153] However, in order to maximize production and minimize the production footprint, fill volumes are typically increased aiming to achieve near 100% maximum operating volume at harvest. The mixing speed is important as the movement of the impeller can be a source of shear stress on mammalian cells which are sensitive to such forces compared to microbial fermentation. To avoid cell damage, the impeller tip speed is typically kept below 1m/s in benchtop bioreactors.[141] Furthermore, mixing speed is used to estimate the volumetric power input (P/V) of the culture broth. The P/V is a measure of how much power is applied to the liquid during mixing and as such is used to ensure proper homogenization of media. This parameter is typically kept between 10-80W/m^3.[141] However, in large scale single-use bioreactors the maximum P/V is typically between 20-30W/m^3 due to physical limitations.[35] As for the number of impellers, it impacts gas transfer and the shear stress applied to cells. The P/V of double impeller bioreactors can be estimated by doubling the power number (Np) of a single impeller.[154] When multiple impellers are used and the same P/V is maintained by adjusting the mixing speed, the gas transfer coefficient, k_La, has been shown to be lower in double impeller configurations than that of single impeller systems. This is counterintuitive as empirical models typically have k_La as a function of P/V rather than agitation speed. The use of a double impeller spreads the mixing force across a larger volume changing the local k_La distribution. A higher k_La in single impeller systems indicates that focusing the mixing power near the site of bubble formation improves gas transfer.[32] On the other hand, a double impeller system allows for a lower mixing speed, and thus impeller tip speed, at the same P/V as a single impeller system which is desirable in reducing shear stress applied to cells.

In this study, we use cumate inducible CHO cell clones to explore the impact of feeding volume and hydrodynamic conditions on recombinant monoclonal antibody production. The cumate gene switch works by constitutively expressing the cymene repressor (CymR) which binds to the operator sites (CuO). In the absence of cumate, binding of CymR to CuO prevents expression of the cumate reverse transactivator (rcTA) that is under the control of the CMV5-CuO promoter.

When added, cumate binds to CymR and causes a conformational change resulting in its disassociation from the CuO site and allowing rcTA to bind to the CR5 promoter, hence driving expression of the transgene of interest.[26] This allows to separate the cell culture into two distinct phases: cell growth and protein production. The separation of the process into two phases results in a higher productivity by allowing for rapid cell growth before induction and boosting protein production at high cell density after induction.[25] Process optimization and scale-up to 10-L was done using the cell clone producing product A. First, feed regimens are explored and their impacts on osmolality and product titer were investigated. Second, the number of impellers along with different aeration strategies is studied. The differences in physicochemical environments caused by the number of impellers have been extensively studied in our work while in the literature few studies present the effect of these specific configurations on cell culture.[155] As for gassing, an aeration cascade is used where air is sparged for dissolved oxygen (DO) control until a specified air flowrate (further referred to as "air cap") is reached after which the air flowrate is supplemented with pure oxygen as needed. The process is scaled-up from 1-L to 10-L by using concurrently the constant P/V and constant gassing as scale-up criteria. The developed 1-L process is also transferred to two different clones of a different mAb (product B) to demonstrate its robustness. The process utilizing the clone production of product B is used to further explore the impact of mixing and gassing microenvironments on cell culture productivity.

4.4 Materials and Methods

4.4.1 Small-Scale Cell Culture Maintenance and Pre-Culture

Two different inducible CHO-GS stable clones with a cumate gene switch producing distinct monoclonal antibodies Palivizumab (PLVZM, hereinafter referred to as Product A) and Omalizumab (OMLZM, hereinafter called Product B) were used. The proprietary cell lines were generated internally as previously reported.[25] The $CHO^{BRI/55E1}$ cell line producing Product A (PLVZM) differs slightly from the $CHO^{BRI2353}$ cell line expressing Product B (OMLZM). Both cell lines come from the same parental CHO^{BRI} cell line which is derived from the DHFR deficient CHO-DXB11.[156] The CHO^{BRI} cell line has been adapted to suspension growth in serum-free culture media. The $CHO^{BRI/55E1}$ parental cell line is equipped with the cumate (p-isopropylbenzoate) inducible expression system as it stably expresses the cymene repressor (CymR) and the cumate reverse transactivator (rcTA). Thus, clones will have high recombinant

protein expression in presence of cumate and low basal expression in absence of cumate.[25] The $CHO^{BRI2353}$ parental cell line is equipped with rcTA only. For constitutive expression, the parental cells are simply transfected with the plasmid DNA containing the gene of interest (GOI) under the control of the cumate promoter (CR5). For inducible expression, cells are transfected with a plasmid DNA containing the GOI along with a second expression cassette for constitutive expression of the CymR repressor. In this later case, cumate addition is required to induce expression of the GOI.[135] The $CHO^{BRI/55E1}$ producing Product A has a higher specific productivity than the $CHO^{BRI2353}$ cell line producing Product B thus is able to achieve higher volumetric product titers in fed-batch cultures.

Cells were stored frozen in BalanCD CHO Growth A medium (Fujifilm Irvine Scientific, USA) with 7.5% (v/v) dimethylsufoxide (DMSO) (Sigma Aldrich, ≥99.7% purity, USA) in liquid nitrogen storage tanks (MVE, Series 800-190, USA) at -180°C. The cells were thawed using a water bath (Fisher Scientific, Isotemp Digital 2320, USA) at 37°C for 5 min. Cells were expanded in shake flasks (Corning, USA) ranging from 125-mL to 2-L in incubators regulating temperature at 37°C, humidity at 75% RH, and mixing at 120 RPM with a 25mm orbit. Cells were passaged every 2-3 days in BalanCD CHO Growth A medium supplemented with 50μM L-methionine sulfoximine (MSX) (Sigma-Aldrich, USA) to maintain cell density between 0.2 and 3.0 million cells/mL.

4.4.2 Bioreactor Cell Culture and Operating Conditions

Five experimental conditions (Table 4.1) were developed to study the effect of bolus feeding volume, aeration, and mixing strategy on cell growth and recombinant protein production. Cell cultures were performed in 1.3-L and 14-L BioFlo120 (Eppendorf, Germany), with maximum working volumes of 1L and 10L respectively, under fed-batch mode. The bioreactors were inoculated at 0.3 million cells/mL. BalanCD CHO Growth A medium was supplemented with 0.1% (w/v) Kolliphor P188 (BASF, Germany) for a total surfactant concentration of 0.2% (w/v) and 50μM MSX (Sigma-Aldrich, USA). Cells were fed with 0.8X BalanCD CHO Feed4 (Fujifilm Irvine Scientific, USA) in a bolus mode on the induction day and fed every two or three days onwards.

The inducible cell system, previously described by our research team[26], allows for two distinct phases during the cell culture: growth and production. The growth phase lasts from -3 to 0 days

post induction (DPI). At the end of the growth phase, the cultures were induced with 2 μg/mL of cumate (4-Isopropylbenzoic acid (Ark Pharm Inc, USA)). Throughout the growth phase and the beginning of the production phase, from -3 to 2 days post induction (DPI), temperature was maintained at 37°C after which it was decreased to 32°C for the remainder of the production phase. pH was maintained at 7.0±0.2 by carbon dioxide sparging and addition of 4% (w/v) sodium hydroxide and 9% (w/v) bicarbonate base solution to the culture. The 1-L benchtop bioreactors were agitated with a 5.8 cm diameter 3-blade 45° pitched-blade impeller at a mixing speed setpoint of 148 RPM such that the volumetric power input was estimated at 35 W/m^3 and 27 W/m^3 for initial and final volumes respectively. The dissolved oxygen (DO) setpoint was 60% of air saturation. The DO control was acheived through constant air surface aeration of 25 mL/min (0.031 vvm, volume of gas per volume of liquid per minute) and cascade sparging aeration which will be described in the following paragraph (Section 2.2.3). Cell cultures were terminated when cell viability reached below 70%.

Table 4.1 Bioreactor operating conditions

Parameter	EXPERIMENTAL CONDITIONS					
	Low Feeding Strategy	**High Feeding Strategy**	**1-Impeller / Medium Air Cap**	**Low Air Cap**	**High Air Cap**	**Scale-Up**
Production Vessel	1.3 L BioFlo120	1.3 L BioFlo120	1.3 L BioFlo120	1.3 L BioFlo120	1.3 L BioFlo120	14 L BioFlo120
Initial Working Volume (mL)	800	800	650	650	650	7000
Feed Regimen	Low Feeding Strategy	High Feeding Strategy	Low Feeding Strategy	Low Feeding Strategy	Low Feeding Strategy	Low Feeding Strategy
Number of Impellers	2	2	1	1	1	1
Impeller Diameter (m)	0.058	0.058	0.058	0.058	0.058	0.1
Agitation Rate (RPM)	148	148	171	148	147-174	130-160
Initial P/V (W/m^3)	35	35	35	23	22 from -3 to 2 DPI	22 from -3 to 2 DPI
Final P/V (W/m^3)	27	27	27	18	29 from 2 DPI	29 from 2 DPI
Surface Air Flow Rate (mL/min)	25	25	25	25	21.5-27	230-330
Initial Surface vvm	0.031	0.031	0.038	0.038	0.033	0.033
Final Surface vvm	0.024	0.024	0.024	0.024	0.033	0.033
Sparging Air Cap (mL/min)	2	2	2	1	2-12.3	22 - 150
Sparging Air Cap vvm	0.0025	0.0025	0.0031	0.0015	0.0031 from -3 to 0 DPI, then 0.015	0.0031 from -3 to 0 DPI, then 0.015

4.4.2.1 Low- and High-Volume Feeding Regimens

1-L bioreactor cell cultures were operated at an initial volume of 800 mL (80% of the maximum fill volume). Cell cultures were fed according to low- or high-volume feeding strategies (Table 4.2) on 2, 4, 7, and 9 DPI. In the low-volume feeding strategy (namely low feeding, LFS), 2M D-(+)-glucose (≥99.5% purity, Sigma Aldrich, USA) is supplemented as needed to maintain glucose concentration above 17mM while in the high-volume feeding strategy (HFS) the culture is supplemented to bring the glucose concentration to 33mM after feeding.

Table 4.2: Low- and high-volume bolus BalanCD CHO Feed4 addition regimens described as a percentage of initial culture volume.

DAYS POST INDUCTION (DPI)	LOW FEEDING STRATEGY (LFS)	HIGH FEEDING STRATEGY (HFS)
0	5%	5%
2	7.5%	7.5%
4	7.5%	12%
7	5%	7%
9	5%	7%
11	7.5%	7.5%
TOTAL	**37.5%**	**46%**

4.4.2.2 Number of Impellers and Mixing

Both the 1- and 2-impeller fed-batch cell cultures were fed following the low feeding strategy (LFS). The initial volume of the 2-impeller configuration was increased to 80% maximum fill volume when compared to the 65% maximum fill volume of the 1-impeller configuration to assure all impellers were submerged for the entirety of the cell culture. The height of the lower impeller

on the 2-impeller configuration (H_i) is as low as possible without spatial hindrance of the probes, gas spargers, samplers, and harvest lines (Figure 4.1). The second impeller is placed immediately above the first one. As both impellers are on the same shaft and rotating in the same directions, the impellers have no way to impact with each other as it might appear on Figure 4.1. The estimated initial volumetric power input (P/V, W/m^3) (Equation 4.1) was maintained for both conditions at 35 W/m^3 by adjusting the impeller mixing speed (N).

$$P/V = \frac{N_p d_i^5 N^3}{V} \quad 4.1$$

where, N_p is the impeller power number, d_i (m) is the impeller diameter, N (s^{-1}) is the impeller mixing speed, and V (m^3) is the liquid volume. The power number of 2 impellers is equal to $2 \times N_{p_1}$ where N_{p_1} is the power number of 1 impeller.[154] Adjusting the mixing speed to maintain the P/V constant for both conditions leads to different impeller tip speeds (v_t, m/s) (Equation 4.2) of 0.45 and 0.52 m/s for the 2- and 1-impeller configuration, respectively.

$$v_t = \pi d_i N \quad 4.2$$

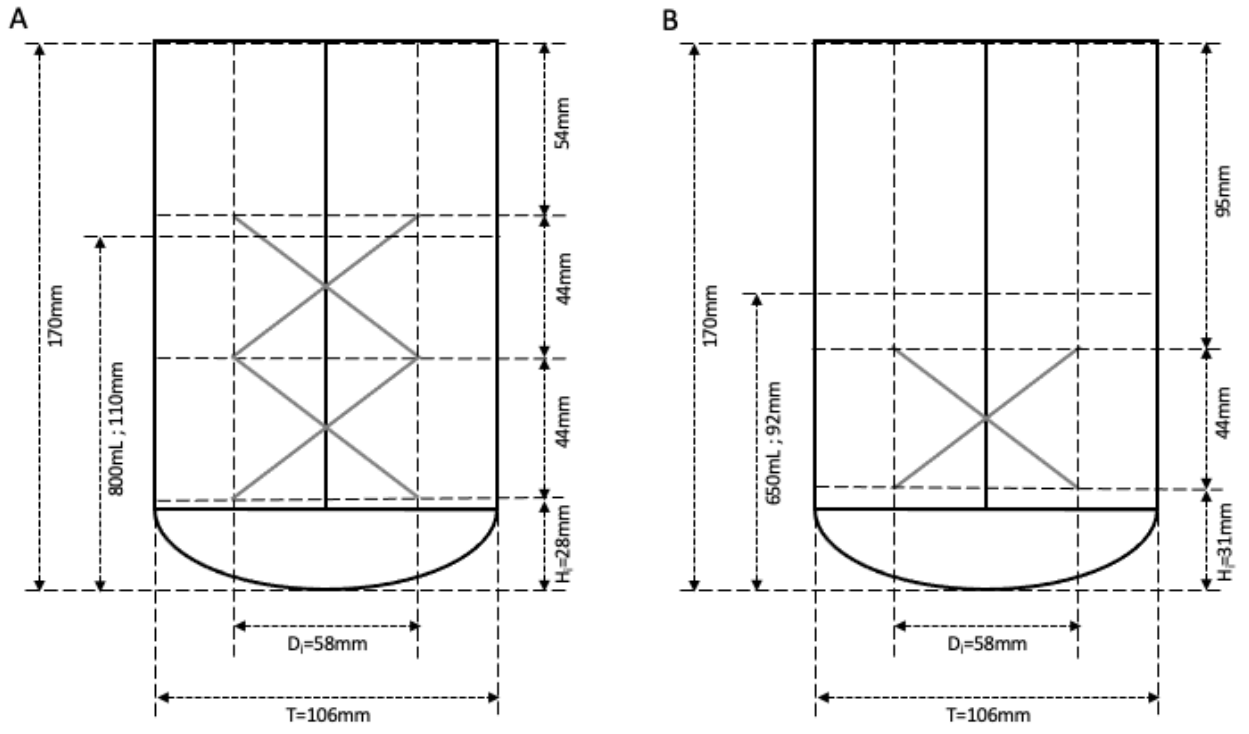

Figure 4.1 Measurements and mixing configuration of the A) 2-impeller and B) 1-impeller bioreactor. 800mL and 650mL are the initial working volumes of the 2- and 1-impeller configurations respectively.

4.4.2.3 Aeration Strategy and Air Cap

Dissolved oxygen control is done by cascade sparging aeration such that air is first sparged for oxygen control until reaching the air cap flowrate (AC) after which sparging is supplemented with pure oxygen as needed. The air caps of 1, 2, and up to 12.3 mL/min correspond to 0.0015, 0.003, and 0.015 volumetric gas flowrate (vvm) when initial volumes of 650mL are used. The high air cap condition uses a constant vvm of 0.015 after induction which results in a maximum air cap of 12.3 This flowrate was used for the high AC condition to ensure culture conditions would have observable differences. These will be referred to as low, mid, and high AC respectively. All air cap conditions used the 1-impeller configuration and the LFS. However, the 1 mL/min treatment used a reduced agitation rate such that the initial P/V was estimated at 23 W/m^3. This was done to determine if lower shear stress environment would allow to maintain cell viability longer when compared to the 2 mL/min AC treatment. The total cumulative oxygen sparged (TCO, [mL]) was calculated using equation 4.3 where F is the gas flowrate (mL/min), Δt is the sampling rate (min), and t_{start} and t_{end} are the start and end times of the cell culture (min).

$$TCO = \sum_{t_{start}}^{t_{end}} \left(0.21 \times F_{air} \times \Delta t + F_{O_2} \times \Delta t\right) \quad 4.3$$

4.4.2.4 Scale-Up to 10-L Bioreactor

Scale-up to 10-L, maximum working volume, bioreactor was done by maintaining the number of impellers, the volumetric power input (P/V), the feeding strategy, and the air cap vvm constant. The volumetric power was kept constant at 22 W/m^3 from -3 to 2 DPI and 29 W/m^3 afterwards by adjusting the mixing speed. The AC vvm was maintained constant at 0.0033 min^{-1} by adjusting the air flowrate as volume increases. These air caps and mixing speeds were selected to ensure the maintenance of the DO set-point in the 10-L unit, given the oxygen sparge flowrate limitations of the experimental setup. The surface air flowrate was increased with feed additions throughout the cell culture to maintain a constant vvm of 0.033 min^{-1} for both bioreactor scales.

4.4.3 Sampling and Handling of Samples

At -3, 0, 2, 4, 7, 9, and 11 DPI, 5mL of culture was purged before sampling another 5mL. Then, 1mL of sample was used for cell counts and viability by means of trypan blue exclusion staining using a Cedex MS20C Automated Cell Counter (Innovatis, Germany). The integral viable cell

concentration (IVCC, cell.day/mL) and doubling time (td, h) were calculated with equations 4.4 and 4.5 respectively where, VCD is the viable cell density, ΔIVCC (cell.day/mL) refers to the change in integral viable cell density, V (mL) refers to the current culture volume, and t (day) is the sampling time. Subscripts 1 and 2 refer to the previous and the current sampling times respectively:

$$IVCC_2 = IVCC_1 + \Delta IVCC = IVCC_1 + \frac{(VCD_2 \times V_2) + (VCD_1 \times V_1)}{2} * \frac{(t_2 - t_1)}{V_2} \quad 4.4$$

$$t_d = \frac{ln(2)}{\mu} = \frac{\ln(2)}{\ln(VCD_2/VCD_1)/24(t_2 - t_1)} \quad 4.5$$

The remainder of the sample was centrifuged at 5000 x g for 5 minutes to obtain the supernatants. Glucose, lactate, and ammonia concentrations of sample supernatants were determined by colorimetric assays using Vitros350 (Ortho-Clinical Diagnostics, USA). Culture media supernatant osmolality was measured by OsmoTECH osmometer (Advanced Instruments, USA). Cell specific consumption rates of glucose (qGlu, pmol/cell/day) and production of lactate (qLac, pmol/cell/day) and ammonia (qNH_3, pmol/cell/day) were calculated using equations 4.6-4.8 respectively where, [Glu] (pmol/mL), [Lac] (pmol/mL), and [NH_3] (pmol/mL) refer to the concentrations of glucose, lactate, and ammonia; subscripts 1 and 2 refer to the previous sampling time (after feeding) and the current sampling time (before feeding) respectively:

$$qGlu = \frac{[Glu]_1 - [Glu]_2}{\Delta IVCC} \quad 4.6$$

$$qLac = \frac{[Lac]_2 - [Lac]_1}{\Delta IVCC} \quad 4.7$$

$$qNH_3 = \frac{[NH_3]_2 - [NH_3]_1}{\Delta IVCC} \quad 4.8$$

The resulting supernatant was filtered in MultiScreen HV 96-well filtration plates at 1500 x g for 2 minutes (Durapore®, 0.45 µm, Millipore, USA) to remove debris. A Protein A HPLC method was used to measure the monoclonal antibody titer using a 2695/2996 HPLC system (WATERS Corporation, USA) with a protein A cartridge (POROS® A20 column, 2.1 mmD x 30 mmH, Thermo Fisher Scientific, Part# 2-1001-00). The column was equilibrated with phosphate buffered saline solution without calcium and magnesium (Cat. No. SH30028.03, Cytiva, USA) and then samples were loaded at 2 mL/min. The column was washed with 1mL, 10 column volumes, to

remove unbound species and cell culture media components. The attached antibodies were eluted using 0.15M NaCl solution at pH 2.0 for 1 minute. Detection of the antibody product is done by UV at 280nm. The standard error of the measurement using this method was typically below 10%. Cell specific mAb production (qP, pg/cell/day) is calculated from equation 4.9 where, P (pg/mL) is the product volumetric concentration measured at two timepoints. The space time yield (STY, [mL/L/day]) is calculated according to equation 4.10 where the product concentration is given in mL/L and the time is given in days.

$$qP = \frac{P_2 - P_1}{\Delta IVCC} \tag{4.9}$$

$$STY = \frac{[Product]_{final}}{Time_{final}} \tag{4.10}$$

4.5 Results and Discussion

4.5.1 Effect of Feeding Strategy

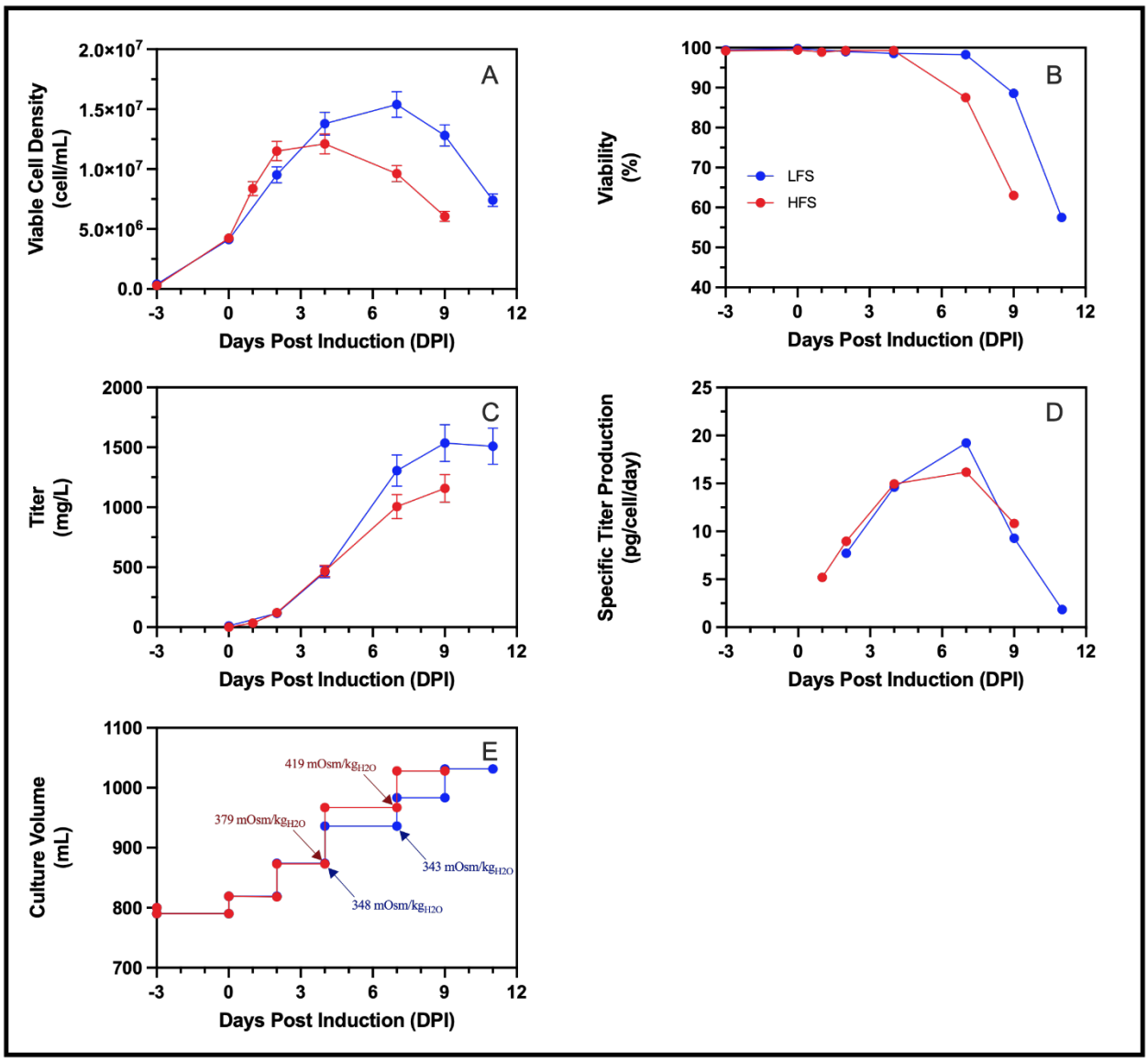

Figure 4.2 The effect of feeding strategy on the A) viable cell density, B) cell viability, C) volumetric titer, D) cell specific titer, and E) cumulative cell culture volume of 1-L benchtop bioreactor cell cultures. Low feeding strategy (-●- LFS); High feeding strategy (-●- HFS). Error bars represent measurement errors for viable cell density (A) and volumetric titers (C).

Cell cultures following low (LFS) and high (HFS) feeding strategies had doubling times of 21.5h and 18.8h, respectively, during the growth phase between -3 and 0 DPI. The difference in doubling times is within the observed range of variability during the seed train while maintaining cells in the

exponential growth phase. This resulted in a comparable viable cell density (VCD) and cell viability (Figure 4.2A and B) at the end of the growth phase (0 DPI). The comparability of both cell cultures extends to metabolite (glucose, lactate, and ammonia) concentrations, as well as cell specific consumption and production. The growth phase exhibits the highest lactate production throughout the cell culture, with 2.4 and 2.8 pmol/cell/day of lactate produced while 0.87 and 1.2 pmol/cell/day of glucose are consumed for the LFS and HFS cell cultures, respectively (Supplemental Figure A.1). This is consistent with literature where rapid cell growth of CHO cells is associated with high glycolytic activity and thus lactate production[157].

At the beginning of the production phase, between 0 and 4 DPI, the difference in VCD for both feeding strategies is at most 17%. During this period, specific glucose consumption stays consistent at just below 1 pmol/cell/day for the LFS culture while the specific glucose consumption for the HFS culture jumps rapidly to 3 pmol/cell/day at 1 DPI before decreasing to near zero at 4 DPI (Supplemental Figure A.1B). Lactate levels reach a peak during this period and cell metabolism enters lactate consumption mode for both feeding conditions (Supplemental Figure A.1C). After induction, cell specific PLVZM mAb production increases linearly until 4 DPI reaching 14.6 and 14.9 pg/cell/day for the LFS and HFS, respectively. LFS and HFS cell cultures attain 459 mg/L and 469 mg/L respectively at 4 DPI, with comparable specific productivities and VCDs. Differences in VCD and glucose consumption are presumed to be due to the difference in glucose supplementation, although this has no significant impact on titer.

Between 4 and 9 DPI, the HFS culture gradually loses cell viability, while the LFS culture maintains cell viability above 98% until 7 DPI, after which it decreases until 11 DPI (Figure 4.2B). The early drop in viability of the HFS culture occurred following culture supplementation at 4 DPI (12% of the initial volume in feed, compared to 7.5% for the LFS culture). With all else being the same between these two cultures, the crash in cell viability was seemingly caused by a larger and rapid increase in osmolality from the addition of a concentrated bolus feeding solution (feed's osmolality is in the range of 780-930 mOsm/kg). As a result of this higher feed volume between 4 and 7 DPI, the osmolality of the culture media increased from 379 to 419 mOsm/kg whereas in the lower feed addition culture (LFS) osmolality was maintained approximately constant at 348 and 343 mOsm/kg (Figure 4.2E). The osmolality of the HFS culture, at 419 mOsm/kg at 7 DPI, is close to the critical osmolality of 450 mOsm/kg for CHO cell cultures, which has been reported to

negatively impact cell viability and VCD.[63,150,158-160] It has previously been noted in the literature that a reduction in bolus feeding amount allowed for lower osmolality and increased product titers.[161] In a separate study done by our research group, large bolus feeding of comparable proportions using similar operating parameters in benchtop bioreactors resulted in early cell death when producing the SARS-CoV-2 recombinant spike protein in a CHO stable cell pool.[150] Since cell death probably resulting from a comparable osmolality increase was also observed in a CHO cell clone producing a different recombinant protein, it is reasonable to argue that overfeeding of this magnitude is detrimental to cell viability. Different strategies have been suggested in the literature to mitigate the adverse effects of high bolus feeding. The CHO cells can be adapted to hyperosmotic conditions over several cell passages to better tolerate high osmotic environments.[162] The feeding technique could also be adapted to feed the same volume continuously which allows for the maintenance of low nutrient concentrations and a manageable osmotic pressure allowing for a longer preservation of cell viability.[150] Overfeeding may have other negative implications on cell culture performance as high concentrations of certain feed nutrients may decrease cell growth, productivity, and protein quality.[163] Specifically, TCA cycle intermediates (malate and citrate) have been observed to accumulate after feeding, which has been linked to growth limitations.[144,163]

Due to the decrease in viability, the VCD of the HFS culture is negatively impacted with respect to the LFS culture. This early reduction in viability with greater feeding is reflected in the cell specific productivity which is constant at ~15pg/cell/day from 4 to 7 DPI after which it decreases as cell viability further descends. With lower feeding, cell specific productivity continues to increase until ~19 pg/cell/day before sharply decreasing during cell death, reaching near zero when cell viability is below 70% (Figure 4.2D). The early loss in cell viability attributed to the bolus increase in osmolality led to a lower volumetric titer (Figure 4.2C). Here, cell specific productivity dropped because of cell death presumably from osmotic stress caused by the increased feed amount. In the literature, the positive effects of osmotic stress on cell-specific productivity towards the end of production have been well documented.[164,165] Specifically, a high osmotic pressure induces an increase in cell size,[166] which in turn is known to boost cell specific productivity.[167,168] Furthermore, a higher volume feeding regimen will lead to a higher final production volume which could dilute the product concentration. As a result, even if a higher product concentration is obtained with a low feeding regimen, it could still lead to a lower total product yield. However, this is not the case here; the low-volume feeding regimen bioreactor yielded 1511mg at a final

volume of 974 mL while the high-volume feeding regimen produced 1190 mg at a final volume of 1018 mL.

4.5.2 Effect of Impeller Number and Aeration Strategy

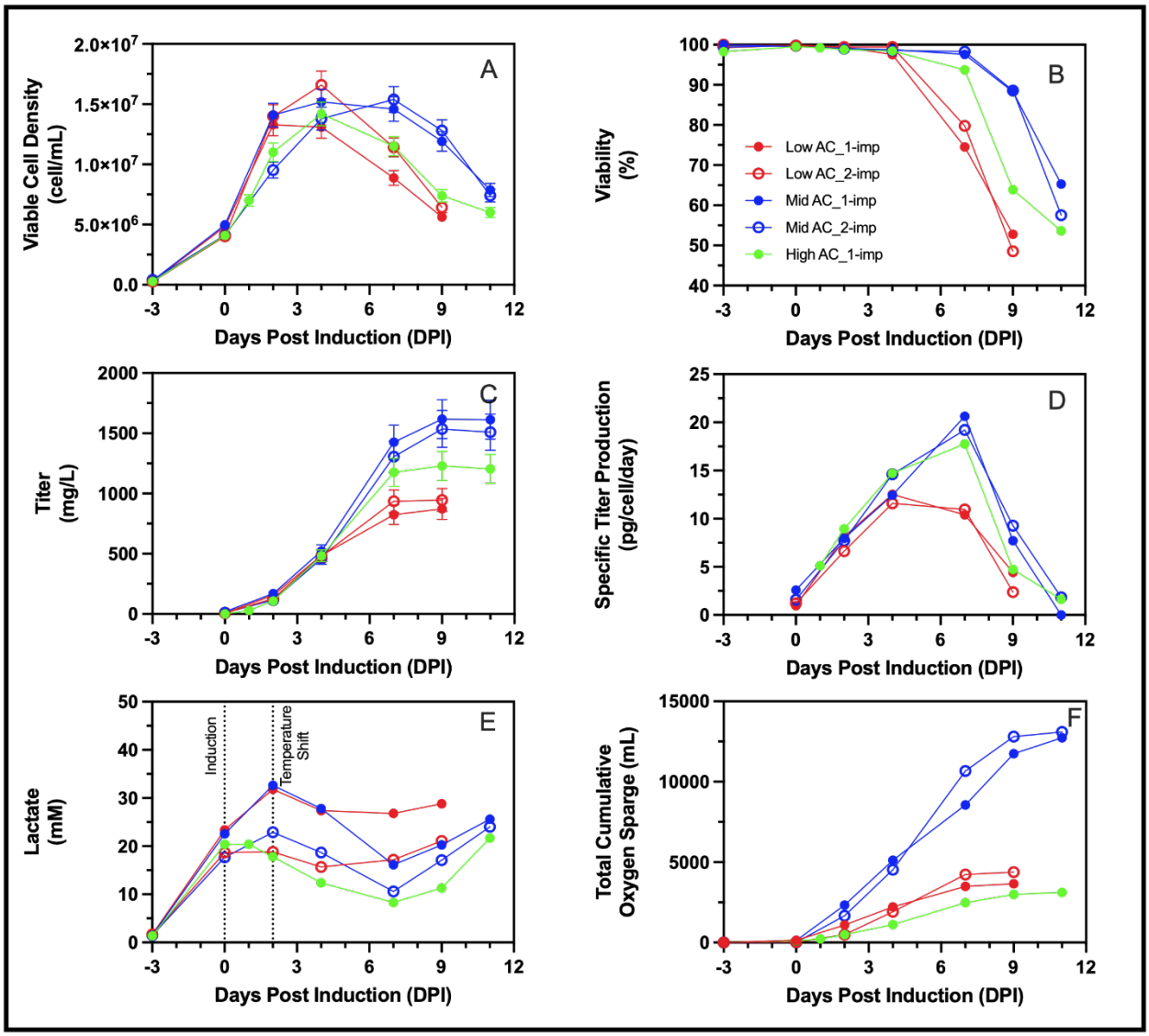

Figure 4.3 Effect of impeller number and aeration strategy on A) viable cell density, B) cell viability, C) volumetric titer, D) cell specific titer, E) lactate concentration, and F) total cumulative oxygen sparged from air and pure oxygen for low (1 mL/min, red), mid (2 mL/min, blue), and high (12.3 mL/min, green) air caps; 1-impeller configuration (full dots) and 2-impeller configuration (empty dots). Error bars represent measurement errors for viable cell density (A) and volumetric titers (C).

Oxygen control of bioreactor cell cultures was acheived through cascade aeration, whereby air is sparged until a pre-set maximal value. When this air cap (AC) flow rate is reached, pure oxygen is supplied on demand to maintain dissolved oxygen setpoints. As no air or oxygen had been sparged during the growth phase, from -3 to 0 DPI, (Figure 4.3F and Supplemental Figure A.2) all studied air cap conditions have comparable cell growth (Figure 4.3A) and differences in cell metabolism prior to induction are expected to be due to cell culture variability. From 0 to 7 DPI, which is the period during which most protein production occurs (Figure 4.3C and D), cell specific glucose consumption is comparable among all culture conditions (data not shown). For all conditions, lactate levels continue to increase until 2 DPI, when a temperature shift occurs, as the cells are still in the exponential growth phase (Figure 4.3E).[169] After the temperature shift, the cell metabolism changes to lactate consumption. In the case of the 1 mL/min low air cap condition, the maintained lactate levels from 4 DPI onwards may be due to early cell death.

Gas sparging during the exponential growth phase has been shown to significantly retard cell growth as the cells adapt to the high shear stress environment.[170] Thus, the aeration cascade gassing strategy may allow for a greater cell growth by minimizing gas sparging (Figure 4.3 F). Headspace air aeration is sufficient to support cell growth from -3 DPI to 0 DPI. Among the three different levels of air cap in this study (low, mid, high), the mid air cap condition with 1-impeller yielded a maximum volumetric product titer of 1617 mg/L at 9 DPI (Figure 4.3C). Meanwhile, in the high AC condition, the maximum volumetric product titer was 1228mg/L at 9 DPI due to an earlier cell death and lower VCD compared to the mid AC condition. Using a higher air cap required a greater total volume of gas sparging which is expected, as a larger proportion of the oxygen supplied to the cells comes from air. At 11 dPI, a total of 34.9L of gas (air, oxygen, and carbon dioxide) was sparged in the mid AC condition compared to 76.6 L of total gas sparged in the high AC condition (Supplemental Figure A.2). This larger total volume of sparged gas applied a greater shear stress on the cells as it is well known that the bursting of bubbles at the surface of the liquid is one of the most significant contributors to shear stress.[53] High sparging rates also improve CO_2 stripping; sustained ultra-low pCO_2 levels have been shown to reduce VCD and cell viability.[69] When using the lower air cap gassing condition with 1-impeller configuration, a maximum titer of 872mg/L was obtained at 9 DPI. The low air cap condition had the earliest observed cell death with 74.5% cell viability at 7 DPI (Figure 4.3B). This early cell death is reflected in the specific titer production which is lower than in the other two conditions at 7 DPI (Figure 4.3D). The low AC condition had

the lowest total gas sparging of 12.1L at 11 DPI. A reduction in gas sparging in turn decreases CO_2 stripping rates. Elevated pCO_2 levels have been shown to reduce cell growth rate and productivity.[63] In addition to this, low pCO_2 is desirable as it has been correlated with improved mAb galactosylation.[69] Although pCO_2 was not measured here, it can be assumed there is no accumulation as this is mainly an issue at larger scales due to longer gas residence times leading to bubbles becoming saturated with CO_2 before reaching the liquid surface.[48,53,68]

The cell growth, viability, and productivity of 1-L bioreactor CHO cell cultures are comparable with 1- and 2-impeller bioreactor configurations (Figure 4.3). In a 2-impeller bioreactor system, with equivalent volumetric power input to a 1-impeller system, the impeller tip speed will be slower allowing a lower local maximum shear rate by spreading out the mixing zones over two impellers.[107] In 1- and 2-impeller systems, cells experience the same shear stress from bursting gas bubbles at the surface. Therefore, dual impeller systems are expected to apply lower overall shear stress to cells than single impeller systems. A lower maximum lactate concentration is observed in the 2-impeller system when compared with the 1-impeller system for both the low AC and mid AC conditions (Figure 4.3E). This is in accordance with the literature as high shear stress environments are known to cause greater lactate production and delayed lactate consumption phases.[150,171] Additionally, multi-impeller systems are known to have more efficient gas distribution, higher gas residence times, and increased gas hold-up.[155] However, in this case, shear stress on cells does not appear to be an issue as both 1- and 2-impeller configuration cell cultures are comparable.

4.5.3 Scale-up from 1-L to 10-L Bioreactor

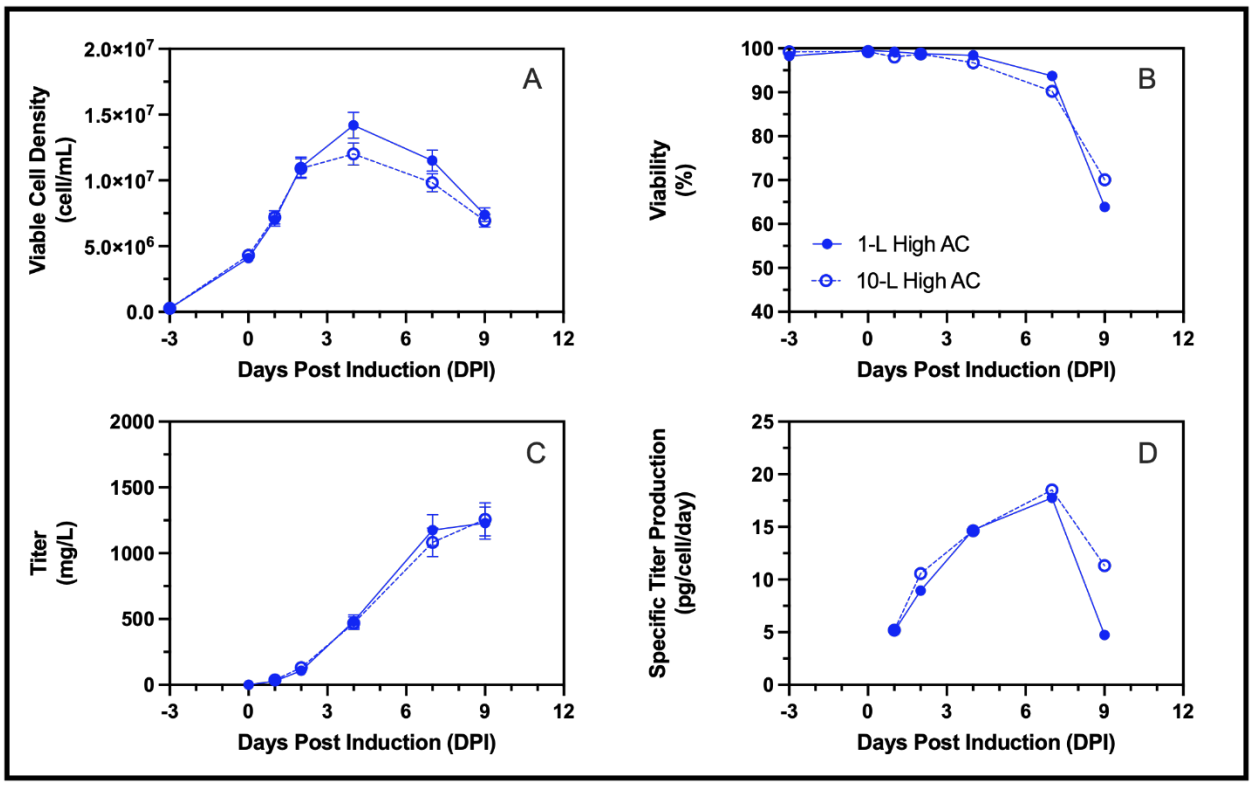

Figure 4.4 Scale-up of 1-L benchtop bioreactor to 10-L bioreactor using constant P/V and vvm as criterion and their measured A) viable cell density, B) cell viability, C) volumetric titer, and D) cell specific titer obtained in 1-L benchtop bioreactor with high AC aeration (-●-) and 10-L benchtop bioreactor with high AC aeration (-○-). Error bars represent measurement errors for viable cell density (A) and volumetric titers (C).

Although the 1-L mid AC aeration condition was observed as the optimal condition for volumetric productivity (Figure 4.3), the 1-L High AC cell culture was selected for process scale up to 10-L. This decision was based on the need for higher vvm typically required in large scale bioreactors to prevent CO_2 accumulation as well as physical gas flowrate limitations of the 10-L bioreactor. The 10-L bioreactor was equipped with thermal mass flow controllers (TMFCs) for both pure oxygen and air. However, the maximum oxygen flow capacity of the TMFC was insufficient to maintain dissolved oxygen (DO) levels at or above the set point when using an air cap vvm similar to the Mid AC condition in previous cultures performed by our research group (data not shown), necessitating the use of the High AC strategy. Scale-up from 1-L to 10-L was performed using a constant volumetric power input (P/V) as a primary scale-up criterion as this was shown to be the most reliable approach for small differences in operating vessel volumes.[141] Volume normalized

gas flow rate (vvm) was selected as a criterion for gas sparging. The combination of constant P/V and vvm across scales has been shown to result in comparable VCD, viability, and product titer between 3-L, 500-L, and 2000-L bioreactors.[58] The constant vvm allows for sufficient CO_2 stripping and oxygen transfer while the constant P/V ensures proper mixing. Due to maximum gas flowrate limitations in the 10-L system, the maximum vvm was increased from 0.006 to 0.015 to ensure DO setpoint levels could be maintained. This scale-up strategy led to comparable cell growth and viability (Figure 4.4A and B), volumetric and cell specific productivities (Figure 4.4C and D) between 1-L and 10-L productions.

4.5.4 Process Transfer to a Different Product

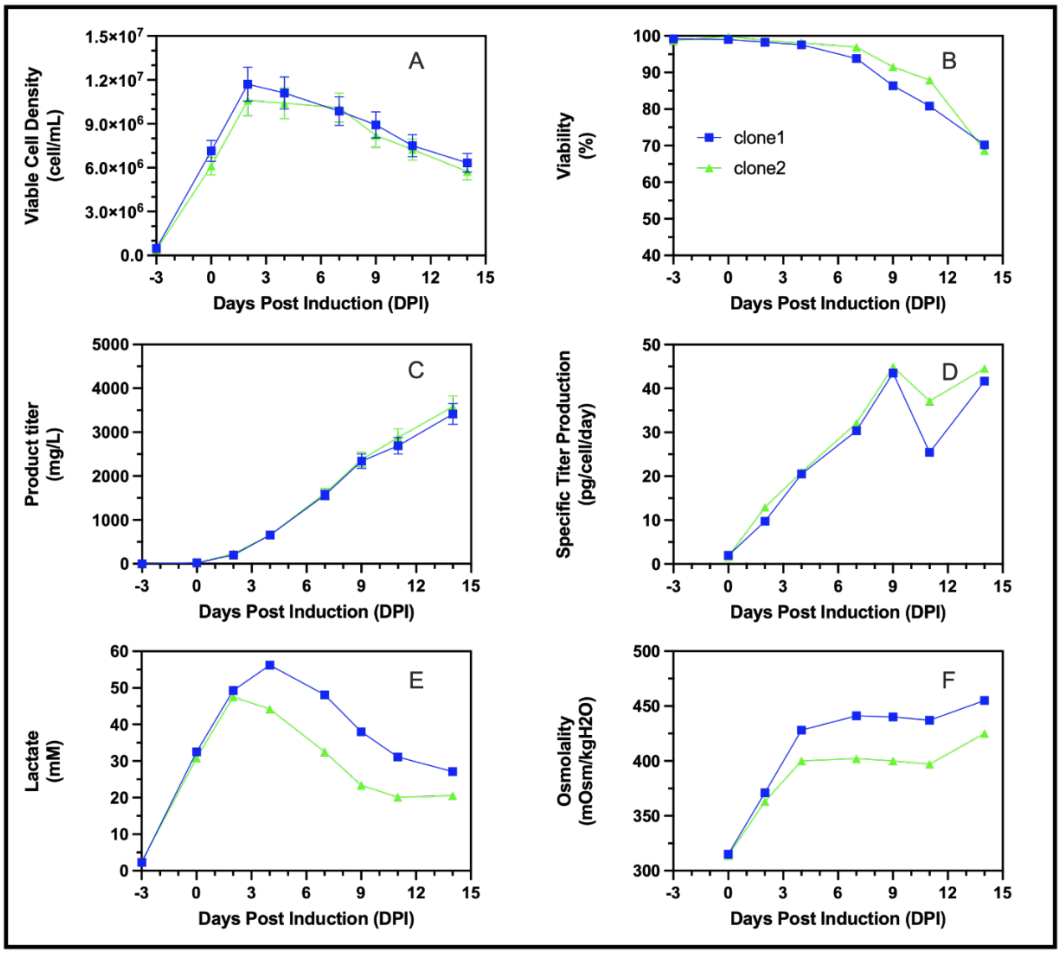

Figure 4.5 Benchtop 1-L bioreactor cell culture performance of clone 1 (-■-), and clone 2 (-▲-) for the production of Product B operating at mid AC with single impeller and LFS A) viable cell density, B) cell viability, C) volumetric titer, D) cell specific titer, E) lactate concentration, and F) osmolality. Error bars represent measurement errors for viable cell density (A) and volumetric titers (C).

The same culture strategy was assessed with two clones expressing another antibody (Product B) in benchtop bioreactors. Both clones were observed to achieve comparable VCD, viability, volumetric and cell specific product profiles (Figure 4.5A, B, C, D). However, in clone 2, the metabolic switch to lactate consumption occurs earlier (after 2 DPI) than in clone 1 (after 4 DPI) (Figure 4.5E). The production of lactate is associated with a reduction of pH as lactate is excreted from cells through a monocarboxylate transporter (MCT) which also excretes an H^+ ion as it is a co-transporter.[172] In pH controlled cell cultures, base is added when pH reaches the lower limits of the deadband. This addition of base in turn increases the osmolality of the culture media. This explains the greater osmolality observed with clone 1 when compared to clone 2 (Figure 4.5F). The switch in lactate metabolism from production to consumption is driven by many different factors such as low glucose levels or depletion, glutamine depletion, high lactate concentration, high H^+ concentration (low pH), and the transition of cell growth to the stationary phase.[173] Another viable explanation for the lactate metabolic switch is that it is controlled by redox balancing.[173] The sole source of lactate production is from the reduction of pyruvate catalyzed by lactate dehydrogenase (LDH). This conversion also oxidizes NADH to NAD^+. Thus, when NADH levels rise, such as during high glycolytic activity, rates of conversion of pyruvate to lactate increase. Meanwhile, it was shown that lactate excretion and consumption rates were solely determined by the concentration gradients of both lactate and H+ ions.[174] Although no difference in cell culture productivity was observed as a result of the difference in lactate and osmolality, clone 2 was deemed a better performer as high lactate and osmolality levels are typically associated with shorter culture duration and lower productivities. Thus, clone 2 was used for investigating the effect of hydrodynamic conditions on productivity in the following section.

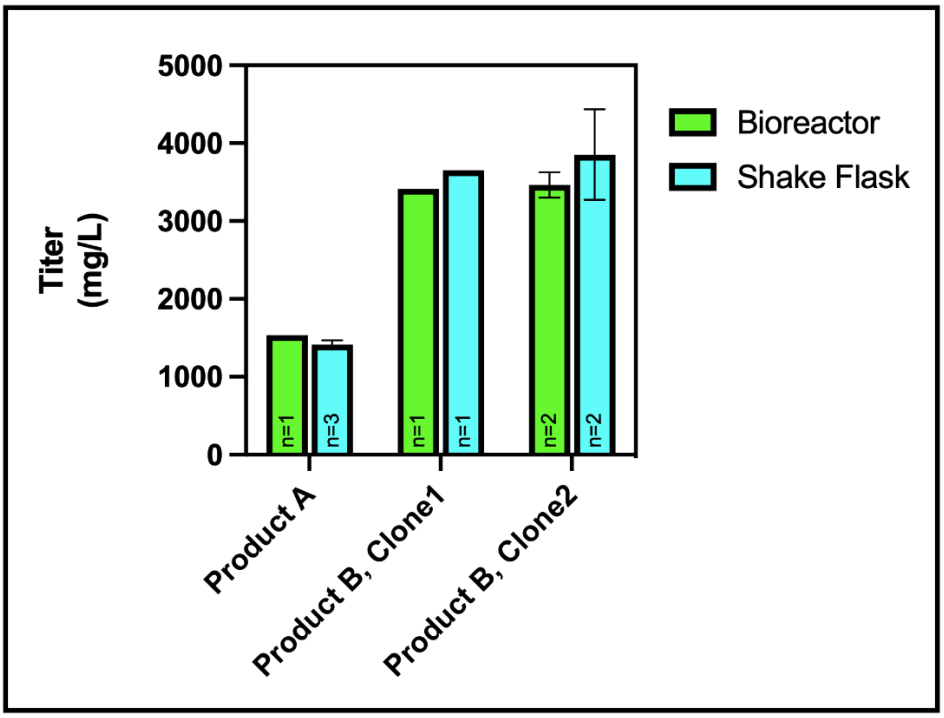

Figure 4.6 Comparison of final volumetric product titer of product A, product B from clone 1, and product B from clone 2 in 1-L bioreactor (green) and shake flask (blue). Error bars of replicates represent standard deviations.

It is worth mentioning that product A, product B clone 1 and clone 2 bioreactor cultures produced 90-109% of the external control shake flasks (125mL baffled flask, 200 RPM, 25 mm orbit) titer at 14 DPI (Figure 4.6) showing the linearity of scale-up. The consistent titers between the flask and bioreactor indicate that the process developed by optimizing feeding regimens, mixing, and gassing strategies is robust, and that comparable parameters are suitable across different mAb products and cell lines.

4.5.5 Effect of Culture Hydrodynamic Conditions on Productivity

In a fed-batch bioreactor, as the culture progresses, the working volume increases which changes variables such as the volumetric power input (P/V) and volumetric gas flowrate (vvm). The P/V is an important engineering parameter in bioreactor process design due to its implications for mixing and distribution of nutrients, gradients of pH, oxygen and carbon dioxide transfer, and shear stress considerations. As for vvm, we have shown in this study the importance of its optimization for improvements in cell longevity and productivity. To assess the impact of both P/V and vvm on cell

growth, viability, and productivity, the process previously developed with LFS, mid AC aeration, and 1-impeller to produce Product B in clone 2 was used as a standard process. However, maintaining P/V and vvm of AC constant throughout the cell culture, by adjusting mixing speed and gas flowrate at AC, has impacts on other crucial engineering variables such as the impeller tip speed, superficial gas velocity, and gas entrance velocity. To further remove the impact of these parameters, an additional culture was performed where the culture volume was kept constant by removing an amount of culture broth equal to the feed volume after each feeding.

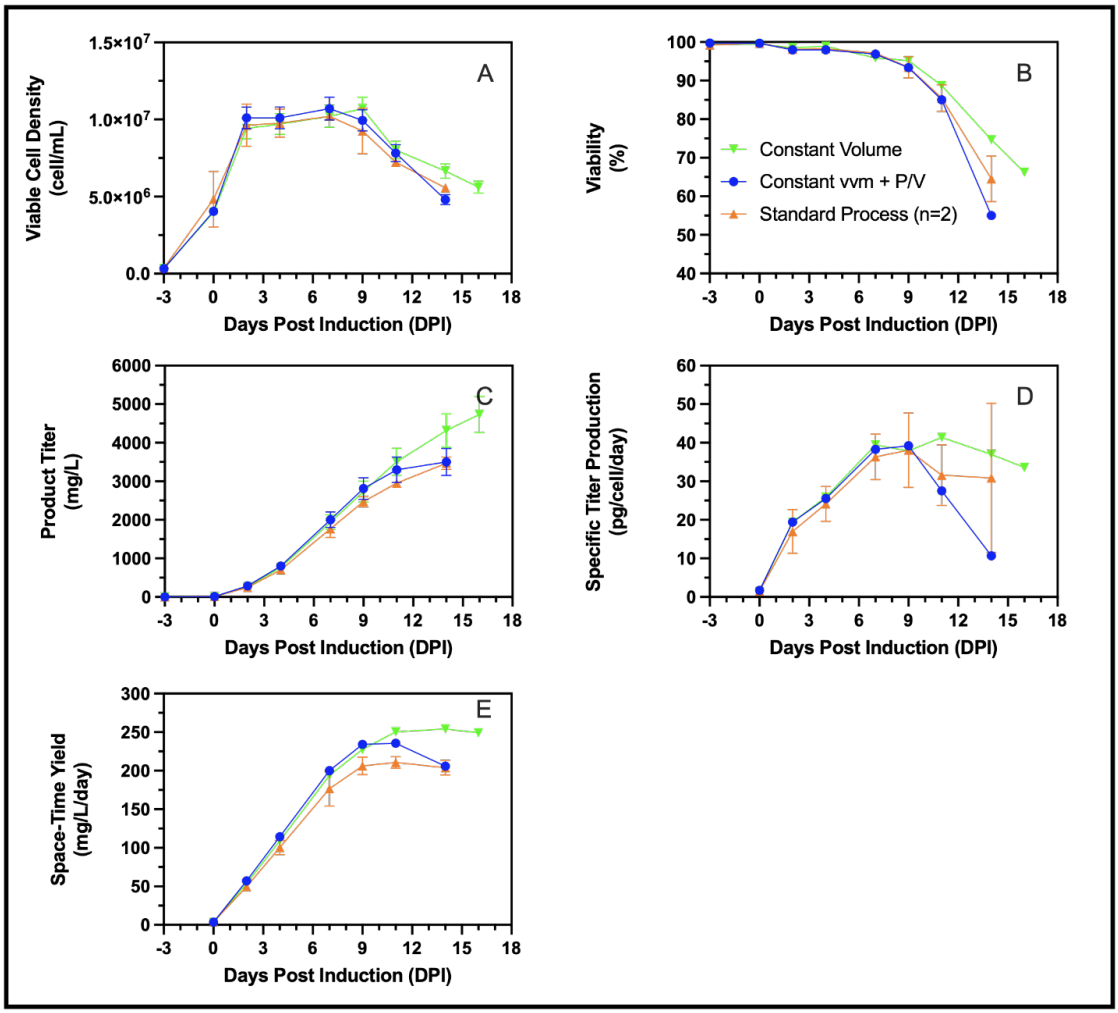

Figure 4.7 Effect of constant volumetric gas flowrate (vvm) at air cap, constant volumetric power input (P/V), and constant volume on A) viable cell density, B) cell viability, C) volumetric titer, D) cell specific titer, E) space-time yield; Constant volume cell cultures (-▼-), constant air cap vvm and P/V cell cultures (no volume adjustments) (-●-), and the standard process with middle AC, constant mixing speed, with variable volume from bolus feeding (-▲-). Error bars of duplicates represent standard deviation while error bar of single runs represent measurement errors for viable cell density (A) and volumetric titers (C).

Maintaining consistent hydrodynamic conditions, either by keeping the culture volume constant or by adjusting mixing speed and air cap flow rate to maintain a constant P/V and air cap volumetric gas flow rate (vvm) throughout cell culture, led to an improvement in space-time yield (STY) up to 11 days post-induction (DPI). This suggests that the uniformity of these engineering variables plays a crucial role in enhancing overall productivity. Furthermore, maintaining a constant culture volume helped sustain a high STY up to 16 DPI (Figure 4.7E). This is potentially because increasing P/V and vvm has impacts on shear stress applied to cells at the impeller tip and liquid surface respectively. Mixing times in small volume bioreactors are generally adequate in all situations when P/V is between 10-80 W/m^3. However, constant volumes allow for maintaining a lower mixing speed while keeping P/V constant. To maintain P/V constant in a fed-batch cell culture, the mixing speed of the impeller must be increased at each bolus feeding point. This will naturally increase the impeller tip speed thereby increasing the shear stress applied to cells. Increasing vvm will cause a higher total gas sparging rate potentially leading to increased cell damage over the course of the cell culture. The constant volume culture yielded a more favorable environment for cell growth and protein production, which underscores the importance of carefully balancing engineering parameters to optimize cell culture performance.

The volumetric power input and gas flowrates not only have an impact on shear stress applied to cells but also on gas transfer. The volumetric gas transfer coefficient, k_La, is used to express the rate of transfer from the gas to the liquid phase. In the case of bioreactors, the gas phase represents the sparged bubbles and the liquid phase is the bulk media. As shown in equation 4.11, k_La is a function of mixing (P/V) and aeration (v_s), where v_s is the superficial gas velocity and K, α, and β are empirically determined constants.[55]

$$k_L a = K \times \left(\frac{P}{V}\right)^{\alpha} \times {v_s}^{\beta} \qquad 4.11$$

In the three process operating conditions presented (Figure 4.7), cell cultures begin with the same volume, agitation rate, and gassing such that the gas transfer rates are the same. The k_La at the beginning of the culture, which was previously measured using the cell-free static gassing out method, was of $14h^{-1}$ (data not shown). In the case of the standard process, the culture volume increases with time due to feed additions, and the agitation speed stays constant over time. This decreased the P/V by 19% which reduced the k_La to $12h^{-1}$ by the end of the cell culture. However,

in the case of the constant P/V and vvm and the constant volume condition, the mixing and aeration rates are adjusted such that k_La is maintained constant throughout the cell culture. The same applies to the constant volume cell culture where mixing speed and gas flowrate at the air cap are fixed theoretically enabling a constant k_La. An unchanged P/V and vvm strategy shows an improvement in titer but requires an increase in agitation speed while a constant volume shows a further increase in titer without the requirement for an increase in mixing speed.

4.6 Conclusion

The objective of this study was to optimize CHO cell cultures in benchtop bioreactors for parameters that are particularly important during scale-up: aeration and mixing. Before aeration and mixing could be optimized, a feeding regimen needed to be selected. It was shown that cell cultures with a high bolus feeding regimen generating spikes in osmolality exhibited an early drop in cell viability. A lower feeding regimen enabled 25% more final volumetric titer concomitantly with a significantly improved cell growth. Different strategies could be employed to avoid the adverse effects of an increase in osmolality. Namely, adapting the clone to a high osmolality environment by gradually increasing the osmolality of the culture media, or similarly, feeding the same quantity continuously rather than in bolus.[150] The importance of optimizing aeration strategies was shown by utilizing different air caps with cascade aeration. As the air cap was increased, a larger total volume of gas was sparged throughout the cell culture. It is suspected that the low VCD and faster decline in cell viability associated with the higher air cap were due to the prolonged shear stress caused by higher gas sparge rates. To assess process scalability, the 1-L process was transferred to a 10-L vessel using a constant P/V and vvm strategy. A comparable cell culture performance, in terms of VCD, viability, and productivity, was observed. For scale-up across larger volumes, constant P/V and vvm have been shown to be successful, when the gas flow rate is sufficient to ensure efficient CO_2 stripping.[141] In cases where these parameters do not produce an environment with sufficient gas transfer rates, constant P/V could be paired with constant k_La at the air cap to ensure that DO is maintained at the setpoint. The optimized 1-L process was then transferred to two different cell lines expressing a different product. A linearity showing 90-109% of shake flask titer was obtained demonstrating the robustness of the developed process. Studying the effect of mixing and aeration on cell culture productivity revealed the delicate interplay between sufficient mixing, efficient gas transfer and the stress applied to cells.

4.7 Author Contributions

Lucas Lemire: Conceptualization; methodology; data curation; investigation; validation; writing – original draft. **Sebastian-Juan Reyes**: Formal analysis; writing – review and editing. **Yves Durocher**: Supervision; resources; formal analysis; writing – review and editing. **Robert Voyer** – Resources; writing – review and editing. **Olivier Henry** and **Phuong Lan Pham**: Supervision; formal analysis; validation; funding acquisition; writing – review and editing; resources; project administration.

4.8 Acknowledgements

This work was supported by the Natural Sciences and Engineering Research Council of Canada (stipend allocated to Lucas Lemire via the NSERC-CREATE PrEEmiuM program). We thank Louis Bisson for HPLC monoclonal antibody titer measurements and Brian Cass for the assistance in bioreactor operations.

4.9 Conflict of Interest Statement

The authors declare no conflicts of interest.

CHAPTER 5 ARTICLE 2: N-1 SEMI-CONTINUOUS TRANSIENT PERFUSION IN SHAKE FLASK FOR ULTRA-HIGH DENSITY SEEDING OF CHO CELL CULTURES IN BENCHTOP BIOREACTORS

5.1 Article Presentation

The article titled "N-1 Semi-Continuous Transient Perfusion in Shake Flask for Ultra-High Density Seeding of CHO Cell Cultures in Benchtop Bioreactors" was accepted for publication in *Biotechnology Progress* on March 20, 2025. This article covers objective 3 of this thesis by detailing the development of a semi-continuous transient perfusion method in shake flasks with the objective of seeding a benchtop bioreactor. The importance of daily, rather than intermittent, media exchange is emphasised and its effects on nutrient concentration are explained. Maximum oxygen transfer rates in shake flasks measured using the sulfite method are used to confirm that maximal cell densities allowable before oxygen limitations are achieved. Ultra-high density seeding with this seed train allowed for a 29.3% increase in space-time yield. For this article I have done conceptualization, methodology, data curation, investigation, validation, and writing – original draft.

Lucas Lemire[1,2], Sebastian-Juan Reyes[1,2], Yves Durocher[2], Robert Voyer[2], Olivier Henry[1*], Phuong Lan Pham[2*]

[1] Department of Chemical Engineering, Polytechnique Montreal, Montreal, QC H3T 1J4, Canada

[2] Human Health Therapeutics Research Centre, National Research Council Canada, 6100 Royalmount Avenue, Montréal, QC H4P 2R2, Canada

Correspondence:

Phuong Lan Pham: phuonglan.pham@nrc-cnrc.gc.ca

Olivier Henry: olivier.henry@polymtl.ca

5.2 Abstract

One strategy to enhance the production of biological therapeutics is using transient perfusion in the preculture (N-1 stage) to seed the production culture (N stage) at ultra-high cell densities (> $10x10^6$

viable cells/mL). This very high seeding density improves cell culture performance by shortening timeline and/or achieving higher final product concentrations. Typically, an N-1 seed train employs bioreactors with alternating tangential flow filtration (ATF) or tangential flow filtration (TFF) perfusion systems or Wave cell bag bioreactor with integrated filtration membrane, which have costs and technical complexity. Here, we propose an alternative method using semi-continuous transient perfusion through media exchange in shake flasks which is suitable for benchtop-scale intensification process development. Daily media exchange was necessary to prevent nutrient limitations. Observed limitation of maximum viable cell densities (VCD) in various flask sizes was demonstrated to be due to oxygen limitations through the measurements of maximum oxygen transfer rates (OTR) using the sulfite system. By increasing agitation frequency from 200 RPM to 300 RPM, maximum OTR in 500-mL shake flasks was increased by 62.3% allowing an increase in maximum VCD of 29.6%. However, in 1000-mL shake flasks, an increase in agitation speed resulted in an early cell death. After demonstrating that media exchange in shake flasks by centrifugation had no significant impact on cell growth rates, metabolism, and productivity, a benchtop bioreactor was seeded from semi-continuous transient perfusion cell expansion. The ultra-high cell density seeding resulted in a 49.3% increase in space-time-yield (STY) when compared to a standard low seeding density culture.

KEYWORDS: Preculture perfusion, cumate inducible system, oxygen transfer, ultra-high seeding density (UHSD), semi-continuous perfusion, pseudo-perfusion, CHO cell culture

5.3 Introduction

Biotherapeutics such as monoclonal antibodies (mAbs) are predominantly produced in large-scale fed-batch bioreactors with CHO cell expression systems. To supply the ever-growing demand of these products, three options are presented: process intensification, scale-out, and scale-up. Scaling-up of mammalian cell cultures can be non-trivial task which inherently includes risks associated to productivity and product quality.[141] As such, alternatives to increase production of biologics including scale-out and process intensification are gaining in popularity. Scale-out is generally more feasible than scale-up, as it is easier to add additional bioreactors than to increase the size of a single bioreactor and can be more cost-effective than scale-up in terms of capital costs. This makes it easier to increase production capacity as demand grows. Process intensification, which often comes in the form of achieving high cell densities, is another method of increasing

recombinant protein productivity. It has been shown that ultra-high seeding density (UHSD) at up to 20 x 10^6 cells/mL cell cultures to produce mAbs have enabled up to a 3-fold increase in final titer or 75%-132% increase in space-time-yield (STY) (Equation 5.1).[116-118,175-178] To seed bioreactors at these elevated cell densities, cells are commonly cultured in transient perfusion mode in the N-1 seed train vessel to satisfy the large number of cells needed.

$$STY = \frac{[Product]_{final}}{Time_{final}} \quad 5.1$$

Various perfusion systems are available which could be used for the N-1 cell expansion for UHSD cell cultures. Conventional perfusion methods utilize static, dynamic or tangential flow (TF) coupled with membrane-based (MB) filtration, or membrane-free (non-MB) dedicated cell retention systems. Static MB retention systems are typically used with rocking bioreactors such as the ReadyToProcess WAVE25 and its Cellbag (Cytiva) or Biostat RM 20 and its Flexsafe RM bag (Sartorius) which aid in reducing membrane fouling through dynamic mixing. Dynamic BM retention systems such as spin and rotating disk filters have lower fouling risks. However, the moving parts housed inside of the bioreactor increase contamination risks thus they are impractical to replace, and they are also not available in single-use formats.[179] To avoid fouling altogether, non-MB such as acoustic filtration, centrifuge, and gravitational settlers have been used.[180] However, these cell retention systems have downsides such as limited scalability of acoustic filters, cell damage, aggregation, and requirement of specialized bioreactor design for centrifugation, and long residence time in sub-optimal culture conditions for gravitational settlers. Due to these limitations, acoustic filters, which were the predominant non-MB cell retention method, have seldom been reported in literature since 2014.[180] TF MBs such as alternating tangential flow filtration (ATF) (Refine Technology, Repligen, and Artemis) and tangential flow filtration (TFF) which are driven by low-shear centrifugation magnetic pumps (Levitronix) have the advantage of being kept outside of the bioreactor allowing modularity and scalability of cell retention. For these reasons, ATF and TFF perfusion systems are the most used cell retainer devices for N-1 perfusion for UHSD cell cultures.[180-182]

Scale-down models of perfusion systems are necessary due to the high operating costs of benchtop bioreactor perfusion equipment and the need to optimize cell specific perfusion rates (CSPR), perfusion rate (vessel volume per day, VVD), feed and media composition, and cell line stability

and scalability. These scale-down models are typically done through semi-continuous transient perfusion in non-instrumented shake tubes, shake flasks, and standard and deep multi-well plates. In 50-mL shake tubes with fill volumes of 10-15 mL, a maximum viable cell density of 30-70x10^6 cells/mL was observed.[183-186] In 125-mL baffled shake flasks with 25 mL (20%, volume/volume) fill volume, a maximum viable cell density of 45x10^6 cells/mL was observed with optimized feed composition.[187] Cell densities of up to 95 x10^6 cells/mL were achieved with transient semi-continuous perfusion in 24 deep-well plates (DWP) at working volumes of 3 mL.[188]

The impact of fill volume (5, 10, 30 mL) in 50-mL shake tubes was explored and it was found that larger fill volumes resulted in lower cell growth. These growth limitations are due to oxygen transfer limitations.[183] Similarly, these oxygen limitations are expected to be observed in shake flasks. The maximum oxygen transfer rate (OTR) achievable in shake flask depends on agitation rate, fill volume, shaking orbit diameter, flask diameter, and osmolarity levels.[189] Increasing shake flask sizes, at the same proportional fill volume, will result in lower OTR_{max} due to volume increasing faster than flask diameter. Additionally, OTR may be an indicator of the late phase exponential growth,[190] metabolic activity,[191,192] and cell concentration.[193,194] These metrics are of importance as bioreactors should be seeded from cells in exponential growth with high cellular metabolic activity. High cell concentration is needed in the N-1 culture to seed the production culture (N stage). The Transfer-Rate Online Monitoring (TOM, Kuhner Inc.) device has been shown to be useful at non-invasively monitoring oxygen uptake rates (OUR) and carbon transfer rate (CTR) in shake flasks in order to determine critical differences in cell line behavior.[195] Another factor which may impact oxygen transfer in shake flasks is the material of construction. The hydrophilicity of the material affects the formation of the thin liquid film formation during agitation. A hydrophilic material, such as glass, will form a thin layer of liquid on the surface allowing for gas transfer while wetting of a hydrophobic material, such as plastic, will not be as efficient.[196] However, in mammalian cell cultures, such as those performed in this study, single-use sterile shake flasks are predominantly used to minimize risk of contamination.

In this article, we present a simple but efficient method of performing semi-continuous transient perfusion (transient pseudo-perfusion) in shake flask with the objective of seeding a benchtop bioreactor for UHSD CHO cell culture production of recombinant protein. This method was developed with a cumate-inducible CHO-GS clonal cell line which truly allows for a two-phase

cell culture.[25] Using the inducible system alleviates the metabolic burden imposed on cells by protein production in cell growth phase, thus allowing for faster growth rate and higher achievable viable cell densities.[197,198] In the present study, we have also demonstrated, through oxygen transfer rate (OTR) measurements, that the highest viable CHO cell density was achieved in shake flask before oxygen transfer limitations are attained.

5.4 Materials And Methods

5.4.1 Cell Culture Maintenance

A proprietary stable clone of CHO-GS cells, inducible through a cumate gene switch and capable of producing the monoclonal antibody palivizumab (PLVZM), was utilized. This cell line was internally developed, as previously detailed.[25] Cells were cryopreserved in BalanCD CHO Growth A media (Fujifilm Irvine Scientific, USA) with 50 µM MSX and 0.1% (w/v) Kolliphor P118 (BASF, Germany) supplemented with 7.5% dimethylsulfoxide (DMSO) (Sigma Aldrich, ≥99.7% purity, USA) and stored in liquid nitrogen tanks (MVE, Series 800-190, USA) at -180°C. For thawing, cell vials were immersed in a 37°C water bath a few minutes until completely thawed. Cells were expanded in shake flasks in 5% CO_2 incubators set to 37°C, 75% relative humidity, and 120 RPM agitation with a 25-mm orbit. Cells were passaged every 2-3 days in growth medium consisted of BalanCD CHO Growth A and 50 µM MSX with cell density maintained between 0.2 and 3.0x10^6cells/mL.

5.4.2 Semi-Continuous Transient Perfusion

The semi-continuous transient perfusion cell cultures were initiated by seeding polycarbonate shake flasks (Corning, Product Numbers 431143, 431144, 431145, and 431147, USA) ranging from 125 to 1000-mL at 0.2-0.4x10^6 cells/mL. All used shake flasks are unbaffled unless otherwise specified. Flasks were agitated in a 5% CO_2 incubator at 37°C, 75% relative humidity, 120-300 RPM agitation with a 25-mm orbit, with a working volume of 20% (v/v) of the flask maximum total volume. Once cell densities reached 1.5-2.5x10^6 cells/mL, full media exchange was done by centrifugation in conical tubes at 300xg for 5 minutes. Samples of cell suspension taken before centrifugation were used for cell counts and key metabolites (glucose, lactate, and ammonia) measurements. The cell pellets were disrupted by gentle taping the tube and resuspended in BalanCD CHO Growth A media supplemented with a pre-defined % (v/v) of 0.8X BalanCD CHO

Feed4 (Fujifilm Irvine Scientific, USA). Medium is supplemented with 0.8X BalanCD CHO Feed4 to avoid nutrient depletion given the high cell densities achieved. Cell cultures were then placed back in incubator conditions until the next sampling and media exchange. Cell cultures were ended when important drops in cell viability were observed to avoid seeding production bioreactors from cells with declining viability below 90%.

5.4.3 Bioreactor Cell Culture

Both cell culture modes, standard seeding density (SSD) and ultra-high seeding density (UHSD), were performed in 1-L BioFlo120 (Eppendorf, Germany) under fed-batch mode with an initial volume of 650 mL. Cells were cultivated in BalanCD CHO Growth A (Fujifilm Irvine Scientific, USA) supplemented with 50 µM MSX, 0.1% (w/v) Kolliphor P118 (BASF, Germany) and fed with 0.8X BalanCD CHO Feed4 (Fujifilm Irvine Scientific, USA) according to an in-house developed bolus feed schedule every 2-3 days based on platform work to optimize for cell growth and productivity. The culture pH was controlled at 7.0 ± 0.2 through carbon dioxide (CO_2) sparging and addition of an in-house 9% (w/v) sodium hydroxide and 9% (w/v) bicarbonate base solution. Cultures are agitated using a 3-blade 45° elephant ear impeller with a 5.8 cm diameter at an estimated volumetric power input (P/V) of 35 W/m^3. The latter relates to volume, agitation speed, impeller dimeter, and impeller number.[141] Dissolved oxygen levels (DO) were controlled through 25 mL/min surface air gassing and a cascade of air and oxygen sparging. Cascade aeration first uses air on-demand to control DO at the desired setpoint until reaching a maximum air flowrate of 2 mL/min after which the air flowrate is supplemented with pure oxygen as needed. At 0 days post induction (DPI), cell cultures were induced with 2 µg/mL of cumate (4-Isopropylbenzoic acid, Ark Pharm Inc, USA). Cell cultures were terminated when measured cell viability reached below 70%.

The SSD cell cultures were seeded at 0.4x10^6 cells/mL at -3 DPI (three days prior to induction day). Temperature was maintained at 37°C until 2 DPI after which temperature was down-shifted to 32°C to the end of the culture. Temperature shift was done because of its positive impact on protein production and culture longevity.[199] The DO was maintained at 60% of air saturation. The UHSD cell cultures were seeded at 15x10^6 cells/mL at 0 DPI. The induction was performed at the time of cell seeding thus eliminating the growth phase in the bioreactors. The temperature was maintained at 32°C throughout the culture. The DO was maintained at 40% of air saturation.

5.4.4 Gas Transfer Rates and Shear Stress Estimations in Shake Flasks

The OTR of cell cultures in shake flasks were measured with the Transfer-rate Online Monitoring (TOM) system (Kuhner Inc., Switzerland). The cell culture conditions during OTR measurement are those described in semi-continuous transient perfusion methods. The flask headspace aeration flowrate was set to 16 mL/min and OTR measurements were performed over 105 minutes with 35 minutes of measuring time and 6 minutes of high flow flushing out time.[200] During the remaining 64 minutes of the cycle, the system operates under surface aeration mode which aims to mimic aeration conditions of shake flasks in an incubator with 5% CO_2 and 75% relative humidity at 37°C. The maximum OTR of the shake flask was measured using the sulfite system.[201] A 0.35 M sodium sulfite solution (≥ 99%; Sigma, USA) in 0.012 M phosphate buffer prepared with deionized water adjusted to pH 8 was used (Na_2HPO_4 ≥ 99% purity; NaH_2PO_4 ≥ 99% purity; Sigma, USA). The reaction was catalyzed by 10^{-7} M cobalt sulfate (≥ 99% purity; Sigma, USA). The maximum OTR with the sulfite system (cell-free system) was conducted in the same flask sizes, fill volumes, and incubating conditions as the cell cultures they replicate.

The average energy dissipation rate ($\varepsilon_{\emptyset}$) can be calculated (Equation 5.2) from agitation rate (n), flask diameter (d), liquid volume (V_L), and the modified Newton number (Ne') as seen in Equation 5.3.[171] The modified Newton number is estimated in unbaffled shake flasks using Reynold's number (Equation 5.3).[202] The Reynold's number can be calculated from Equation 5.4 including the liquid density (ρ), the agitation rate (n), the flask diameter (d), and dynamic fluid viscosity (η).[171] In unbaffled shake flask, the maximum energy dissipation rate (ε_{max}) is equal to the average energy dissipation rate for Reynolds numbers below 60000 and can be calculated from Equation 5.5 for Reynolds numbers above 60000.[29] From ε_{max} and the kinematic viscosity (ν), the Kolmogorov length (λ_K) can be calculated (Equation 5.6).

$$\varepsilon_{\emptyset} = Ne' \times \frac{n^3 \times d^4}{V_L^{2/3}} \quad 5.2$$

$$Ne' = 70Re^{-1} + 25Re^{-0.6} + 1.5Re^{-0.2} \quad 5.3$$

$$Re = \frac{\rho \times n \times d^2}{\eta} \quad 5.4$$

$$\varepsilon_{max} = \frac{0.1(\pi \times n \times d)^3}{1.11 \times d_0^{0.18} \times d^{-0.11} \times n^{0.44} \times V_L^{0.34}} \quad 5.5$$

$$\lambda_K = \sqrt[4]{\frac{\nu^3}{\varepsilon_{max}}} \quad 5.6$$

5.4.5 Sample Handling

Cell counts and viability measurements were done by means of trypan blue exclusion staining using a Cedex MS20C Automated Cell Counter (Innovatis, Germany). Sample supernatants obtained by centrifugation at 5000xg for 5 minutes were used for glucose, lactate, ammonia, monoclonal antibody (mAb), and amino acid concentration measurements. Glucose, lactate, and ammonia concentrations were measured by colorimetric assays using Vitros350 (Ortho-Clinical Diagnostics, USA). Amino acid measurements were done following the AccQ-Tag Ultra Derivatization Kit (Waters Corporation, USA) protocol using the Acquity H-Class UPLC system (Waters Corporation, USA). The mAb titer determination was done by Protein A HPLC. The sample supernatants were filtered in MultiScreen HV 96-well filtration plates at 1500 x g for 2 minutes (Durapore®, 0.45 µm, Millipore, USA) to remove cellular debris. The HPLC was performed using a 2695/2996 HPLC system (WATERS Corporation, USA) with a protein A cartridge (POROS® A20 column, 2.1 mm D x 30 mm H, Thermo Fisher Scientific, Part# 2-1001-00). A phosphate buffer saline solution without calcium and magnesium (Cat. No. SH30028.03, Cytiva, USA) is injected into the column before loading the samples at 2 mL/min. The column was washed with 1 mL, 10 column volumes, to remove unbound species and cell culture media components. A 0.15M NaCl elution buffer at pH 2.0 was used for 1 minute to detach the antibodies from the column. The mAb product was detected by UV at 280nm with a typical error below 10%.

5.5 Results and Discussion

5.5.1 Time-of-Action Study

A time-of-action study was performed to determine a suitable timing for the first media exchange of semi-continuous transient perfusion in shake flasks. A batch cell culture was performed in a 250-mL baffled shake flask (Corning, USA) at a working volume of 50 mL and an initial viable cell density of 0.2 x 10^6 cells/mL. The viable cell density (VCD), cell viability, and cell doubling time were monitored daily to identify at which cell density either the cell viability begins to drop

or doubling times increase indicating the culture is no longer in exponential growth (Figure 5.1). Historical cell doubling times during exponential growth for this cell line were on average 18.6 ± 2.0hr (n=46). A VCD of 3.31 x 10^6 cells/mL was selected as the maximum density at which media exchange will be initiated. A doubling time of 21.09hr was observed which falls within 2 standard deviations of the historical mean. As such, going forward, media exchange was started at VCD of 1.5-2.5 x 10^6 cells/mL to ensure media exchange is begun before cells enter late exponential and plateau phase of cell growth. The cell density of 3.31 x 10^6 cells/mL being at the end of the exponential growth phase is in line with observations from literature where batch CHO cells cultures in shake flasks typically reach the late exponential phase by 4-6 x 10^6 cells/mL.[167,203-206]

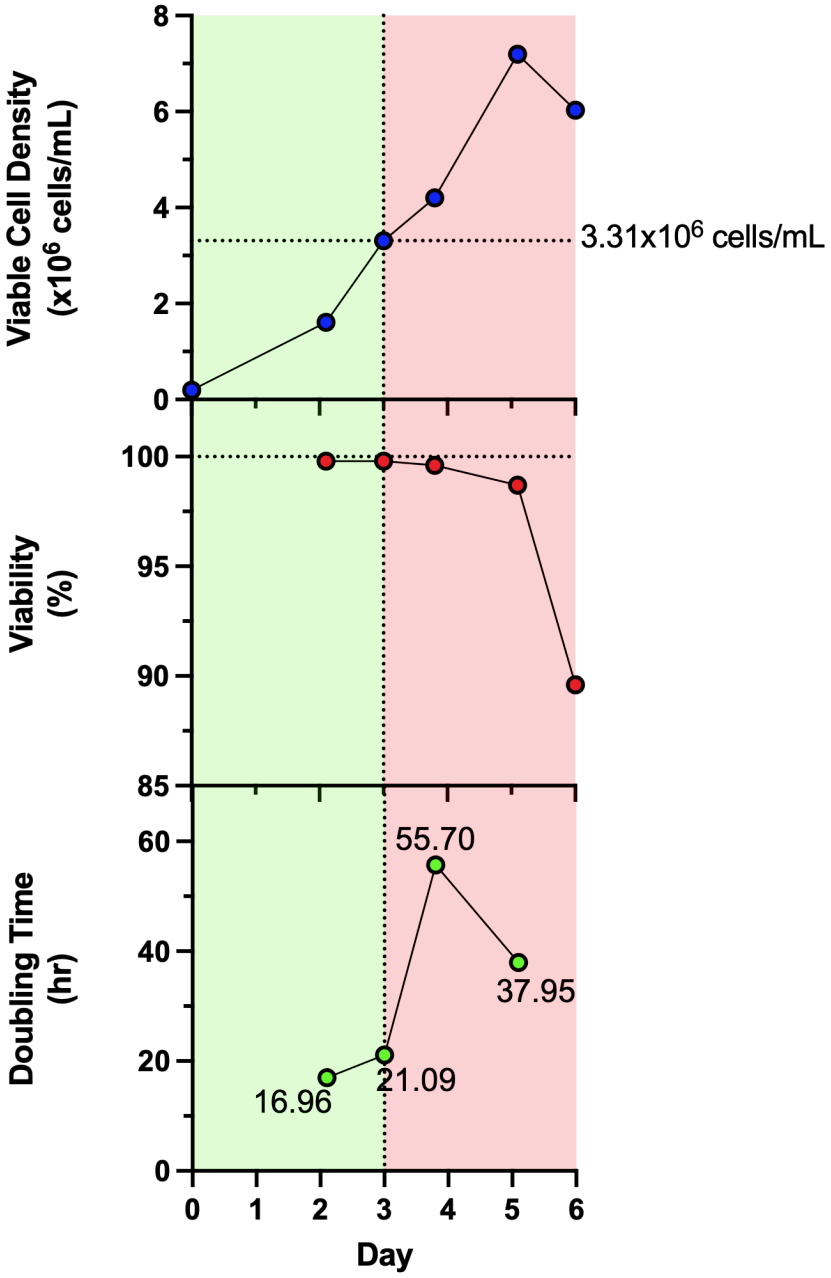

Figure 5.1 Time-of-action study for determination of beginning of media replacement for semi-continuous transient perfusion in shake flasks. Viable cell density (blue), cell viability (red), and cell doubling time (green) of a 50 mL batch cell culture in 250-mL shake flasks. Green area represents cell densities at which viability is maintained at >98% and when cells are under exponential growth as shown by the corresponding doubling times.

5.5.2 Effect of Media Exchange Frequency

During cell expansion, cell cultures passages were performed every 2-3 days to ensure cells are kept in the exponential growth phase. The first media exchange experiment in shake flasks simply replaced cell dilution with media exchange. In this case, cell dilution and media exchange serve the same purpose: removal of metabolic waste such as lactate and ammonia and replenishment of nutrients such as glucose, key amino acids, and other substrates. The 125-mL unbaffled shake flask was first used to test the effect of intermittent media exchanges (IME) (performed on days 0, 2, 4, and 7) starting at a VCD of 1.5-2.5x10^6 cells/mL (Figure 5.2A and B). From day 0 to 4, cell viability is maintained a >98% value and a VCD of 20.3x10^6 cells/mL is achieved which represents a doubling time of 30.66 hrs. This prolongment in doubling time due to cell biomass accumulation is expected and has previously been observed and modeled for perfusion cultures.[116,207] On day 7, cell growth rate had strongly decreased with a doubling time of 47.88 hrs and cell viability had decreased to 80.4%. This drop in cell viability can be explained by glucose depletion at day 7. Specific glucose consumption rate of this cell line during cell growth phase is ~1pmol/cell/day. With this consumption rate and an estimated VCD at day 7, a glucose concentration of ~80mM is required. However, high glucose concentrations (>55mM) have been reported to decrease cell growth rate.[208] To solve this issue and maintain glucose concentrations low without depletion, media exchange was done daily (DME) in 125-mL unbaffled shake flask beginning media exchange on day 0 at a cell concentration of 1.5-2.5x10^6 cells/mL (Figure 5.2A and B). With daily media exchange (DME), glucose concentrations were successfully maintained between 6mM and 45mM, cell viability was shown high at >98%, and a peak VCD of 65.5 ± 7.2x10^6 cells/mL (n=2) was achieved on day 7 at a doubling time of 30.1 ± 1.2 hrs (n=2). Although no cell growth is observed between day 7 and 8, no significant loss of viability was detected.

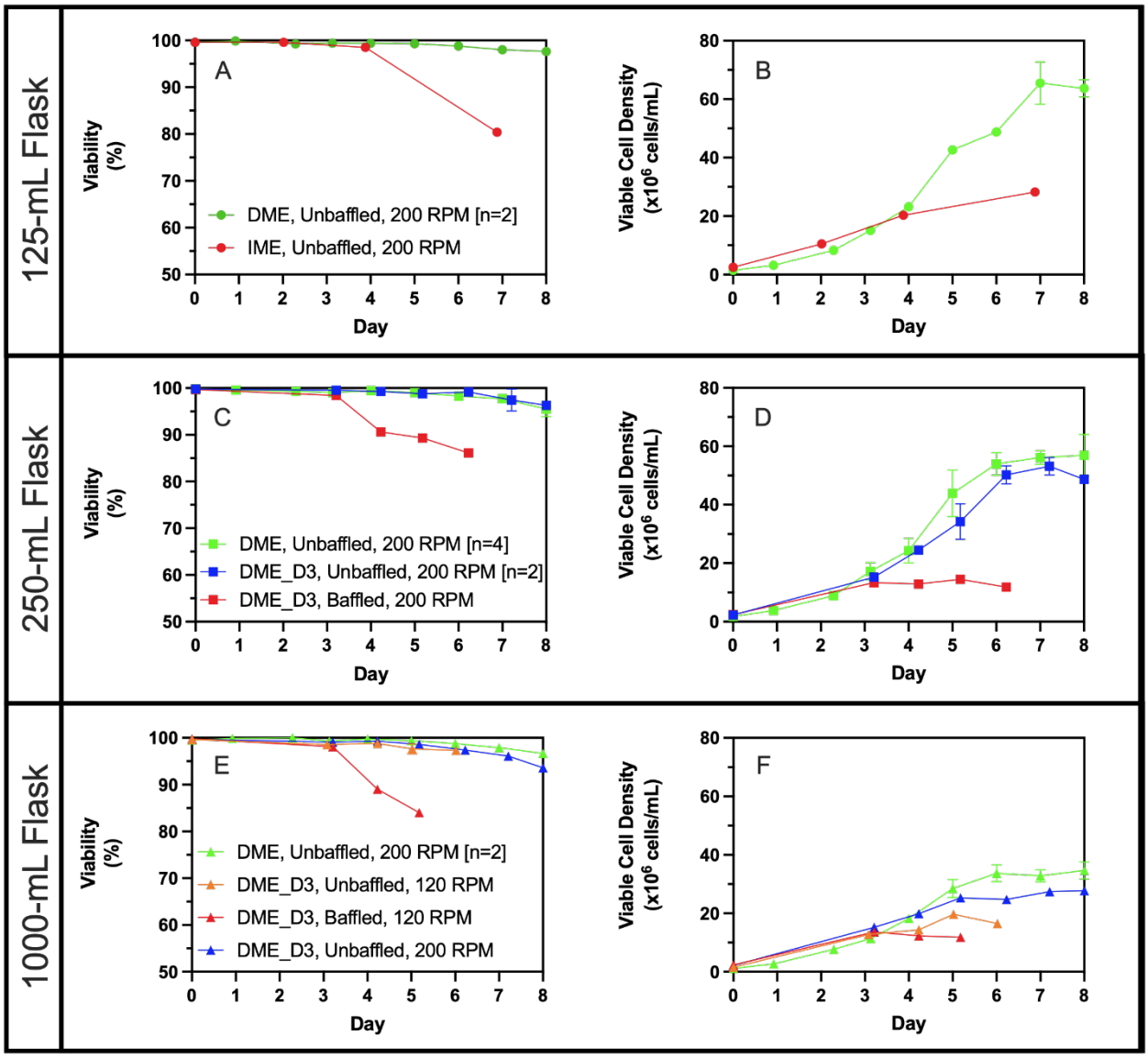

Figure 5.2 Effect of Media Exchange Frequency performed in shake flasks. A) Viable cell density and B) cell viability of daily media exchange (DME, -●-) and cell passages replaced by media exchange (IME, -●-) in unbaffled 125-mL shake flasks; C) Viable cell density and D) cell viability of daily media exchange in unbaffled flasks (DME, -■-), daily media exchange beginning at day 3 in unbaffled flasks (DME_D3, -■-), and daily media exchange beginning at day 3 in baffled flasks (DME_D3, -■-) for 250-mL shake flasks; E) Viable cell density and F) cell viability of daily media exchange in unbaffled flasks agitated at 200 RPM (DME, -▲-), daily media exchange beginning at day 3 in unbaffled flasks agitated at 200 RPM (DME_D3, -▲-), daily media exchange beginning at day 3 in unbaffled flasks agitated at 120 RPM (DME_D3, -▲-), and daily media exchange beginning at day 3 in baffled flasks agitated at 120 RPM (DME_D3, -▲-) for 1000-mL shake flasks. DME refers to daily media exchange; IME refers to the intermittent media exchange of cell passages replaced by media exchange; DME_D3 refers to media exchange at day 0 and daily media exchange beginning on day 3. Error bars of duplicates represent minimum and maximum values while error bars of quadruplicates represent standard deviation of replicates.

The semi-continuous transient perfusion cell expansion process with daily media exchange (DME) was performed in 250-mL shake flasks (Figure 5.2C and D) and in 1000-mL shake flasks (Figure 5.2E and F). Maximum cell concentrations of 56.1 ± 7.1x10^6 cells/mL (n=4) at day 7 and 33.7 ± 2.9x10^6 cells/mL (n=2) at day 6 respectively were achieved with >98% cell viability. As OTR in shake flasks is a function of flask size,[189] the reduced maximum VCD in larger flasks was suspected to be due to oxygen transfer limitations (as confirmed further in this study). Unbaffled shake flasks were thus switched for baffled flasks which are known to increase OTR.[209] Initially, to reduce media consumption of the process, media exchange was not performed on day 1 and 2 when VCD is low enough such that glucose would not be depleted in this time frame as seen in the 125-mL shake flask cultures. However, these conditions resulted in early cell death after day 3 in both 250-mL and 1000-mL baffled flasks (Figure 5.2C, D, E, and F). As a result of early cell death in baffled flasks, maximum VCD was significantly lower than in daily media exchanged unbaffled flasks. Premature cell decline observed in baffled shake flask cultures without media exchange on day 1 and 2 was attributed to shear stress rather than nutrient limitation. This conclusion was supported by experiments using unbaffled flasks without media exchange on days 1 and 2, conducted in 250-mL shake flasks (Figure 5.2C and D) and 1000-mL shake flasks (Figure 5.2E and F). This is consistent with literature where cell death was observed in baffled shake flasks after prolonged exposure to a higher shear stress environment.[210] Maximum cell concentrations of 53.2 ± 3.0x10^6 cells/mL (n=2) and 27.4x10^6 cells/mL respectively at day 7 were achieved with >93% cell viability. To further demonstrate the impact of oxygen limitations, media exchange cell culture was performed in 1000-mL flasks agitated at a lower orbital agitation rate of 120 RPM (Figure 5.2E and F). Although cell viability was maintained at >98%, a maximum VCD of only 19.7x10^6 cells/mL was achieved on day 5. This observation is in line with expected oxygen transfer limitations.

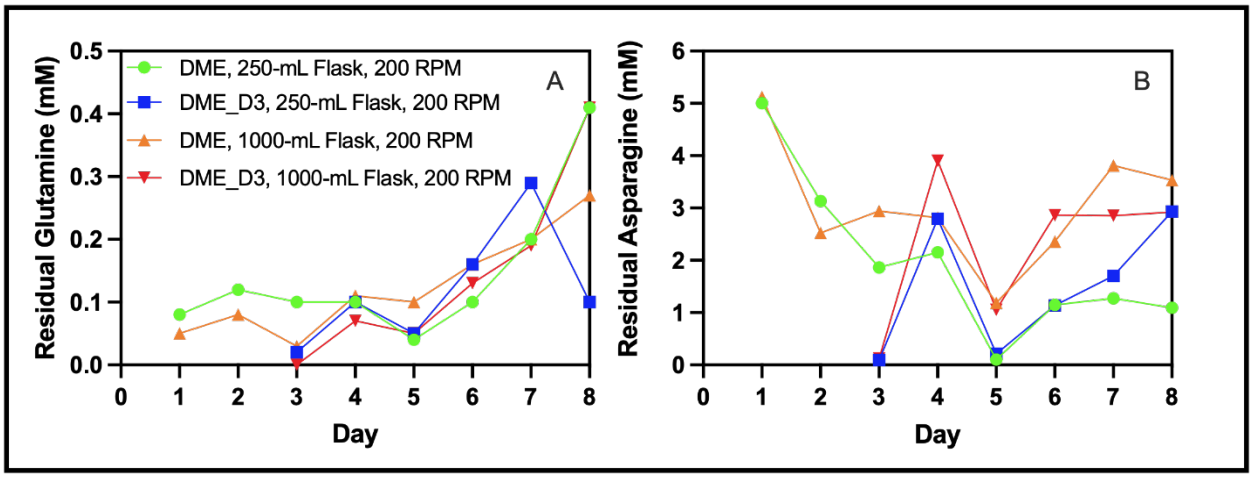

Figure 5.3 L-Glutamine and L-Asparagine kinetic profile in 250- and 1000-mL shake flask. A) Residual glutamine and B) residual asparagine of semi-continuous transient perfusion cell cultures with daily media exchange (DME) in 250-mL flasks (-●-) and 1000-mL flasks (-▲-) and daily media exchange with day 1 and 2 omitted (DME_D3) in 250-mL flasks (-■-) and 1000-mL flasks (-▼-).

From the 20 protein-forming amino acids measured, only asparagine (Asn) and glutamine (Gln) were observed to be depleted during semi-continuous transient perfusion in shake flasks with media exchange (Supplemental Figure B.3). In both daily media exchange (DME) and daily media exchange with day 1 and 2 omitted (DME_D3) performed in 250-mL and 1000-mL shake flasks, glutamine levels remain low throughout cell culture showing slightly higher levels towards the end of the culture (Figure 5.3A). Low glutamine levels are typical for CHO-GS cells which can synthesize glutamine from glutamate and ammonia due to the expression of glutamate synthetase enzyme. It is worth mentioning the low endogenous GS expression in CHO cells in general. Consequently, no additional glutamine supplementation was performed in the media and feed formulated for CHO-GS cells, as previously described.[25] This small quantity of glutamine produced is rapidly consumed by the cells leading to a low residual level detected transiently in the cell culture. Moreover, the frequent media exchange also prevents its accumulation. Asparagine has been observed to be depleted on day 3 in both 250-mL and 1000-mL shake flasks when media exchange is omitted on days 1 and 2 (Figure 5.3B). Both glutamine and asparagine, which can be used interchangeably by cells, are particularly important during early exponential cell growth phase for their contribution of carbon and nitrogen sources into the TCA cycle.[211] Asparagine, which enters the TCA cycle through its conversion to aspartate by asparaginase then converted to oxaloacetate catalysed by glutamic-oxaloacetic transaminase 1,[212] contributing to the total carbon

flux to the TCA cycle.[213] Although glutamine and asparagine can be used interchangeably as nutrient sources for the TCA cycle, in the DME_D3 semi-continuous transient perfusion cell culture, both of these amino acids are rapidly depleted on day 3 as no nutrients are supplied on days 1 and 2. Furthermore, asparagine was shown to be crucial in CHO-GS cell growth and its lack could result in cell growth arrest.[214] Growth arrest of asparagine depleted DME_D3 cell cultures can also be confirmed by the slower rate of increase in OTR, which is expected to be proportional to VCD, before day 3 and then restored after media exchange of day 3 (Supplemental Figure B.4).[200] Asparagine depletion is also observed in 250-mL flasks for both DME and DME_D3 media exchange schedules due to elevated cell concentrations. However, glutamine, which can be used concomitantly with asparagine, is not completely depleted on day 5.

5.5.3 Effect of Flask Size on Semi-Continuous Transient Perfusion

The impact of flask size on maximum VCD and oxygen transfer limitations was evaluated using 125-mL, 250-mL, 500-mL, and 1000-mL shake flasks, each at 20% of maximum nominal volume (Figure 5.4). The OTR was monitored throughout the semi-continuous transient perfusion cultures using the TOM system. To maximize VCD, cultures were agitated at 200 RPM in unbaffled flasks with daily media exchange starting from day 0, based on previous frequency of media exchange optimization studies. Cell viability is maintained at >98% for all flask sizes while in exponential cell growth (Figure 5.4). The observed maximum VCD and OTR are inversely proportional to the flask size (Table 5.1). The maximum VCD is proportional to the maximum OTR indicating that the specific respiration rate of the cells at the maximum cell density achieved in each flask is the same at 2.8 ± 0.2 pmol/cell/day. This specific respiration rate value falls within the expected range of 1-10 pmol/cell/day for CHO cells.[195,215] The observed OTR curve throughout cell culture follows the expected tendency for oxygen limiting cell cultures where OTR increases during cell growth until reaching a plateau and maintaining this plateau for some time.[216]

Table 5.1 Maximum observed viable cell densities and oxygen transfer rates of semi-continuous transient perfusion cell cultures with daily media exchange in 125-mL, 250-mL, 500-mL, and 1000-mL shake flasks at a fill volume of 20% and an agitation rate of 200 RPM.

Flask size	**Maximum Observed Viable Cell Density (x10^6 cells/mL)**	**Maximum Observed Oxygen Transfer Rate (mmol/L/h)**
125-mL	65.5 ± 7.2 (n=2)	8.04
250-mL	56.1 ± 7.1 (n=4)	7.04
500-mL	46.7 ± 3.9 (n=4)	4.99
1000-mL	33.7 ± 2.9 (n=2)	3.91

Equation 5.7 allows estimation of maximum OTR in shake flasks as a function of osmolarity (Osmol), agitation rate (n), operating volume (V_L), flask diameter (d), orbital shaking diameter (d_0), operating pressure (p_R), and oxygen molar fraction (y_{O2}).[189] Although this equation has an outstandingly small error of ±5 mmol/L/h for bacterial cell cultures, it does not allow to determine if the observed maximum OTR is due to oxygen transfer limitations in the present mammalian cell cultures. This correlation was created for use with bacteria which have much higher oxygen consumption rate than mammalian cells. Since the measured maximum OTRs of this study fall in the lower portion (4-8 mmol/L/h) of the range of applicability of this correlation (0-80 mmol/L/h), the error makes it impossible to determine if different flask sizes theoretically result in significantly different maximum OTRs.

$$OTR_{max} = 3.72 \times 10^{-7} \times Osmol^{0.05} \times n^{\left(1.18-\frac{Osmol}{10.1}\right)} \times V_L^{-0.74} \times d_0^{0.33} \times d^{1.88} \times p_R \times y_{O2} \quad 5.7$$

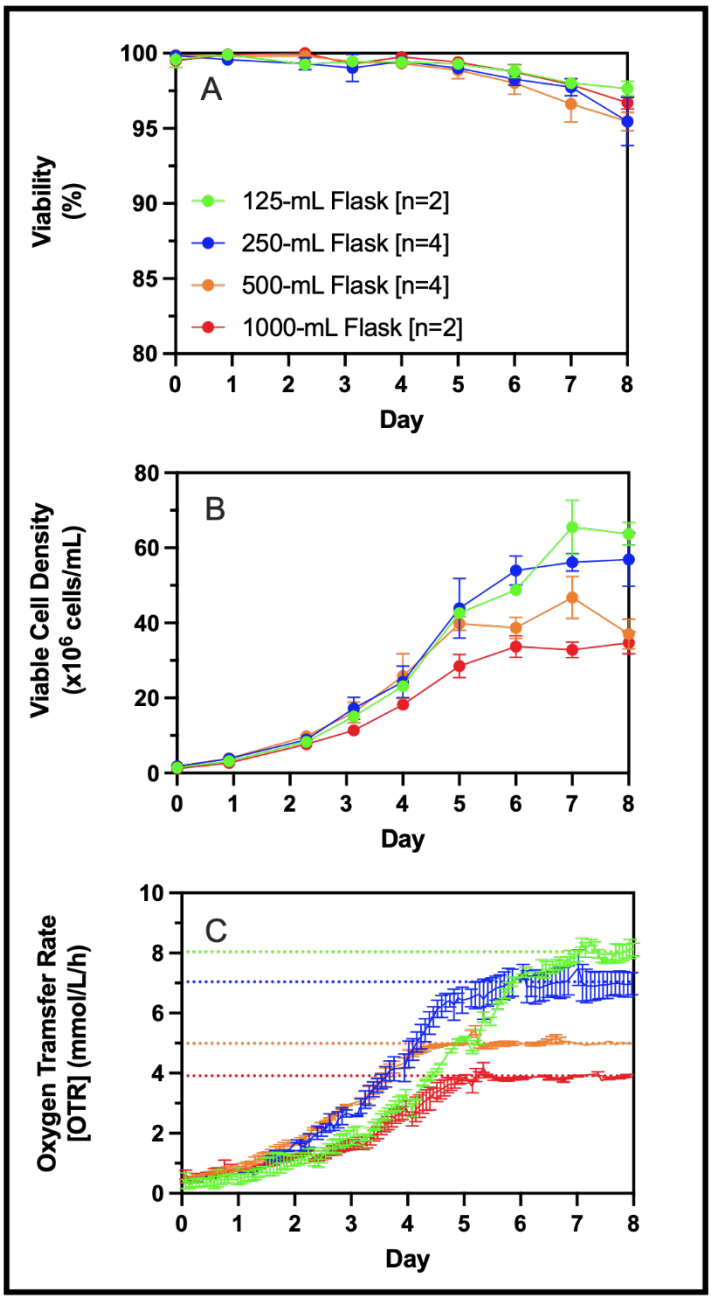

Figure 5.4 Effect of flask size on cell growth and OTR profile. A) Cell viability, B) viable cell density, and C) oxygen transfer rate (OTR) of cell cultures undergoing complete daily media exchange. Horizontal bars indicate the maximum OTR observed for each flask size (C). Cell cultures were performed in unbaffled flask 125-mL (-●-), 250-mL (-●-), 500-mL (-●-), and 1000-mL (-●-) at fill volumes of 20% and agitated at 200 RPM. Error bars of duplicates represent minimum and maximum values while error bars of quadruplicates represent standard deviation of replicates. OTR measurements for 250-mL and 500-mL flasks were done in duplicates [n=2].

A sulfite system was used to measure maximum OTR to confirm that oxygen transfer limitations, rather than other factors such as nutrient depletion or metabolic waste accumulation, caused the observed maximum OTR in media exchanged cell cultures (Figure 5.4C). To do this, sodium sulfite is used to simulate rapid oxygen consumption as it is converted to sodium sulfate by catalysis of cobalt sulfate (II) at sufficiently high rates such that the OTR is considered the rate limiting step.[217,218] The maximum OTR measured with the sulfite system for 125-mL, 250-mL, 500-mL, and 1000-mL flasks at a 20% fill volume were inversely proportional to flask size (Table 5.2 raw data presented in Supplemental Figure B.5). The maximum OTR measurements obtained with the sulfite system (cell-free) were compared to the maximum OTR observed in the biological system which are the maximum OTRs achieved during daily media exchange in shake flasks agitated at 200 RPM (Figure 5.4C). These maximum OTRs (cell-free sulfite system) represent a 2% - 26% difference compared to the maximum OTRs observed in the biological system when doing the daily media exchange (Table 5.2).

Table 5.2 Maximum oxygen transfer rates observed in biological systems and measured in sulfite systems (cell-free) for 125-mL, 250-mL, 500-mL, and 1000-mL unbaffled shake flasks at 20% fill volume agitated at 200 RPM. Maximum OTR measurements in the sulfite system were done in triplicates (OTRmax sulfite, n=3). Maximum OTR measurements in the biological system were done in duplicates (OTRmax bio, n=2).

	Flask Size			
	125-mL	**250-mL**	**500-mL**	**1000-mL**
$OTR_{max,sulfite}$ (mmol/L/h)	9.6 ± 0.1	6.9 ± 0.3	6.1 ± 0.5	4.9 ± 0.1
$OTR_{max,bio}$ (mmol/L/h)	8.04	7.04	4.99	3.91
Difference (%)	18.7	1.8	22.2	25.8
$OTR_{max,bio}/OTR_{max,sulfite}$	0.84	1.02	0.82	0.80

There exists a difference between measured maximum OTR of the sulfite system and the biological system. This difference can be in part attributed to the differences in osmolarity and diffusion coefficients of the solutions.[189] Although differences between culture media and sulfite system at different concentrations of sodium sulfite exist, a concentration of sodium sulfite of 0.35M was shown to have comparable gas transfer kinetics to culture media.[201] As such, a 0.35M concentration

of sodium sulfite was used to reduce difference between biological maximum OTR and sulfite system maximum OTR. Furthermore, to measure maximum OTR with the sulfite system, the reaction kinetics must be adjusted to a "non-accelerated" reaction regime which allows only negligible reaction of oxygen and sulfite in the liquid side boundary layer. This allows for most of the oxygen to be consumed in the bulk liquid, similarly to biological systems where oxygen transfer occurs at the liquid film formed on the surface of the flask and oxygen consumption occurs in the bulk liquid. Using a 10^{-7} M concentration of the cobalt sulfate (II) catalyst allows for a "non-accelerated" reaction regime with the sulfite system.[201] Thus, through the general trend of the OTR curve and sulfite system measurements of maximum shake flask OTR, it was shown that the maximum cell density of this CHO cell line was attained in shake flasks due to oxygen transfer limitations.

5.5.4 Effect of Orbital Agitation Speed on Cell Growth and OTR

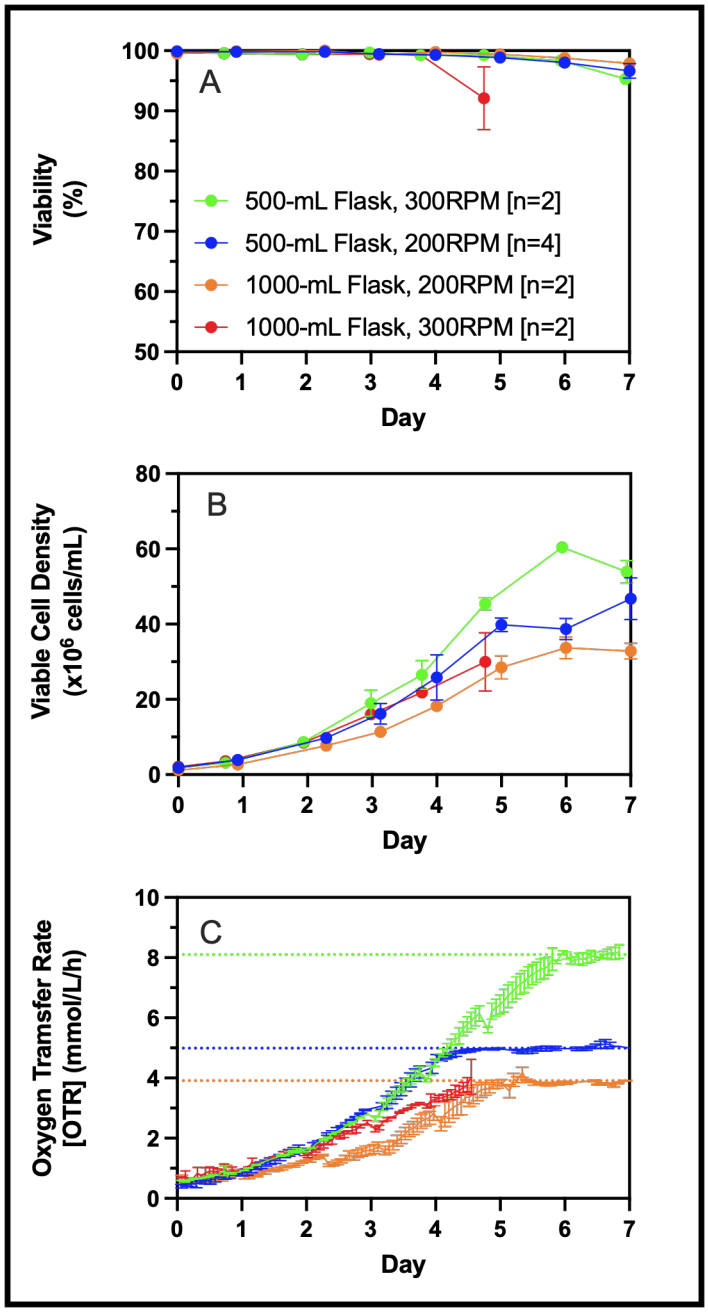

Figure 5.5 Effect of orbital shaking speed on cell growth and OTR**.** A) Cell viability, B) viable cell density, and C) oxygen transfer rate (OTR) of cell cultures undergoing complete daily media exchange. Cell cultures were performed in unbaffled flasks at shaking frequencies of 200 and 300 RPM: 500-mL at 300 RPM (-●-), 500-mL at 200 RPM (-●-), 1000-mL at 200 RPM (-●-), and 1000-mL at 300 RPM (-●-). Error bars of duplicates represent minimum and maximum values and error bars of quadruplicates represent standard deviation of replicates. OTR measurements for 500-mL flasks at 200 RPM (blue curve, C) were done in duplicate [n=2] due to technical issues.

As it was shown that the maximum sustainable VCD by oxygen transfer was achieved, reaching greater VCD in shake flasks by semi-continuous transient perfusion requires increasing the maximum OTR of the system. The OTR of shake flasks can be increased by the addition of baffles which induces greater turbulence.[218] However, the addition of baffles was shown to lead to early decrease of cell viability (Figure 5.2). The maximum OTR of a shake flask can also be increased by decreasing operating volume, increasing shaking diameter, or increasing shaking frequency (Equation 5.7). Shaking frequency was selected to increase maximum OTR as shaking diameter has a lesser effect on maximum OTR[189]. On the other hand, reducing operating volume would reduce the total quantity of cells produced by semi-continuous transient perfusion which goes against the purpose of cell expansion for seeding of a benchtop bioreactor. Shaking frequency was increased from 200 RPM to 300 RPM for 500-mL and 1000-mL flasks for semi-continuous transient perfusion with daily media exchange (Figure 5.5). In 500-mL flasks, the increase in shaking rate resulted in an observed maximum OTR of 4.99 mmol/L/h to 8.10 mmol/L/h. This increase in maximum OTR allowed for an improvement of maximum VCD from $46.7 \pm 3.9 \times 10^6$ cells/mL (n=4) at 200 RPM to $60.5 \pm 0.2 \times 10^6$ cells/mL (n=2) at 300 RPM. However, in the case of the 1000-mL flask, the increase in agitation rate did not result in a rise of maximum VCD and maximum OTR as cell viability began to decrease after day 4. The cell culture in the 1000-mL flask at 300 RPM was terminated early due to an observed early decline in cell viability.

Table 5.3 Reynolds numbers (Re), average ($\varepsilon_{\emptyset}$) and maximum (ε_{max}) energy dissipation rates, and Kolmogorov lengths (λ_K) in 500-mL and 1000-mL shake flasks at 20% fill volume and different agitation rates.

Flask size	**500-mL**	**500-mL**	**1000-mL**	**1000-mL**
Agitation rate (RPM)	200	300	200	300
Re	49138	73707	78921	118382
$\varepsilon_{\emptyset}$ (W/kg)	0.38	1.2	0.54	1.7
ε_{max} (W/kg)	0.38	6.1	3.6	10
λ_K(μm)	30.8	15.4	17.6	13.6

An increase in shaking speed results in increased shear stress in shake flasks.[209] Furthermore, shake flasks with larger volume, and thus larger flask diameter, are subjected to higher levels of shear stress at the same shaking frequency when compared to smaller flasks.[171,219] The average energy dissipation rates increase by 1.6-fold when shake flask sizes are varied from 500-mL to 1000-mL and by 3.2-fold when agitation rates are increased from 200 to 300 RPM (Table 5.3). The Kolmogorov length represents the size of the smaller eddies formed in mixing. When the size of these eddies is smaller than cell size, cell damage may occur.[220] In 1000-mL shake flasks, a Kolmogorov length of 13.6μm is estimated which is below that of the average CHO cell diameter of 15μm. Thus, cell death in the 1000-mL flask at 300 RPM is most likely due to prolonged exposure to elevated shear stress conditions.

5.5.5 Effect of Semi-Continuous Transient Perfusion on Cell Doubling Time and Productivity

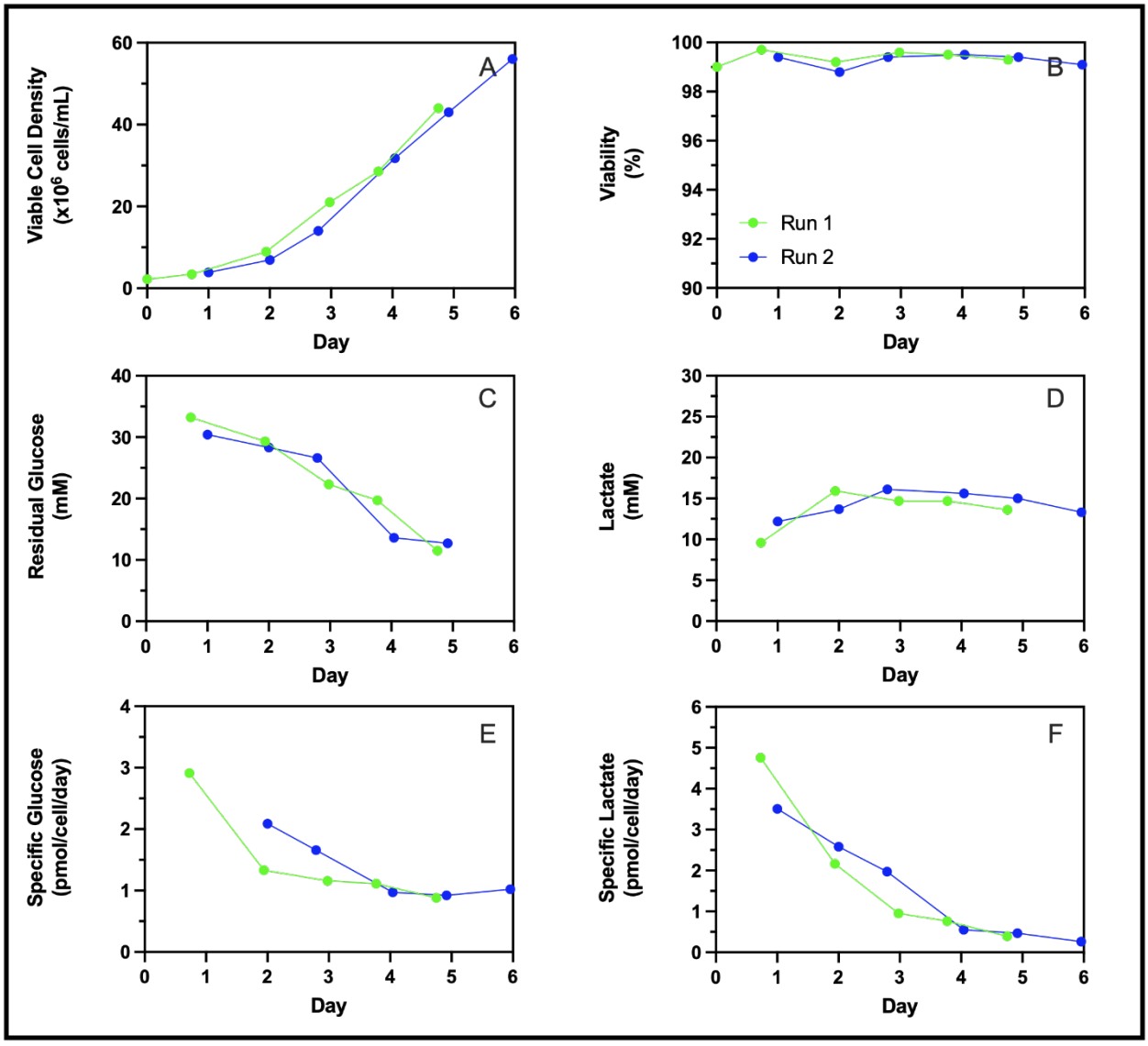

Figure 5.6 Effect of daily medium replacement on shake flask cell growth performance. A) Viable cell density, B) cell viability, C) residual glucose, D) lactate, E) cell specific glucose consumption, and F) cell specific lactate production for Run 1 (-●-) and Run 2 (-●-) of daily media exchange in 125-mL unbaffled shake flasks at 20% fill volume agitated at 300 RPM. Run 1 refers to the semi-continuous transient perfusion cell expansion from thawed cells. Run 2 refers to semi-continuous transient perfusion cell expansion from Run 1 cells at day 5 after reaching >40x10^6 cells/mL.

To determine the effect of medium replacement on cell growth rate, daily media exchange was performed on cells grown in a 125-mL shake flask at 20% fill volume (25 mL) agitated at 300 RPM

from 2x10^6 cells/mL (labeled "Run 1"). When reaching 40x10^6 cells/mL, cells were diluted back to 2x10^6 cells/mL and daily media exchange was performed once again until cells had reached over 40x10^6 cells/mL (labeled "Run 2"). The cell viability was maintained at >98% throughout both Run 1 and Run 2 cell expansions (Figure 5.6B). The growth curves of Run 1 and Run 2 overlap (Figure 5.6A) indicating that semi-continuous transient perfusion in shake flasks through complete daily media exchange has no short-term impact on cell growth rate. Furthermore, residual glucose and lactate levels as well as specific glucose consumption and lactate production were comparable in Run 1 and Run 2 of semi-continuous transient perfusion cell expansion (Figure 5.6C, D, E, and F).

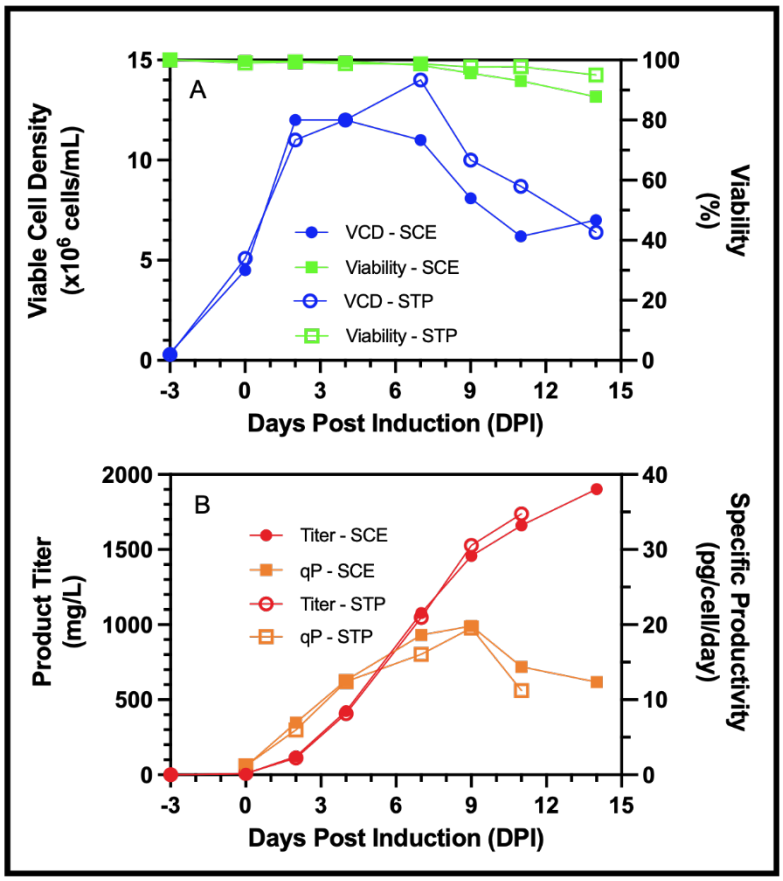

Figure 5.7 Effect of daily medium replacement cell expansion on shake flask fed-batch production. A) Viable cell density & cell viability and B) volumetric product titer & cell specific productivity of cell cultures in 125-mL baffled shake flasks seeded from standard cell expansion (SCE) and semi-continuous transient perfusion (STP).

To determine the effect of daily media exchange on culture productivity, two cell cultures were performed in shake flask under identical conditions but with different seed trains. One flask was

seeded using standard cell expansion (SCE) where cells were maintained in exponential growth by diluting the cells to maintain viable cell density between 0.2 to $3x10^6$ cells/mL. A second flask was seeded with cells coming from semi-continuous transient perfusion (STP) where cells were subjected to daily media exchange from 2.2 $x10^6$ cells/mL on day 0 until day 5 when the cells reached >$40x10^6$ cells/mL. Cells were diluted to $2x10^6$ cells/mL and daily media exchange was performed until day 11 when the cells reached $56x10^6$ cells/mL (Figure 5.6A). Shake flask cell cultures seeded from SCE and STP both had comparable growth rates during the growth phase until 2 DPI. The decrease in VCD throughout the production phase (2-14 DPI) is comparable for both cultures (Figure 5.7A). Cell specific productivities were similar throughout cell cultures seeded with both SCE and STP (Figure 5.7B). As a result of comparable specific productivity and VCD, volumetric product titers were similar for cultures seeded from both cell expansion methods. These results show that the STP has no observable impact on cell growth and glycolytic metabolism (Figure 5.6) and does not impact cell growth and viability as well as cell specific and volumetric mAb productivity (Figure 5.7).

5.5.6 Improvement of Increased Seeding Density

To demonstrate that STP in shake flasks through daily medium exchange can be used to seed benchtop bioreactors at high cell density, a 1-L vessel was inoculated at Ultra High Seeding Density (UHSD) ($15x10^6$ cells/mL) from a STP N-1 seed train. A second 1-L benchtop bioreactor was seeded at Standard Seeding Density (SSD) ($0.3x10^6$ cells/mL) from a SCE N-1 seed train. The UHSD process begun at $15x10^6$ cells/mL at induction while the SSD process was still only at ~$5x10^6$ cells/mL at induction. The SSD reached ~$15x10^6$ cells/mL 2 days later than the UHSD process (Figure 5.8A). Both processes were maintained at >95% viability for ~5 days (Figure 5.8B). The UHSD process achieving earlier peak cell viability but having an earlier decline in cell viability which is typical of high-density seeding processes as previously observed in high seeding density studies.[176,221] Attaining high VCD earlier in the cell culture allowed for a shorter cell culture in the UHSD process compared to the SSD process. The high-density seeding process produced 1206 mg/L of mAb in 6 days while the standard process produced 1616 mg/L in 12 days. This represents only 25.4% loss of product concentration for a process that is 50% shorter in timeline. As such, the space-time-yield (STY) of the UHSD process was of 201 mg/L/day while the STY of the SSD process was of only 135 mg/L/day representing a 49.3% increase in STY. The shorter

culture time in the UHSD process is achieved by bypassing the pre-induction growth phase (-3 to 0 DPI) and starting the production phase (0 to 2 DPI) at a higher cell density, leading to an earlier productivity peak. Further optimization of UHSD cultures can be done which is outside the scope of this study. Further optimizations can include enhanced feeding regimen, supplement addition such as short chain fatty acids such as sodium butyrate, valeric acid or valproic acid which have been shown to arrest cell growth and promote specific cell productivity,[176] real-time glucose measurements to enable a low glucose level control strategy, and key amino acid supplementation.[178]

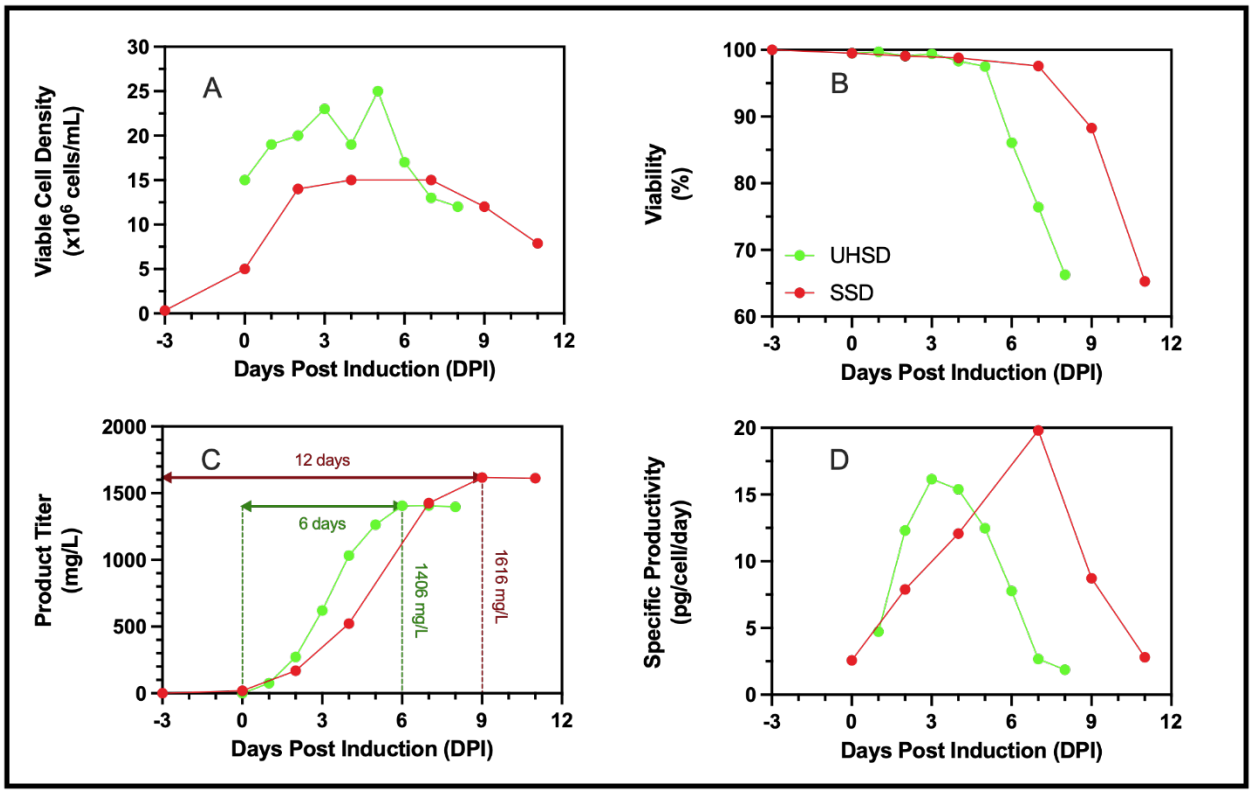

Figure 5.8 Effect of Ultra High Seeding Density (UHSD) on fed-batch bioreactor production performance**.** A) Viable cell density, B) cell viability, C) volumetric product titer, and D) cell specific titer of ultra-high seeding density (UHSD) (-●-) and standard seeding density (SSD) (-●-) cell cultures in 1-L benchtop bioreactors.

5.6 Conclusion

The prime objective of this study to seed a benchtop bioreactor at ultra-high cell densities using shake-flasks in N-1 precultures to reduce process costs and enable process simplicity was achieved. Additionally, the improvements of UHSD process were demonstrated by comparing to a standard

SSD process where the UHSD process had a 49.3% reduction in space-time-yield before process optimization.

The development of the N-1 seed train aims to mimic transient perfusion, such as is done commonly with ATF/TFF perfusion systems, to reach viable cell densities capable of seeding a benchtop bioreactor at $15x10^6$ cells/mL. Semi-continuous transient perfusion done through media exchange in shake flasks was used to approximate transient perfusion in bioreactor. The first step in this development was to determine the necessary frequency of media exchange. The results demonstrated that at lower frequencies (every 2-3 days), total glucose consumptions would become high enough that glucose would be depleted, or high enough glucose concentrations would be necessary that would become inhibitory to cell growth. Daily media exchange from day 0, beginning at $1.5\text{-}2.5x10^6$ cells/mL, was necessary to achieve the highest viable cell density. In fact, when media exchange was omitted on days 1 and 2 to reduce media consumption, lower maximum viable cell densities were achieved due to nutrient limitations.

It was then shown, through OTR measurements of cell cultures using the TOM instrument (Kuhner Shaker Inc.), that maximum cell densities are achieved when oxygen becomes a limiting nutrient. Measured maximum OTR using the sulfite system confirms that cell cultures reached viable cell densities which are oxygen-limiting in 125-mL, 250-mL, 500-mL, and 1000-mL shake flasks at 20% fill volume agitated at 200 RPM. An increase in agitation rate from 200 RPM to 300 RPM for the 500-mL flasks resulted in an increase of maximum OTR from 4.99 to 8.10 allowing an improvement in maximum VCD of 29.6%. However, for the 1000-mL flask, raising agitation rate from 200 RPM to 300 RPM resulted in an early cell death and thus a lower maximum VCD. The early cell death is attributed to the higher shear stress present in larger shake flasks with higher agitation rate. Since cell viability is not negatively impacted at 200 RPM in 1000-mL shake flasks but is impacted at 300 RPM, agitation rate of this flask could be further optimized (between 200 and 300 RPM) to find a maximum OTR which does not impact cell viability.

Semi-continuous transient perfusion in shake flasks was successfully used as a N-1 preculture for the ultra-high density seeding of 1-L benchtop bioreactors thus circumventing the need for expensive and specialised perfusion equipment. The use of ultra-high seeding density (UHSD) ($15x10^6$ cells/mL) in benchtop bioreactor cell cultures resulted in 87% of the volumetric product titer obtained with standard seeding densities (SSD) ($0.3x10^6$ cells/mL). However, the UHSD cell

culture had a 50% shorter culture time when compared to the SSD cell culture. The much shorter culture time paired with comparable volumetric product titers allowed for a 49.3% increase in space-time-yield (STY). This increased STY is mainly due to the elimination of the growth phase performed prior to the N production. When this growth phase time is considered, the difference in space-time yield is much smaller due to the achieved final titers being comparable. Nonetheless, with further optimization, literature shows that higher titers are achievable in high density seeding cultures.[118] Finally, using N-1 perfusion seed train allows for shorter usage of the N production bioreactor enabling a better equipment flexibility and a high asset turnover ratio.

5.7 Author Contributions

Lucas Lemire: Conceptualization; methodology; data curation; investigation; validation; writing – original draft. **Yves Durocher**: Supervision; resources; formal analysis. **Sebastian-Juan Reyes**: Formal analysis; writing – review and editing. **Olivier Henry** and **Phuong Lan Pham**: Supervision; formal analysis; validation; funding acquisition; writing – review and editing; resources; project administration.

5.8 Acknowledgments

This work was supported by the Natural Sciences and Engineering Research Council of Canada (stipend allocated to Lucas Lemire via the NSERC-CREATE PrEEmiuM program). We thank Louis Bisson for HPLC monoclonal antibody titer measurements and Catherine Sabourin-Poirier for UPLC amino acid quantification.

5.9 Conflict of Interest Statement

The authors declare no conflicts of interest.

CHAPTER 6 GENERAL DISCUSSION

The production of recombinant protein biotherapeutics utilizes the well-established Chinese Hamster Ovary (CHO) cell platform. These cells are used for their ability to perform post-translational modifications, producing human-like glycosylated proteins.[6,7,120,141] Furthermore, CHO cell genomes have been extensively optimized to achieve high product yields of 3-10 g/L.[8-10] Several considerations must be taken during process development and scale-up to reach industrial-scale production. It is challenging to maintain the same operating conditions at different scales; thus, strategies focus on keeping volumetric power input (P/V), oxygen mass transfer, gas flowrate (vvm), and impeller tip speed constant. Among these factors, aeration and mixing are the most critical for influencing cell growth, viability, and productivity during culture scale-up.[222] The choice of gas sparger, whether a microsparger or macrosparger, significantly affects shear stress applied to cells, oxygen transfer efficiency, and carbon dioxide stripping. Shear stress from gassing occurs during bubble formation, bubble ascent, and when the bubble bursts at the gas-liquid interface. Most of the stress arises from the bursting of the bubble, where the release of Laplace pressure is inversely proportional to bubble size; thus, microspargers tend to cause greater cell damage at the same gas flowrate.[53] However, smaller bubbles enhance gas transfer efficiency from the bubble to the bulk liquid by increasing the surface area-to-volume ratio[223]. Regarding carbon dioxide stripping, it is not directly dependent on bubble size but rather on the saturation of the bubbles in CO_2.[48] Therefore, the ratio of CO_2 saturation time to gas residence time becomes crucial, as longer gas residence times in larger bioreactors allow bubbles to become saturated. While this understanding sheds light on the effects of sparger types on various aspects of gassing, the interplay between these phenomena is complex. For instance, although the bursting of bubbles produced by a macrosparger generates less stress on cells compared to a microsparger, higher gas flow rates are required with a macrosparger to maintain dissolved oxygen (DO) setpoints. In addition to the three possible gas sparger configurations (microsparger only, macrosparger only, and a combination of both), the strategy for gassing can also be explored. Implementing an aeration cascade, where air is first sparged for DO control until reaching a predetermined flow rate—termed the air cap—allows for robust DO management throughout the cell culture process. Initially, when cell densities are low, air is used to gently adjust pO_2 levels, as small flowrates of oxygen can easily overshoot the DO setpoint, leading to unnecessary fluctuations linked to decreased cell growth and productivity.[224]

Evaluation of IVCC, endpoint cell viability, and final product titers across different sparger configurations, with and without aeration cascade, revealed that the dual sparger (macro and microsparger) achieved the highest titer due to its elevated endpoint viability. In comparison, the microsparger with an air cap condition exhibited a similar average product titer, attributed to having the highest IVCC. Analyzing these results proved sometimes challenging primarily due to batch-to-batch variability, which stemmed from the use of a stable cell pool rather than a clone. Cell pools inherently have variability due to their heterogeneous population.[134] Trends showing an inverse correlation between maximum lactate concentrations and final titer illustrated that cascade aeration generally facilitated lower lactate production. An aeration cascade increases the total gas sparged by utilizing air as part of the total oxygen required to maintain dissolved oxygen (DO) at the desired setpoint. This increased gas flowrate results in decreased pCO_2 levels, which have been linked to lower peak lactate levels.[46] Furthermore, multivariate data analysis, specifically principal component analysis (PCA), can help reduce noise in large datasets when considering multiple variables.[127] By consolidating various factors (endpoint viability, endpoint lactate, endpoint ammonia, endpoint IVCC, endpoint pH, endpoint titer, total base addition, total CO_2 sparge, total O_2 sparge, total glucose consumed, and maximum lactate) into a single component, we can better establish which process variables impact culture outcomes. This analysis further confirmed that both the dual sparger and the microsparger with an air cap demonstrate superior performance regarding product titer, owing to their lower lactate production. For further process optimization and exploration of the effects of gassing strategy and mixing, the microsparger with an air cap was chosen over the dual configuration for its simplicity, as all gases pass through a single gas sparger.

Before further optimizing aeration and mixing, we compared low and high feeding strategies to select between two different platform feeding regimens. Both the low and high feeding regimens had previously demonstrated efficiency in other processes developed by our research group (data not shown). Feeding larger volumes can help avoid nutrient deficiencies that may lead to decreased cell growth and productivity.[143-145] However, high-volume bolus feeds can cause rapid spikes in osmolarity, which are known to induce cell death and result in lower titers.[63,150,161] The high feed regimen studied increased osmolality from 379 to 419 mOsm/kg between 4 to 7 days post-induction, while the low feed regimen maintained osmolality levels of 348 and 343 mOsm/kg during the same period. As a result, the low feeding regimen maintained high cell viability (>97%) for four days longer than the high feeding regimen. This study on feeding strategies is limited to

only two platform feeding regimens due to the scope of this thesis. Further investigation into continuous feeding, rather than bolus additions, and dynamic feeding based on cell growth and density, oxygen uptake, and nutrient concentrations such as amino acids could further improve product titers.

The beneficial effects of cascade aeration prompted an investigation into the impact of airflow at air cap rates on cell culture performance. An optimal air cap flowrate of 2 mL/min was identified, maintaining high cell viability over extended periods, which in turn allowed for the highest specific productivity and maximum volumetric titer. In contrast, increasing the air cap flowrate to 12.3 mL/min increased the total gas sparging requirement and led to earlier cell death, likely due to heightened shear stress. Similarly, a lower air cap flowrate of 1 mL/min resulted in a reduced final product titer, due to early cell death and decreased specific productivity. While the findings on different sparger types, configurations, and air cap flowrates offer insights into optimizing product titers through aeration strategies, these studies were conducted at a single concentration of surfactant (Pluronic F-68). As discussed in section 2.4.5 of this thesis, Pluronic F-68 significantly reduces the shear stress applied to cells which is known to be impacted by sparging. Therefore, varying the concentration of Pluronic F-68 would be desirable to test to assess the generality of the conclusions regarding the effects of aeration strategies. In examining the effect of mixing with a second impeller, challenges arose in determining the positioning of the additional impeller. Due to the size of the impellers and vessel, simply adding a second impeller 1 to 2 impeller diameters above the first would result in the top impeller being mostly out of the bulk liquid for most of the cell culture. To ensure both impellers remained submerged throughout the entire cell culture duration, thus allowing for the most accurate estimations of volumetric power input, the lower impeller was placed as low as possible without interfering with the gas sparger or harvest line, while the top impeller was positioned immediately above it. Additionally, the initial volume of the cell culture was increased.

The successful scale-up from 1-L to 10-L bioreactors demonstrated comparable growth and productivity, but it presented certain challenges and limitations inherent to the system employed. The 10-L system utilized a thermal mass flow controller (TMFC) with a maximum flowrate of 20 mL/min, which was inadequate for maintaining DO levels at the achieved cell densities. Preliminary experiments indicated that the air cap vvm for the mid AC condition, which was

optimal in the 1-L vessels, was insufficient to maintain DO levels in the 10-L vessel. As a result, the high AC condition was chosen for scaling up the process. Given the small volume difference between the 1-L and 10-L vessels, the scale-up could have been simplified; literature suggests that maintaining a constant P/V alone is often sufficient for achieving comparable performance across small differences in scale. This implies that a more complex approach, such as maintaining both constant P/V and constant vvm at the air cap, might not have been necessary in this instance. However, for scaling beyond 10-L, establishing a constant vvm at the air cap or even a constant k_La at air cap may be beneficial for maintaining pCO_2 and pO_2 within appropriate ranges.

To further enhance the performance of the 1-L bioreactor process, we aimed to transition from standard cell density seeding to ultra-high density seeding. It has been shown that increasing the seeding density to up to 20 million cells/mL can improve product titer and space-time yield (product/time).[116-118,175-178] Typically, preculture transient perfusion is carried out in bioreactors using systems like ATF. To avoid the complexities and costs associated with such equipment, we developed a simple, yet effective, method utilizing semi-continuous transient perfusion through media exchange in shake flasks. Similar to bioreactors, optimizing gas transfer in shake flasks is essential for achieving high cell densities. In this cultivation system, oxygen transfer occurs at the thin film of liquid media on the flask walls during agitation.[201] Therefore, the agitation rate is crucial for supplying the oxygen needed for cell growth. However, increased agitation rates in shake flasks also raises shear stress applied to cells.[209] As such, there is a balance to be made between enhancing oxygen transfer for cell growth and minimizing shear stress to prevent cell death. Daily media exchange was shown to be necessary to avoid glucose and amino acid depletion. Even in the absence of nutrient limitations, semi-continuous transient perfusion cultures in shake flasks reached VCD plateaus that were function of flask size. Measurements of oxygen transfer rates during media exchange, along with maximum oxygen transfer rates determined using the sulfite method, indicated that gas transfer was a limiting factor. While increasing the agitation rate led to a greater VCD in 500-mL shake flasks, more vigorous mixing in 1000-mL flasks caused early cell death. Although this method was successfully used to seed a 1-L benchtop bioreactor at 15 million cells/mL, resulting in a 50% increase in space-time yield, it had certain limitations compared to the use of conventional perfusion systems. Media exchange in shake flasks involves multiple manipulations, such as transferring cell cultures to centrifuge tubes and back into the shake flasks, which increases the risk of contamination. Additionally, while sufficient cells were

produced to seed a 1-L benchtop bioreactor, the maximum VCD achieved (60 million cells/mL in a 500-mL flask at 20% fill volume) was lower than what is routinely obtained with perfusion systems in bioreactor (>100 million cells/mL). As a result of the increase in maximum VCD combined with the absence of cell death due to shear stress observed in the 500-mL flask at 300 RPM, it can be assumed that further increases in the agitation rate could lead to a greater maximum VCD. However, the Kuhner TOM incubator's flask shaker does not permit agitation rates higher than 300 RPM. In the case of the 1000-mL flask, the agitation rate could be fine-tuned to identify an optimal rate that maximizes OTR while preventing cell death due to shear stress.

CHAPTER 7 CONCLUSION AND RECOMMENDATIONS

7.1 Conclusion

The primary objective of this doctoral thesis was to investigate the effects of gas transfer in CHO cell cultures with a focus on process intensification and scale-up. This research has resulted in the publication of a research article (Chapter 5), as well as the submission of a second research article (Chapter 4). In bioreactors, gas transfer is achieved through sparging of air and oxygen through either a macrosparger (drilled hole sparger) or a microsparger (frit sparger). The type of sparger used primarily influences the size of the bubbles produced, which in turn affects gas transfer rates of oxygen and carbon dioxide, as well as the shear stress experienced by the cells. While the impact of individual bubble size is well understood, there has been limited research explicitly examining how different sparger configurations affect the performance of CHO cell cultures in terms of product titers. This gap is evident in the lack of consensus on sparger configuration choices, especially in small-scale bioreactors. In shake flasks, gas transfer occurs at the liquid film on the walls during orbital agitation, with the rate of transfer mainly determined by flask size, fill volume, and agitation rate. Similar to bioreactors, these factors also influence shear stress, which becomes critical when high cell densities lead to oxygen becoming a limiting nutrient for the culture. Therefore, it is essential to balance adequate oxygen supply with shear stress in both bioreactors and shake flasks. The findings presented in this thesis represent significant advancements in understanding the impact of aeration in these systems.

Objective #1 focused on examining the effects of sparger type and configuration on cell culture growth and production. This was accomplished by systematically evaluating the integral viable cell density (IVCC), endpoint product titers, and endpoint cell viability across different sparger configurations and aeration strategies in 1-L benchtop bioreactors. The dual sparger demonstrated enhanced carbon dioxide stripping capabilities and oxygen transfer, which helped maintain a favorable culture environment, resulting in improved cell growth and productivity. Although microsparger configurations with an air cap also achieved high IVCCs and comparable product titers to the dual sparger, macrosparger configurations exhibited significantly lower performance. Aeration strategies that employed cascade aeration with air caps showed improved lactate control, contributing to higher volumetric titers. This study is of special interest as the effect of bubble size on individual parameters (ie. shear stress, oxygen transfer, and carbon dioxide stripping) is well

known, however the combined interplay of effects on cell culture performance is not explicitly demonstrated in literature.

Objective #2 aimed to establish process conditions that enhance the growth and productivity of cell culture processes through the selection of feeding regimens and parameters critical for process scale-up, such as mixing and aeration. This objective was addressed by comparing low and high-volume feeding regimens, examining the impact of the number of impellers, and optimizing the air cap of an aeration cascade. Additionally, the 1-L process was scaled up to a 10-L vessel transferred to the production of a different recombinant protein. It was found that cultures with a high bolus feeding regimen, which caused spikes in osmolality, experienced an early decline in cell viability while a lower feeding regimen resulted in a 25% increase in final volumetric titer. For this process, an optimal air cap of 2mL/min was determined. Increasing the magnitude of the air cap allowed for a greater total volume of gas to be sparged into the cell culture which resulted in low viable cell density (VCD) and early decline in cell viability, likely due to prolonged shear stress. Comparable cell culture performance, regarding VCD, viability, and productivity, was observed when scale-up was done based on constant P/V and constant air cap vvm. Additionally, maintaining constant hydrodynamic conditions (P/V and vvm) throughout cell culture, either by keeping a constant volume or by adjusting the agitation rate and flowrate at the air cap, improved process performance. The originality of this study lies in the use of cascade aeration and the effect of the flowrate at the air cap on productivity, as these gassing strategies are seldom described in the literature. Furthermore, recognizing that constant hydrodynamic conditions throughout cell cultures aids in understanding how highly concentrated feeds enhance cell culture performance.

We have described the development of a semi-continuous transient perfusion methodology which satisfies objective #3. Daily media exchanges starting on day 0 were crucial for achieving maximum viable cell density and preventing nutrient limitations. Measurements of the oxygen transfer rates (OTR) revealed that maximum cell densities are reached when oxygen becomes limiting. The semi-continuous transient perfusion in shake flasks effectively acted as an N-1 preculture for ultra-high density seeding in 1-L benchtop bioreactors, thereby eliminating the need for expensive perfusion equipment. Using an ultra-high seeding density of 15 million cells/mL achieved 87% of the volumetric product titer compared to standard seeding densities of 0.3 million cells/mL, all while reducing culture time by 50%. This decrease in culture time, coupled with

similar volumetric product titers, resulted in a 49.3% increase in space-time yield (STY), primarily due to the elimination of the growth phase prior to N production. This study demonstrates a method capable of achieving maximum viable cell densities with mammalian cells in flasks of various sizes, notably in larger flasks which has previously been a challenge in literature. Furthermore, measurements of the oxygen transfer rate explain why these are the maximum viable cell densities as well as expose the delicate interplay between oxygen transfer and shear stress in shake flasks of different sizes.

7.2 Recommendations and Future Work

From the findings and conclusions of this thesis, the following recommendations and potential avenues for further research and development emerge:

The scale-up of the 1-L cell culture with the established cell culture condition was only brought to a 10-L vessel. Further scale-up to industrial scale units (>200L) could reveal issues such as improper CO_2 stripping and shear stress from high impeller tip speed due to maintaining a constant P/V. Using the knowledge of sparger type and configuration from this thesis, gassing could be adapted to control CO_2 accumulation. In the case where tip speed causes issues with shear stress, the agitation rate could be reduced while maintain k_La constant at the air cap. In the case where CO_2 levels increase affecting cell growth and productivity, the sparger configuration could be changed to a dual sparger where air is sparger through a macrosparger. Alternatively, rather than a specified air cap, air flowrate could be used in pH control which in turn would lower pCO_2 levels.

The type and configuration of spargers and aeration strategies such as cascade aeration at varying flowrates influence pCO_2 levels. Measuring dissolved carbon dioxide concentrations would allow to create an accurate scale-down model of large-scale productions which are known to regularly encounter issues with pCO_2 accumulation. Scale-down models are an efficient way to study process parameters of large-scale productions.

The method of N-1 semi-transient perfusion in shake flasks developed in this thesis allowed to achieve the highest VCD allowable before oxygen transfer limitations. Applying this methodology to other cells lines could be useful in selecting clones with the best potential for scalability to bioreactor perfusion. Cell lines that would reach the highest VCD in media exchange shake flask cultures would demonstrate the lowest requirement for oxygen consumption at high densities. The use of cell lines that require lower oxygen consumption reduces the total gas sparging needed to

maintain DO levels and thus lowers the shear stress cells are subjected to. Furthermore, these cultures could be scaled-up from flask to bioreactor using a constant P/V criteria, which has been shown to be successful in replicating metabolite and final titers.[225]

This work has revealed how bolus overfeeding in fed-batch cell cultures results in early cell death due to high osmolality. Using a continuous feeding strategy rather than bolus additions would likely prevent rapid changes in osmolarity and allow cells to gradually consume nutrients and adapt to the higher osmolarity environment. This can be particularly useful when large feeding volumes are necessary such as in high density cell cultures.

This thesis highlighted the detrimental effects of overfeeding on culture performance. It would be interesting to explore the use of dynamic feeding strategies, based on online signals, such as oxygen consumption measured by an off-gas analyzer or cell density measured by capacitance. By adapting feed volumes to the culture's needs in real time, overfeeding could be avoided.

Maintaining stable hydrodynamic conditions throughout cell culture led to increased recombinant protein yields. Keeping the culture volume consistent proved effective in maintaining P/V and vvm constant. Consequently, employing a more concentrated feed solution such as ThermoFischer EfficientFeed+, which requires smaller feed amounts, is expected to further enhance cell culture performance.

REFERENCES

1. Allied Analytics LLP. *Biopharmaceuticals Market By Type and Application - Global Opportunity Analysis And Industry Forecast, 2018-2025*. 2018.

2. Lu R-M, Hwang Y-C, Liu IJ, et al. Development of therapeutic antibodies for the treatment of diseases. *Journal of Biomedical Science*. 2020/01/02 2020;27(1):1. doi:10.1186/s12929-019-0592-z

3. Wang C, Li W, Drabek D, et al. A human monoclonal antibody blocking SARS-CoV-2 infection. *Nature Communications*. 2020/05/04 2020;11(1):2251. doi:10.1038/s41467-020-16256-y

4. Baum A, Fulton BO, Wloga E, et al. Antibody cocktail to SARS-CoV-2 spike protein prevents rapid mutational escape seen with individual antibodies. *Science*. 2020;369(6506):1014-1018. doi:10.1126/science.abd0831

5. Zost SJ, Gilchuk P, Case JB, et al. Potently neutralizing and protective human antibodies against SARS-CoV-2. *Nature*. 2020/08/01 2020;584(7821):443-449. doi:10.1038/s41586-020-2548-6

6. Shirahata H, Diab S, Sugiyama H, Gerogiorgis DI. Dynamic modelling, simulation and economic evaluation of two CHO cell-based production modes towards developing biopharmaceutical manufacturing processes. *Chemical Engineering Research and Design*. 2019;150:218-233.

7. Becker M, Junghans L, Teleki A, Bechmann J, Takors R. The Less the Better: How Suppressed Base Addition Boosts Production of Monoclonal Antibodies With Chinese Hamster Ovary Cells. Original Research. *Front Bioeng Biotechnol*. 2019-April-11 2019;7(76)doi:10.3389/fbioe.2019.00076

8. Rader RA, Langer ES. Years of upstream productivity improvements. *BioProcess Int*. 2015;13(2):2015.

9. Takagi Y, Kikuchi T, Wada R, Omasa T. The enhancement of antibody concentration and achievement of high cell density CHO cell cultivation by adding nucleoside. *Cytotechnology*. 2017;69(3):511-521.

10. Huang YM, Hu W, Rustandi E, Chang K, Yusuf-Makagiansar H, Ryll T. Maximizing productivity of CHO cell-based fed-batch culture using chemically defined media conditions and typical manufacturing equipment. *Biotechnology progress*. 2010;26(5):1400-1410.

11. Urlaub G, Chasin LA. Isolation of Chinese hamster cell mutants deficient in dihydrofolate reductase activity. *Proceedings of the National Academy of Sciences of the United States of America*. 1980;77(7):4216-4220. doi:10.1073/pnas.77.7.4216

12. Xu P, Clark C, Ryder T, et al. Characterization of TAP Ambr 250 disposable bioreactors, as a reliable scale-down model for biologics process development. *Biotechnol Prog*. Mar 2017;33(2):478-489. doi:10.1002/btpr.2417

13. Feary M, Racher AJ, Young RJ, Smales CM. Methionine sulfoximine supplementation enhances productivity in GS–CHOK1SV cell lines through glutathione biosynthesis. *Biotechnology Progress*. 2017;33(1):17-25. doi:10.1002/btpr.2372

14. Noh SM, Shin S, Lee GM. Comprehensive characterization of glutamine synthetase-mediated selection for the establishment of recombinant CHO cells producing monoclonal antibodies. *Sci Rep*. Mar 29 2018;8(1):5361. doi:10.1038/s41598-018-23720-9

15. Zhang L, Shen H, Zhang Y. Fed-batch culture of hybridoma cells in serum-free medium using an optimized feeding strategy. *Journal of Chemical Technology & Biotechnology*. 2004;79(2):171-181. doi:10.1002/jctb.940

16. Lefloch F, Tessier B, Chenuet S, et al. Related effects of cell adaptation to serum-free conditions on murine EPO production and glycosylation by CHO cells. *Cytotechnology*. 2006;52(1):39-53. doi:10.1007/s10616-006-9039-y

17. Miki H, Takagi M. Design of serum-free medium for suspension culture of CHO cells on the basis of general commercial media. *Cytotechnology*. 2015;67(4):689-697. doi:10.1007/s10616-014-9778-0

18. Junker B, Lester M, Leporati J, et al. Sustainable reduction of bioreactor contamination in an industrial fermentation pilot plant. *Journal of Bioscience and Bioengineering*. 2006/10/01/ 2006;102(4):251-268. doi:https://doi.org/10.1263/jbb.102.251

19. Ong EC, Smidt P, McGrew JT. Limiting the metabolic burden of recombinant protein expression during selection yields pools with higher expression levels. *Biotechnol Prog*. Sep 2019;35(5):e2839. doi:10.1002/btpr.2839

20. Misaghi S, Chang J, Snedecor B. It's time to regulate: Coping with product-induced nongenetic clonal instability in CHO cell lines via regulated protein expression. *Biotechnology Progress*. 2014;30(6):1432-1440. doi:10.1002/btpr.1970

21. Lam C, Santell L, Wilson B, et al. Taming hyperactive hDNase I: Stable inducible expression of a hyperactive salt- and actin-resistant variant of human deoxyribonuclease I in CHO cells. *Biotechnology Progress*. 2017;33(2):523-533. doi:10.1002/btpr.2439

22. No D, Yao TP, Evans RM. Ecdysone-inducible gene expression in mammalian cells and transgenic mice. *Proceedings of the National Academy of Sciences of the United States of America*. 1996;93(8):3346-3351. doi:10.1073/pnas.93.8.3346

23. Figueroa Jr. B, Ailor E, Osborne D, Hardwick JM, Reff M, Betenbaugh MJ. Enhanced cell culture performance using inducible anti-apoptotic genes E1B-19K and Aven in the production of a monoclonal antibody with Chinese hamster ovary cells. *Biotechnology and Bioengineering*. 2007;97(4):877-892. doi:10.1002/bit.21222

24. Mellahi K, Cambay F, Brochu D, et al. Process development for an inducible rituximab-expressing Chinese hamster ovary cell line. *Biotechnology Progress*. 2019;35(1):e2742. doi:10.1002/btpr.2742

25. Poulain A, Perret S, Malenfant F, Mullick A, Massie B, Durocher Y. Rapid protein production from stable CHO cell pools using plasmid vector and the cumate gene-switch. *Journal of Biotechnology*. 2017/08/10/ 2017;255:16-27. doi:https://doi.org/10.1016/j.jbiotec.2017.06.009

26. Mullick A, Xu Y, Warren R, et al. The cumate gene-switch: a system for regulated expression in mammalian cells. *BMC Biotechnology*. 2006/11/03 2006;6(1):43. doi:10.1186/1472-6750-6-43

27. Carpio M. Current Challenges with Cell Culture Scale-up for Biologics Production. *BioPharm International*. 2020;33(10):23-27.

28. Macdonald GJ. Scale-Out Plus Single-Use Can Multiply Yields: Single-use technology reduces some biomanufacturing equations to scale-out> scale-up. *Genetic Engineering & Biotechnology News*. 2019;39(11):46-48, 50.

29. Klöckner W, Büchs J. Advances in shaking technologies. *Trends in Biotechnology*. 2012/06/01/ 2012;30(6):307-314. doi:https://doi.org/10.1016/j.tibtech.2012.03.001

30. Klöckner W, Gacem R, Anderlei T, et al. Correlation between mass transfer coefficient kLa and relevant operating parameters in cylindrical disposable shaken bioreactors on a bench-to-pilot scale. *Journal of Biological Engineering*. 2013/12/02 2013;7(1):28. doi:10.1186/1754-1611-7-28

31. Chaturvedi K, Sun SY, O'Brien T, Liu YJ, Brooks JW. Comparison of the behavior of CHO cells during cultivation in 24-square deep well microplates and conventional shake flask systems. *Biotechnology Reports*. 2014/06/01/ 2014;1-2:22-26. doi:https://doi.org/10.1016/j.btre.2014.04.001

32. Sieblist C, Jenzsch M, Pohlscheidt M, Lubbert A. Insights into large-scale cell-culture reactors: I. Liquid mixing and oxygen supply. *Biotechnol J*. Dec 2011;6(12):1532-46. doi:10.1002/biot.201000408

33. Paul Smelko J, Rae Wiltberger K, Francis Hickman E, Janey Morris B, James Blackburn T, Ryll T. Performance of high intensity fed-batch mammalian cell cultures in disposable bioreactor systems. *Biotechnology Progress*. 2011;27(5):1358-1364. doi:https://doi.org/10.1002/btpr.634

34. Sherman M, Lam V, Carpio M, Hutchinson N, Fenge C. Continuous cell culture operation at 2,000-L scale. *BioProcess International*. 2016;14(10)

35. Dorceus M. Cell Culture Scale-Up in Stirred-Tank Single-Use Bioreactors. *BioProcess Int*. 2018;

36. Kaisermayer C, Yang J. Highly efficient inoculum propagation in perfusion culture using WAVE Bioreactor™ systems. *BMC Proceedings*. 2013/12/04 2013;7(6):P7. doi:10.1186/1753-6561-7-S6-P7

37. Wright B, Bruninghaus M, Vrabel M, et al. A novel seed-train process: Using high-density cell banking, a disposable bioreactor, and perfusion technologies. *BioProcess International*. 03/01 2015;13

38. Imseng N, Steiger N, Frasson D, et al. Single-use wave-mixed versus stirred bioreactors for insect-cell/BEVS-based protein expression at benchtop scale. *Engineering in Life Sciences*. 05/01 2014;14doi:10.1002/elsc.201300131

39. Busse C, Biechele P, de Vries I, Reardon KF, Solle D, Scheper T. Sensors for disposable bioreactors. *Engineering in Life Sciences*. 2017;17(8):940-952. doi:10.1002/elsc.201700049

40. Nienow AW. Aeration in Biotechnology. *Kirk-Othmer Encyclopedia of Chemical Technology*. 2015:1-23.

41. Hsu WT, Aulakh RP, Traul DL, Yuk IH. Advanced microscale bioreactor system: a representative scale-down model for bench-top bioreactors. *Cytotechnology*. Dec 2012;64(6):667-78. doi:10.1007/s10616-012-9446-1

42. Nienow AW, Rielly CD, Brosnan K, et al. The physical characterisation of a microscale parallel bioreactor platform with an industrial CHO cell line expressing an IgG4. *Biochemical Engineering Journal*. 2013/07/15/ 2013;76:25-36. doi:https://doi.org/10.1016/j.bej.2013.04.011

43. Zhang X, Moroney J, Hoshan L, Jiang R, Xu S. Systematic evaluation of high-throughput scale-down models for single-use bioreactors (SUB) using volumetric gas flow rate as the criterion. *Biochemical Engineering Journal*. 2019/11/15/ 2019;151:107307. doi:https://doi.org/10.1016/j.bej.2019.107307

44. Xu S, Jiang R, Mueller R, et al. Probing lactate metabolism variations in large-scale bioreactors. *Biotechnology Progress*. 2018;34(3):756-766. doi:10.1002/btpr.2620

45. Xing Z, Kenty BM, Li ZJ, Lee SS. Scale-up analysis for a CHO cell culture process in large-scale bioreactors. *Biotechnology and Bioengineering*. 2009;103(4):733-746. doi:10.1002/bit.22287

46. Hoshan L, Jiang R, Moroney J, et al. Effective bioreactor pH control using only sparging gases. *Biotechnology Progress*. 2019;35(1):e2743. doi:10.1002/btpr.2743

47. He C, Ye P, Wang H, Liu X, Li F. A systematic mass-transfer modeling approach for mammalian cell culture bioreactor scale-up. *Biochemical Engineering Journal*. 2019/01/15/ 2019;141:173-181. doi:https://doi.org/10.1016/j.bej.2018.09.019

48. Xing Z, Lewis AM, Borys MC, Li ZJ. A carbon dioxide stripping model for mammalian cell culture in manufacturing scale bioreactors. *Biotechnology and Bioengineering*. 2017;114(6):1184-1194. doi:10.1002/bit.26232

49. Baez A, Shiloach J. Effect of elevated oxygen concentration on bacteria, yeasts, and cells propagated for production of biological compounds. *Microbial cell factories*. 2014;13:181-181. doi:10.1186/s12934-014-0181-5

50. Handlogten MW, Zhu M, Ahuja S. Intracellular response of CHO cells to oxidative stress and its influence on metabolism and antibody production. *Biochemical Engineering Journal*. 2018/05/15/ 2018;133:12-20. doi:https://doi.org/10.1016/j.bej.2018.01.031

51. Gao Y, Ray S, Dai S, et al. Combined metabolomics and proteomics reveals hypoxia as a cause of lower productivity on scale-up to a 5000-liter CHO bioprocess. *Biotechnology Journal*. 2016;11(9):1190-1200. doi:10.1002/biot.201600030

52. Velez-Suberbie ML, Tarrant RDR, Tait AS, Spencer DIR, Bracewell DG. Impact of aeration strategy on CHO cell performance during antibody production. *Biotechnology Progress*. 2013;29(1):116-126. doi:10.1002/btpr.1647

53. Nienow AW. Reactor engineering in large scale animal cell culture. *Cytotechnology*. 2006;50(1-3):9-33. doi:10.1007/s10616-006-9005-8

54. Tharmalingam T, Goudar CT. Evaluating the impact of high Pluronic® F68 concentrations on antibody producing CHO cell lines. *Biotechnology and Bioengineering*. 2015;112(4):832-837. doi:https://doi.org/10.1002/bit.25491

55. Van't Riet K. Review of Measuring Methods and Results in Nonviscous Gas-Liquid Mass Transfer in Stirred Vessels. *Industrial & Engineering Chemistry Process Design and Development*. 1979/07/01 1979;18(3):357-364. doi:10.1021/i260071a001

56. Mostafa SS, Gu X. Strategies for improved dCO2 removal in large-scale fed-batch cultures. *Biotechnol Prog*. Jan-Feb 2003;19(1):45-51. doi:10.1021/bp0256263

57. Matsunaga N, Kano K, Maki Y, Dobashi T. Culture scale-up studies as seen from the viewpoint of oxygen supply and dissolved carbon dioxide stripping. *Journal of Bioscience and Bioengineering*. 2009;107(4):412-418. doi:10.1016/j.jbiosc.2008.12.016

58. Xu S, Hoshan L, Jiang R, et al. A practical approach in bioreactor scale-up and process transfer using a combination of constant P/V and vvm as the criterion. *Biotechnology Progress*. 2017;33(4):1146-1159. doi:10.1002/btpr.2489

59. Dreher T, Husemann U, Adams T, de Wilde D, Greller G. Design space definition for a stirred single-use bioreactor family from 50 to 2000 L scale. *Engineering in Life Sciences*. 2014;14(3):304-310. doi:10.1002/elsc.201300067

60. Blombach B, Takors R. CO2 - Intrinsic Product, Essential Substrate, and Regulatory Trigger of Microbial and Mammalian Production Processes. *Front Bioeng Biotechnol*. 2015;3:108-108. doi:10.3389/fbioe.2015.00108

61. Pattison RN, Swamy J, Mendenhall B, Hwang C, Frohlich BT. Measurement and Control of Dissolved Carbon Dioxide in Mammalian Cell Culture Processes Using an in Situ Fiber Optic Chemical Sensor. *Biotechnology Progress*. 2000;16(5):769-774. doi:https://doi.org/10.1021/bp000089c

62. Takuma S, Hirashima C, Piret JM. Effects of Glucose and CO2 Concentrations on CHO Cell Physiology. Springer Netherlands; 2003:99-103.

63. Zhu MM, Goyal A, Rank DL, Gupta SK, Boom TV, Lee SS. Effects of Elevated pCO2 and Osmolality on Growth of CHO Cells and Production of Antibody-Fusion Protein B1: A Case Study. *Biotechnology Progress*. 2005;21(1):70-77. doi:10.1021/bp049815s

64. Matanguihan R, Sajan E, Zachariou M, et al. Solution to the high Dissolved CO2 Problem in High-Density Perfusion Culture of Mammalian Cells. In: Lindner-Olsson E, Chatzissavidou N, Lüllau E, eds. *Animal Cell Technology: From Target to Market: Proceedings of the 17th ESACT Meeting Tylösand, Sweden, June 10–14, 2001*. Springer Netherlands; 2001:399-402.

65. Hossler P, Khattak SF, Li ZJ. Optimal and consistent protein glycosylation in mammalian cell culture. *Glycobiology*. Sep 2009;19(9):936-49. doi:10.1093/glycob/cwp079

66. Min Lee G, Koo J. Osmolarity effects, Chinese hamster ovary cell culture. *Encyclopedia of Industrial Biotechnology: Bioprocess, Bioseparation, and Cell Technology*. 2009:1-8.

67. Ryu JS, Lee GM. Application of hypoosmolar medium to fed-batch culture of hybridoma cells for improvement of culture longevity. *Biotechnology and Bioengineering*. 1999;62(1):120-123. doi:https://doi.org/10.1002/(SICI)1097-0290(19990105)62:1<120::AID-BIT14>3.0.CO;2-R

68. Sieblist C, Hageholz O, Aehle M, Jenzsch M, Pohlscheidt M, Lubbert A. Insights into large-scale cell-culture reactors: II. Gas-phase mixing and CO(2) stripping. *Biotechnol J*. Dec 2011;6(12):1547-56. doi:10.1002/biot.201100153

69. Wang C, Wang J, Chen M, Fan L, Zhao L, Tan W-S. Ultra-low carbon dioxide partial pressure improves the galactosylation of a monoclonal antibody produced in Chinese hamster ovary cells in a bioreactor. *Biotechnology Letters*. 2018;40(8):1201-1208. doi:10.1007/s10529-018-2586-4

70. Xu S, Bowers J, Seamans TC, Nyberg G. Bioreactor Scale-Up. *Kirk-Othmer Encyclopedia of Chemical Technology*. 2018:1-35.

71. Sieblist C, Jenzsch M, Pohlscheidt M. Equipment characterization to mitigate risks during transfers of cell culture manufacturing processes. *Cytotechnology*. 2016;68(4):1381-1401. doi:10.1007/s10616-015-9899-0

72. Paul K, Herwig C. Scale-down simulators for mammalian cell culture as tools to access the impact of inhomogeneities occurring in large-scale bioreactors. *Engineering in Life Sciences*. 2020;20(5-6):197-204. doi:10.1002/elsc.201900162

73. Restelli V, Wang M-D, Huzel N, Ethier M, Perreault H, Butler M. The effect of dissolved oxygen on the production and the glycosylation profile of recombinant human erythropoietin produced from CHO cells. *Biotechnology and Bioengineering*. 2006;94(3):481-494. doi:10.1002/bit.20875

74. Brunner M, Braun P, Doppler P, et al. The impact of pH inhomogeneities on CHO cell physiology and fed-batch process performance - two-compartment scale-down modelling and intracellular pH excursion. *Biotechnol J*. Jul 2017;12(7)doi:10.1002/biot.201600633

75. Boulton-Stone JM, Blake JR. Gas bubbles bursting at a free surface. *Journal of Fluid Mechanics*. 1993;254:437-466. doi:10.1017/S0022112093002216

76. Keane JT, Ryan D, Gray PP. Effect of shear stress on expression of a recombinant protein by Chinese hamster ovary cells. *Biotechnology and Bioengineering*. 2003;81(2):211-220. doi:10.1002/bit.10472

77. Johnson C, Natarajan V, Antoniou C. Verification of energy dissipation rate scalability in pilot and production scale bioreactors using computational fluid dynamics. *Biotechnology Progress*. 2014;30(3):760-764. doi:10.1002/btpr.1896

78. Hu W, Berdugo C, Chalmers JJ. The potential of hydrodynamic damage to animal cells of industrial relevance: current understanding. *Cytotechnology*. 2011;63(5):445-460. doi:10.1007/s10616-011-9368-3

79. Sieck JB, Cordes T, Budach WE, et al. Development of a Scale-Down Model of hydrodynamic stress to study the performance of an industrial CHO cell line under simulated production scale bioreactor conditions. *Journal of Biotechnology*. 2013/03/10/ 2013;164(1):41-49. doi:https://doi.org/10.1016/j.jbiotec.2012.11.012

80. Sabourin M, Huang Y, Dhulipala P, et al. Increasing antibody yield and modulating final product quality using the Freedom(TM) CHO-S(TM) production platform. *BMC proceedings*. 2011;5 Suppl 8(Suppl 8):P102-P102. doi:10.1186/1753-6561-5-S8-P102

81. Ramirez OT, Mutharasan R. The role of the plasma membrane fluidity on the shear sensitivity of hybridomas grown under hydrodynamic stress. *Biotechnology and bioengineering*. 1990;36(9):911-920.

82. Zhang Z, Al-Rubeai M, Thomas CR. Effect of Pluronic F-68 on the mechanical properties of mammalian cells. *Enzyme and Microbial Technology*. 1992/12/01/ 1992;14(12):980-983. doi:https://doi.org/10.1016/0141-0229(92)90081-X

83. Gigout A, Buschmann MD, Jolicoeur M. The fate of Pluronic F-68 in chondrocytes and CHO cells. *Biotechnology and Bioengineering*. 2008;100(5):975-987. doi:10.1002/bit.21840

84. Doi T, Kajihara H, Chuman Y, Kuwae S, Kaminagayoshi T, Omasa T. Development of a scale-up strategy for Chinese hamster ovary cell culture processes using the kL a ratio as a direct indicator of gas stripping conditions. *Biotechnol Prog*. Apr 16 2020;n/a(n/a):e3000. doi:10.1002/btpr.3000

85. Alsayyari AA, Pan X, Dalm C, et al. Transcriptome analysis for the scale-down of a CHO cell fed-batch process. *J Biotechnol*. Aug 10 2018;279:61-72. doi:10.1016/j.jbiotec.2018.05.012

86. Manahan M, Nelson M, Cacciatore JJ, Weng J, Xu S, Pollard J. Scale-down model qualification of ambr® 250 high-throughput mini-bioreactor system for two commercial-scale mAb processes. *Biotechnology Progress*. 2019;35(6):e2870. doi:10.1002/btpr.2870

87. Ruhl S, de Almeida N, Carpio M, Rupprecht J, Greller G, Matuszczyk J-C. A Rapid, Low-Risk Approach Process Transfer of Biologics from Development to Manufacturing Scale. *BioProcess International*. 2020;18:5.

88. Gimenez L, Simonet C, Malphettes L. Scale-up considerations for monoclonal antibody production process: an oxygen transfer flux approach. *BMC Proceedings*. 2013;7(Suppl 6):P49-P49. doi:10.1186/1753-6561-7-S6-P49

89. Xu S, Gavin J, Jiang R, Chen H. Bioreactor productivity and media cost comparison for different intensified cell culture processes. *Biotechnology progress*. 2017;33(4):867-878.

90. De Wilde D, Dreher T, Zahnow C, et al. Superior scalability of single-use bioreactors. *Innovations in Cell Culture*. 2014;14:14-19.

91. Metze S, Ruhl S, Greller G, Grimm C, Scholz J. Monitoring online biomass with a capacitance sensor during scale-up of industrially relevant CHO cell culture fed-batch processes in single-use bioreactors. *Bioprocess and biosystems engineering*. 2020;43(2):193-205. doi:10.1007/s00449-019-02216-4

92. Nienow AW, Scott WH, Hewitt CJ, et al. Scale-down studies for assessing the impact of different stress parameters on growth and product quality during animal cell culture. *Chemical Engineering Research and Design*. 2013;91(11):2265-2274. doi:10.1016/j.cherd.2013.04.002

93. Shuler ML, Kargi F. *Bioprocess Engineering: Basic Concepts*. Second Edition ed. Prentice Hall; 2001.

94. Platas Barradas O, Jandt U, Minh Phan LD, et al. Evaluation of criteria for bioreactor comparison and operation standardization for mammalian cell culture. *Engineering in Life Sciences*. 2012;12(5):518-528. doi:https://doi.org/10.1002/elsc.201100163

95. Serrato JA, Palomares LA, Meneses-Acosta A, Ramírez OT. Heterogeneous conditions in dissolved oxygen affect N-glycosylation but not productivity of a monoclonal antibody in hybridoma cultures. *Biotechnology and Bioengineering*. 2004;88(2):176-188. doi:10.1002/bit.20232

96. Tescione L, Lambropoulos J, Paranandi MR, Makagiansar H, Ryll T. Application of bioreactor design principles and multivariate analysis for development of cell culture scale down models. *Biotechnol Bioeng*. Jan 2015;112(1):84-97. doi:10.1002/bit.25330

97. Marks DM. Equipment design considerations for large scale cell culture. *Cytotechnology*. 2003;42(1):21-33. doi:10.1023/A:1026103405618

98. Janakiraman V, Kwiatkowski C, Kshirsagar R, Ryll T, Huang YM. Application of high-throughput mini-bioreactor system for systematic scale-down modeling, process characterization, and control strategy development. *Biotechnology Progress*. 2015;31(6):1623-1632. doi:10.1002/btpr.2162

99. Nie L, Gao D, Jiang H, et al. Development and Qualification of a Scale-Down Mammalian Cell Culture Model and Application in Design Space Development by Definitive Screening Design. *AAPS PharmSciTech*. 2019/07/08 2019;20(6):246. doi:10.1208/s12249-019-1451-7

100. Möller J, Hernández Rodríguez T, Müller J, et al. Model uncertainty-based evaluation of process strategies during scale-up of biopharmaceutical processes. *Computers & Chemical Engineering*. 2020/03/04/ 2020;134:106693. doi:https://doi.org/10.1016/j.compchemeng.2019.106693

101. Chaudhary G, Luo R, George M, Tescione L, Khetan A, Lin H. Understanding the effect of high gas entrance velocity on Chinese hamster ovary (CHO) cell culture performance and its implications on bioreactor scale-up and sparger design. *Biotechnology and Bioengineering*. 2020;117(6):1684-1695. doi:10.1002/bit.27314

102. Hong JK, Yeo HC, Lakshmanan M, et al. In silico model-based characterization of metabolic response to harsh sparging stress in fed-batch CHO cell cultures. *Journal of Biotechnology*. 2020/01/20/ 2020;308:10-20. doi:https://doi.org/10.1016/j.jbiotec.2019.11.011

103. Varley J, Birch J. Reactor design for large scale suspension animal cell culture. *Cytotechnology*. 1999/03/01 1999;29(3):177. doi:10.1023/A:1008008021481

104. Li X, Scott K, Kelly WJ, Huang Z. Development of a Computational Fluid Dynamics Model for Scaling-up Ambr Bioreactors. *Biotechnology and Bioprocess Engineering*. 2018/11/01 2018;23(6):710-725. doi:10.1007/s12257-018-0063-5

105. Wutz J, Steiner R, Assfalg K, Wucherpfennig T. Establishment of a CFD-based kLa model in microtiter plates to support CHO cell culture scale-up during clone selection. *Biotechnology Progress*. 2018;34(5):1120-1128. doi:10.1002/btpr.2707

106. Wutz J, Lapin A, Siebler F, et al. Predictability of kLa in stirred tank reactors under multiple operating conditions using an Euler–Lagrange approach. *Engineering in Life Sciences*. 2016;16(7):633-642. doi:10.1002/elsc.201500135

107. Villiger TK, Neunstoecklin B, Karst DJ, et al. Experimental and CFD physical characterization of animal cell bioreactors: From micro- to production scale. *Biochemical Engineering Journal*. 2018/03/15/ 2018;131:84-94. doi:https://doi.org/10.1016/j.bej.2017.12.004

108. Scully J, Considine LB, Smith MT, et al. Beyond heuristics: CFD-based novel multiparameter scale-up for geometrically disparate bioreactors demonstrated at industrial 2kL–10kL scales. *Biotechnology and Bioengineering*. 2020;117(6):1710-1723. doi:10.1002/bit.27323

109. Maltby R, Lewis W, Wright S, Smith A, Chew J. Multiphase CFD modelling of single-use-technology bioreactors for industrial biotechnology applications. Emerald Group Publishing Ltd.; 2016:

110. Amer M, Feng Y, Ramsey JD. Using CFD simulations and statistical analysis to correlate oxygen mass transfer coefficient to both geometrical parameters and operating conditions in a stirred-tank bioreactor. *Biotechnology Progress*. 2019;35(3):e2785. doi:10.1002/btpr.2785

111. Li C, Teng X, Peng H, et al. Novel scale-up strategy based on three-dimensional shear space for animal cell culture. *Chemical Engineering Science*. 2020/02/02/ 2020;212:115329. doi:https://doi.org/10.1016/j.ces.2019.115329

112. Delafosse A, Calvo S, Collignon M-L, Toye D. Comparison of hydrodynamics in standard stainless steel and single-use bioreactors by means of an Euler-Lagrange approach. *Chemical Engineering Science*. 2018/10/12/ 2018;188:52-64. doi:https://doi.org/10.1016/j.ces.2018.01.034

113. Borys BS, Le A, Roberts EL, et al. Using computational fluid dynamics (CFD) modeling to understand murine embryonic stem cell aggregate size and pluripotency distributions in stirred suspension bioreactors. *Journal of Biotechnology*. 2019/10/10/ 2019;304:16-27. doi:https://doi.org/10.1016/j.jbiotec.2019.08.002

114. Zhu L, Song B, Wang Z. Developing an orbitally shaken bioreactor featuring a hollow cylinder vessel wall. *Journal of Chemical Technology & Biotechnology*. 2019;94(7):2212-2218. doi:10.1002/jctb.6005

115. Paul K, Böttinger K, Mitic BM, et al. Development, characterization, and application of a 2-Compartment system to investigate the impact of pH inhomogeneities in large-scale CHO-based processes. *Engineering in Life Sciences*. 2020;20(8):368-378. doi:https://doi.org/10.1002/elsc.202000009

116. Stepper L, Filser FA, Fischer S, Schaub J, Gorr I, Voges R. Pre-stage perfusion and ultra-high seeding cell density in CHO fed-batch culture: a case study for process intensification guided by systems biotechnology. *Bioprocess and Biosystems Engineering*. 2020/08/01 2020;43(8):1431-1443. doi:10.1007/s00449-020-02337-1

117. Xu J, Rehmann MS, Xu M, et al. Development of an intensified fed-batch production platform with doubled titers using N-1 perfusion seed for cell culture manufacturing. *Bioresources and Bioprocessing*. 2020/03/23 2020;7(1):17. doi:10.1186/s40643-020-00304-y

118. Yongky A, Xu J, Tian J, et al. Process intensification in fed-batch production bioreactors using non-perfusion seed cultures. *mAbs*. 2019/11/17 2019;11(8):1502-1514. doi:10.1080/19420862.2019.1652075

119. Pollock J, Coffman J, Ho SV, Farid SS. Integrated continuous bioprocessing: Economic, operational, and environmental feasibility for clinical and commercial antibody manufacture. *Biotechnology progress*. 2017;33(4):854-866. doi:10.1002/btpr.2492

120. Bielser J-M, Wolf M, Souquet J, Broly H, Morbidelli M. Perfusion mammalian cell culture for recombinant protein manufacturing – A critical review. *Biotechnology Advances*. 2018/07/01/ 2018;36(4):1328-1340. doi:https://doi.org/10.1016/j.biotechadv.2018.04.011

121. Warikoo V, Godawat R, Brower K, et al. Integrated continuous production of recombinant therapeutic proteins. *Biotechnology and bioengineering*. 2012;109(12):3018-3029.

122. Lim J, Sinclair A, Shevitz J, Bonham-Carter J. An economic comparison of three cell culture techniques. *BioPharm International*. 2011;24(2):54-60.

123. Raja V, Desan S, Bhatnagar A, Goel A, Iyer H. Challenges in scaling up a perfusion process. *BMC proceedings*. 2011;5 Suppl 8(Suppl 8):P122-P122. doi:10.1186/1753-6561-5-S8-P122

124. Matzmorr W. Integrating Technology Transfer and Facilities Startup for Biologics. *BioPharm International*. 2016;29(46-48)

125. Xu G, Yu C, Wang W, et al. Quality comparability assessment of a SARS-CoV-2-neutralizing antibody across transient, mini-pool-derived and single-clone CHO cells. *mAbs*. 2022/12/31 2022;14(1):2005507. doi:10.1080/19420862.2021.2005507

126. Ye J, Alvin K, Latif H, et al. Rapid protein production using CHO stable transfection pools. *Biotechnology Progress*. 2010;26(5):1431-1437. doi:https://doi.org/10.1002/btpr.469

127. Reyes S-J, Lemire L, Molina R-S, et al. Multivariate data analysis of process parameters affecting the growth and productivity of stable Chinese hamster ovary cell pools expressing SARS-CoV-2 spike protein as vaccine antigen in early process development. *Biotechnology Progress*. 2024;40(5):e3467. doi:https://doi.org/10.1002/btpr.3467

128. Liu Y, Zhang L, Zhou L. Development of modeling and simulation of bubble-liquid hydrodynamics in bubble column. *Energy Science & Engineering*. 2020;8(2):327-339.

129. Tran TT, Lee EG, Lee IS, et al. Hydrodynamic extensional stress during the bubble bursting process for bioreactor system design. *Korea-Australia Rheology Journal*. 2016/11/01 2016;28(4):315-326. doi:10.1007/s13367-016-0032-5

130. Walls PLL, McRae O, Natarajan V, Johnson C, Antoniou C, Bird JC. Quantifying the potential for bursting bubbles to damage suspended cells. *Sci Rep*. Nov 8 2017;7(1):15102. doi:10.1038/s41598-017-14531-5

131. Stuible M, Gervais C, Lord-Dufour S, et al. Rapid, high-yield production of full-length SARS-CoV-2 spike ectodomain by transient gene expression in CHO cells. *Journal of biotechnology*. 2021;326:21-27.

132. Buchsteiner M, Quek L-E, Gray P, Nielsen LK. Improving culture performance and antibody production in CHO cell culture processes by reducing the Warburg effect. *Biotechnology and Bioengineering*. 2018/09/01 2018;115(9):2315-2327. doi:https://doi.org/10.1002/bit.26724

133. Brunner M, Doppler P, Klein T, Herwig C, Fricke J. Elevated pCO2 affects the lactate metabolic shift in CHO cell culture processes. *Engineering in Life Sciences*. 2018;18(3):204-214. doi:10.1002/elsc.201700131

134. Wurm FM, Wurm MJ. Cloning of CHO Cells, Productivity and Genetic Stability—A Discussion. *Processes*. 2017;5(2):20.

135. Joubert S, Stuible M, Lord-Dufour S, et al. A CHO stable pool production platform for rapid clinical development of trimeric SARS-CoV-2 spike subunit vaccine antigens. *Biotechnology and Bioengineering*. 2023;120(7):1746-1761. doi:https://doi.org/10.1002/bit.28387

136. Barnard GC, Zhou M, Shen A, Yuk IH, Laird MW. Utilizing targeted integration CHO pools to potentially accelerate the GMP manufacturing of monoclonal and bispecific antibodies. *Biotechnol Prog*. Jan-Feb 2024;40(1):e3399. doi:10.1002/btpr.3399

137. Joubert S, Guimond J, Perret S, et al. Production of afucosylated antibodies in CHO cells by coexpression of an anti-FUT8 intrabody. *Biotechnology and Bioengineering*. 2022;119(8):2206-2220. doi:https://doi.org/10.1002/bit.28127

138. Srirangan K, Loignon M, Durocher Y. The use of site-specific recombination and cassette exchange technologies for monoclonal antibody production in Chinese Hamster ovary cells: retrospective analysis and future directions. *Critical Reviews in Biotechnology*. 2020/08/17 2020;40(6):833-851. doi:10.1080/07388551.2020.1768043

139. Huang Z, Xu J, Yongky A, et al. CHO cell productivity improvement by genome-scale modeling and pathway analysis: Application to feed supplements. *Biochemical Engineering Journal*. 2020/08/15/ 2020;160:107638. doi:https://doi.org/10.1016/j.bej.2020.107638

140. Goudar CT, Matanguihan R, Long E, et al. Decreased pCO(2) accumulation by eliminating bicarbonate addition to high cell-density cultures. *Biotechnol Bioeng*. Apr 15 2007;96(6):1107-17. doi:10.1002/bit.21116

141. Lemire L, Pham PL, Durocher Y, Henry O. Practical Considerations for the Scale-Up of Chinese Hamster Ovary (CHO) Cell Cultures. *Cell Culture Engineering and Technology*. Springer; 2021:367-400.

142. Lu S, Sun X, Zhang Y. Insight into metabolism of CHO cells at low glucose concentration on the basis of the determination of intracellular metabolites. *Process Biochemistry*. 2005/04/01/ 2005;40(5):1917-1921. doi:https://doi.org/10.1016/j.procbio.2004.07.004

143. Vergara M, Torres M, Müller A, et al. High glucose and low specific cell growth but not mild hypothermia improve specific r-protein productivity in chemostat culture of CHO cells. *PLOS ONE*. 2018;13(8):e0202098. doi:10.1371/journal.pone.0202098

144. Sellick CA, Croxford AS, Maqsood AR, et al. Metabolite profiling of CHO cells: Molecular reflections of bioprocessing effectiveness. *Biotechnology Journal*. 2015;10(9):1434-1445. doi:https://doi.org/10.1002/biot.201400664

145. Sellick CA, Croxford AS, Maqsood AR, et al. Metabolite profiling of recombinant CHO cells: designing tailored feeding regimes that enhance recombinant antibody production. *Biotechnology and bioengineering*. 2011;108(12):3025-3031.

146. Tabuchi H, Sugiyama T. Cooverexpression of alanine aminotransferase 1 in Chinese hamster ovary cells overexpressing taurine transporter further stimulates metabolism and enhances product yield. *Biotechnology and Bioengineering*. 2013/08/01 2013;110(8):2208-2215. doi:https://doi.org/10.1002/bit.24881

147. Li J, Wong CL, Vijayasankaran N, Hudson T, Amanullah A. Feeding lactate for CHO cell culture processes: Impact on culture metabolism and performance. *Biotechnology and Bioengineering*. 2012;109(5):1173-1186. doi:https://doi.org/10.1002/bit.24389

148. Reinhart D, Damjanovic L, Kaisermayer C, Kunert R. Benchmarking of commercially available CHO cell culture media for antibody production. *Applied Microbiology and Biotechnology*. 2015/06/01 2015;99(11):4645-4657. doi:10.1007/s00253-015-6514-4

149. Mulukutla BC, Kale J, Kalomeris T, Jacobs M, Hiller GW. Identification and control of novel growth inhibitors in fed-batch cultures of Chinese hamster ovary cells. *Biotechnology and Bioengineering*. 2017;114(8):1779-1790. doi:https://doi.org/10.1002/bit.26313

150. Reyes S-J, Pham PL, Durocher Y, Henry O. CHO stable pool fed-batch process development of SARS-CoV-2 spike protein production: Impact of aeration conditions and feeding strategies. *Biotechnology Progress*. 2024;(n/a):e3507. doi:https://doi.org/10.1002/btpr.3507

151. Chen P, Harcum SW. Effects of elevated ammonium on glycosylation gene expression in CHO cells. *Metabolic Engineering*. 2006/03/01/ 2006;8(2):123-132. doi:https://doi.org/10.1016/j.ymben.2005.10.002

152. Nienow AW. Scale-up, stirred tank reactors. *Encyclopedia of Industrial Biotechnology: Bioprocess, Bioseparation, and Cell Technology*. 2009:1-38.

153. Fisher JT, Gurney TO, Mason BM, Fisher JK, Kelly WJ. Mixing and oxygen transfer characteristics of a microplate bioreactor with surface-attached microposts. *Biotechnol J*. May 2021;16(5):e2000257. doi:10.1002/biot.202000257

154. Furukawa H, Kamiya T, Kato Y. Correlation of Power Consumption of Double Impeller Based on Impeller Spacing in Laminar Region. *International Journal of Chemical Engineering*. 2019/10/16 2019;2019:4564589. doi:10.1155/2019/4564589

155. Gogate PR, Beenackers AACM, Pandit AB. Multiple-impeller systems with a special emphasis on bioreactors: a critical review. *Biochemical Engineering Journal*. 2000/10/01/ 2000;6(2):109-144. doi:https://doi.org/10.1016/S1369-703X(00)00081-4

156. Urlaub G, Chasin LA. Isolation of Chinese hamster cell mutants deficient in dihydrofolate reductase activity. *Proceedings of the National Academy of Sciences*. 1980;77(7):4216-4220.

157. Coulet M, Kepp O, Kroemer G, Basmaciogullari S. Metabolic Profiling of CHO Cells during the Production of Biotherapeutics. *Cells*. Jun 15 2022;11(12)doi:10.3390/cells11121929

158. Takagi M, Hayashi H, Yoshida T. The effect of osmolarity on metabolism and morphology in adhesion and suspension chinese hamster ovary cells producing tissue plasminogen activator. *Cytotechnology*. 2000/03/01 2000;32(3):171-179. doi:10.1023/A:1008171921282

159. Han YK, Kim Y-G, Kim JY, Lee GM. Hyperosmotic stress induces autophagy and apoptosis in recombinant Chinese hamster ovary cell culture. *Biotechnology and Bioengineering*. 2010;105(6):1187-1192. doi:https://doi.org/10.1002/bit.22643

160. Kim NS, Lee GM. Response of recombinant Chinese hamster ovary cells to hyperosmotic pressure: effect of Bcl-2 overexpression. *Journal of Biotechnology*. 2002/05/23/ 2002;95(3):237-248. doi:https://doi.org/10.1016/S0168-1656(02)00011-1

161. Kochanowski N, Siriez G, Roosens S, Malphettes L. Medium and feed optimization for fed-batch production of a monoclonal antibody in CHO cells. *BMC Proceedings*. 2011/11/22 2011;5(8):P75. doi:10.1186/1753-6561-5-S8-P75

162. Kamachi Y, Omasa T. Development of hyper osmotic resistant CHO host cells for enhanced antibody production. *Journal of Bioscience and Bioengineering*. 2018/04/01/ 2018;125(4):470-478. doi:https://doi.org/10.1016/j.jbiosc.2017.11.002

163. Pereira S, Kildegaard HF, Andersen MR. Impact of CHO Metabolism on Cell Growth and Protein Production: An Overview of Toxic and Inhibiting Metabolites and Nutrients. *Biotechnology Journal*. 2018;13(3):1700499. doi:https://doi.org/10.1002/biot.201700499

164. Alhuthali S, Kotidis P, Kontoravdi C. Osmolality Effects on CHO Cell Growth, Cell Volume, Antibody Productivity and Glycosylation. *Int J Mol Sci*. Mar 24 2021;22(7)doi:10.3390/ijms22073290

165. Shen D, Kiehl TR, Khattak SF, et al. Transcriptomic responses to sodium chloride-induced osmotic stress: A study of industrial fed-batch CHO cell cultures. *Biotechnology Progress*. 2010;26(4):1104-1115. doi:https://doi.org/10.1002/btpr.398

166. Kiehl TR, Shen D, Khattak SF, Jian Li Z, Sharfstein ST. Observations of cell size dynamics under osmotic stress. *Cytometry Part A*. 2011;79A(7):560-569. doi:https://doi.org/10.1002/cyto.a.21076

167. Pan X, Dalm C, Wijffels RH, Martens DE. Metabolic characterization of a CHO cell size increase phase in fed-batch cultures. *Appl Microbiol Biotechnol*. Nov 2017;101(22):8101-8113. doi:10.1007/s00253-017-8531-y

168. Lloyd DR, Holmes P, Jackson LP, Emery AN, Al-Rubeai M. Relationship between cell size, cell cycle and specific recombinant protein productivity. *Cytotechnology*. Oct 2000;34(1-2):59-70. doi:10.1023/a:1008103730027

169. Zagari F, Jordan M, Stettler M, Broly H, Wurm FM. Lactate metabolism shift in CHO cell culture: the role of mitochondrial oxidative activity. *New biotechnology*. 2013;30(2):238-245.

170. Betts JPJ, Warr SRC, Finka GB, et al. Impact of aeration strategies on fed-batch cell culture kinetics in a single-use 24-well miniature bioreactor. *Biochemical Engineering Journal*. 2014/01/15/ 2014;82:105-116. doi:https://doi.org/10.1016/j.bej.2013.11.010

171. Neuss A, Tomas Borges JS, von Vegesack N, Büchs J, Magnus JB. Impact of hydromechanical stress on CHO cells' metabolism and productivity: Insights from shake flask cultivations with online monitoring of the respiration activity. *New Biotechnology*. 2024/12/25/ 2024;84:96-104. doi:https://doi.org/10.1016/j.nbt.2024.09.008

172. Halestrap AP, Price NT. The proton-linked monocarboxylate transporter (MCT) family: structure, function and regulation. *Biochemical Journal*. 1999;343(2):281-299. doi:10.1042/bj3430281

173. Hartley F, Walker T, Chung V, Morten K. Mechanisms driving the lactate switch in Chinese hamster ovary cells. *Biotechnology and Bioengineering*. 2018;115(8):1890-1903. doi:https://doi.org/10.1002/bit.26603

174. Halestrap AP, Wilson MC. The monocarboxylate transporter family—Role and regulation. *IUBMB Life*. 2012;64(2):109-119. doi:https://doi.org/10.1002/iub.572

175. Bokelmann C, Ehsani A, Schaub J, Stiefel F. Deciphering Metabolic Pathways in High Seeding Density Fed-Batch Processes for Monoclonal Antibody Production: A Computational Modeling Perspective. 2024;

176. Schulze M, Niemann J, Wijffels RH, Matuszczyk J, Martens DE. Rapid intensification of an established CHO cell fed-batch process. *Biotechnology Progress*. 2022;38(1):e3213. doi:https://doi.org/10.1002/btpr.3213

177. Mahé A, Martiné A, Fagète S, Girod P-A. Exploring the limits of conventional small-scale CHO fed-batch for accelerated on demand monoclonal antibody production. *Bioprocess and Biosystems Engineering*. 2022/02/01 2022;45(2):297-307. doi:10.1007/s00449-021-02657-w

178. Olin M, Wolnick N, Crittenden H, et al. An automated high inoculation density fed-batch bioreactor, enabled through N-1 perfusion, accommodates clonal diversity and doubles titers. *Biotechnology Progress*. 2024;40(2):e3410. doi:https://doi.org/10.1002/btpr.3410

179. Woodside SM, Bowen BD, Piret JM. Mammalian cell retention devices for stirred perfusion bioreactors. *Cytotechnology*. 1998/11/01 1998;28(1):163-175. doi:10.1023/A:1008050202561

180. MacDonald MA, Nöbel M, Roche Recinos D, et al. Perfusion culture of Chinese Hamster Ovary cells for bioprocessing applications. *Critical reviews in biotechnology*. 2022;42(7):1099-1115.

181. Clincke M-F, Mölleryd C, Zhang Y, Lindskog E, Walsh K, Chotteau V. Very high density of CHO cells in perfusion by ATF or TFF in WAVE bioreactor™. Part I. Effect of the cell density on the process. *Biotechnology Progress*. 2013;29(3):754-767. doi:https://doi.org/10.1002/btpr.1704

182. Rittershaus ESC, Rehmann MS, Xu J, et al. N-1 Perfusion Platform Development Using a Capacitance Probe for Biomanufacturing. *Bioengineering*. 2022;9(4):128.

183. Mayrhofer P, Castan A, Kunert R. Shake tube perfusion cell cultures are suitable tools for the prediction of limiting substrate, CSPR, bleeding strategy, growth and productivity behavior. *Journal of Chemical Technology & Biotechnology*. 2021;96(10):2930-2939. doi:https://doi.org/10.1002/jctb.6848

184. Wolf MKF, Müller A, Souquet J, Broly H, Morbidelli M. Process design and development of a mammalian cell perfusion culture in shake-tube and benchtop bioreactors. *Biotechnology and Bioengineering*. 2019;116(8):1973-1985. doi:https://doi.org/10.1002/bit.26999

185. Bielser J-M, Domaradzki J, Souquet J, Broly H, Morbidelli M. Semi-continuous scale-down models for clone and operating parameter screening in perfusion bioreactors. *Biotechnology Progress*. 2019;35(3):e2790. doi:https://doi.org/10.1002/btpr.2790

186. Mayrhofer P, Reinhart D, Castan A, Kunert R. Rapid development of clone-specific, high-performing perfusion media from established feed supplements. *Biotechnology Progress*. 2020;36(2):e2933. doi:https://doi.org/10.1002/btpr.2933

187. Janoschek S, Schulze M, Zijlstra G, Greller G, Matuszczyk J. A protocol to transfer a fed-batch platform process into semi-perfusion mode: The benefit of automated small-scale bioreactors compared to shake flasks as scale-down model. *Biotechnology Progress*. 2019;35(2):e2757. doi:https://doi.org/10.1002/btpr.2757

188. Lin H, Leighty RW, Godfrey S, Wang SB. Principles and approach to developing mammalian cell culture media for high cell density perfusion process leveraging established fed-batch media. *Biotechnology Progress*. 2017;33(4):891-901. doi:https://doi.org/10.1002/btpr.2472

189. Meier K, Klöckner W, Bonhage B, Antonov E, Regestein L, Büchs J. Correlation for the maximum oxygen transfer capacity in shake flasks for a wide range of operating conditions and for different culture media. *Biochemical Engineering Journal*. 2016/05/15/ 2016;109:228-235. doi:https://doi.org/10.1016/j.bej.2016.01.014

190. Schoenherr I, Stapp T, Ryll T. A Comparison of Different Methods To Determine the End of Exponential Growth in CHO Cell Cultures for Optimization of Scale-Up. *Biotechnology Progress*. 2000;16(5):815-821. doi:https://doi.org/10.1021/bp000074e

191. Wahrheit J, Nonnenmacher Y, Sperber S, Heinzle E. High-throughput respiration screening of single mitochondrial substrates using permeabilized CHO cells highlights control of mitochondria metabolism. *Engineering in Life Sciences*. 2015;15(2):184-194. doi:https://doi.org/10.1002/elsc.201400175

192. Deshpande RR, Heinzle E. On-line oxygen uptake rate and culture viability measurement of animal cell culture using microplates with integrated oxygen sensors. *Biotechnology Letters*. 2004/05/01 2004;26(9):763-767. doi:10.1023/B:BILE.0000024101.57683.6d

193. Kamen AA, Bédard C, Tom R, Perret S, Jardin B. On-line monitoring of respiration in recombinant-baculovirus infected and uninfected insect cell bioreactor cultures. *Biotechnology and Bioengineering*. 1996;50(1):36-48. doi:https://doi.org/10.1002/(SICI)1097-0290(19960405)50:1<36::AID-BIT5>3.0.CO;2-2

194. Gálvez J, Lecina M, Solà C, Cairó JJ, Gòdia F. Optimization of HEK-293S cell cultures for the production of adenoviral vectors in bioreactors using on-line OUR measurements. *Journal of Biotechnology*. 2012/01/01/ 2012;157(1):214-222. doi:https://doi.org/10.1016/j.jbiotec.2011.11.007

195. Ihling N, Munkler LP, Paul R, et al. Non-invasive and time-resolved measurement of the respiration activity of Chinese hamster ovary cells enables prediction of key culture parameters in shake flasks. *Biotechnology Journal*. 2022;17(8):2100677. doi:https://doi.org/10.1002/biot.202100677

196. Maier U, Büchs J. Characterisation of the gas–liquid mass transfer in shaking bioreactors. *Biochemical Engineering Journal*. 2001;7(2):99-106.

197. Maltais J-S, Lord-Dufour S, Morasse A, Stuible M, Loignon M, Durocher Y. Repressing expression of difficult-to-express recombinant proteins during the selection process increases productivity of CHO stable pools. *Biotechnology and Bioengineering*. 2023;120(10):2840-2852. doi:https://doi.org/10.1002/bit.28435

198. Poulain A, Mullick A, Massie B, Durocher Y. Reducing recombinant protein expression during CHO pool selection enhances frequency of high-producing cells. *Journal of biotechnology*. 2019;296:32-41.

199. Xu J, Tang P, Yongky A, et al. Systematic development of temperature shift strategies for Chinese hamster ovary cells based on short duration cultures and kinetic modeling. *MAbs*. Jan 2019;11(1):191-204. doi:10.1080/19420862.2018.1525262

200. Reyes S-J, Lemire L, Durocher Y, Voyer R, Henry O, Pham PL. Investigating the metabolic load of monoclonal antibody production conveyed to an inducible CHO cell line using a transfer-rate online monitoring system. *Journal of Biotechnology*. 2025/03/01/ 2025;399:47-62. doi:https://doi.org/10.1016/j.jbiotec.2025.01.008

201. Giese H, Azizan A, Kümmel A, et al. Liquid films on shake flask walls explain increasing maximum oxygen transfer capacities with elevating viscosity. *Biotechnology and Bioengineering*. 2014;111(2):295-308.

202. Büchs J, Maier U, Milbradt C, Zoels B. Power consumption in shaking flasks on rotary shaking machines: II. Nondimensional description of specific power consumption and flow regimes in unbaffled flasks at elevated liquid viscosity. *Biotechnology and Bioengineering*.

2000;68(6):594-601. doi:https://doi.org/10.1002/(SICI)1097-0290(20000620)68:6<594::AID-BIT2>3.0.CO;2-U

203. Schmitz J, Hertel O, Yermakov B, Noll T, Grünberger A. Growth and eGFP production of CHO-K1 suspension cells cultivated from single cell to laboratory scale. *Front Bioeng Biotechnol*. 2021;9:716343.

204. Shang M, Kwon T, Hamel J-FP, Lim CT, Khoo BL, Han J. Investigating the influence of physiologically relevant hydrostatic pressure on CHO cell batch culture. *Scientific Reports*. 2021/01/08 2021;11(1):162. doi:10.1038/s41598-020-80576-8

205. López-Meza J, Araíz-Hernández D, Carrillo-Cocom LM, López-Pacheco F, Rocha-Pizaña Mdel R, Alvarez MM. Using simple models to describe the kinetics of growth, glucose consumption, and monoclonal antibody formation in naive and infliximab producer CHO cells. *Cytotechnology*. Aug 2016;68(4):1287-300. doi:10.1007/s10616-015-9889-2

206. Torres M, Betts Z, Scholey R, et al. Long term culture promotes changes to growth, gene expression, and metabolism in CHO cells that are independent of production stability. *Biotechnology and Bioengineering*. 2023;120(9):2389-2402. doi:https://doi.org/10.1002/bit.28399

207. Richelle A, Corbett B, Agarwal P, Vernersson A, Trygg J, McCready C. Model-based intensification of CHO cell cultures: one-step strategy from fed-batch to perfusion. *Front Bioeng Biotechnol*. 2022;10:948905.

208. Lin H-H, Lee T-Y, Liu T-W, Tseng C-P. High glucose enhances cAMP level and extracellular signal-regulated kinase phosphorylation in Chinese hamster ovary cell: Usage of Br-cAMP in foreign protein β-galactosidase expression. *Journal of Bioscience and Bioengineering*. 2017/07/01/ 2017;124(1):108-114. doi:https://doi.org/10.1016/j.jbiosc.2017.02.010

209. Li C, Xia J-Y, Chu J, Wang Y-H, Zhuang Y-P, Zhang S-L. CFD analysis of the turbulent flow in baffled shake flasks. *Biochemical engineering journal*. 2013;70:140-150.

210. Rawat J, Gadgil M. Shear stress increases cytotoxicity and reduces transfection efficiency of liposomal gene delivery to CHO-S cells. *Cytotechnology*. Dec 2016;68(6):2529-2538. doi:10.1007/s10616-016-9974-1

211. Kirsch BJ, Bennun SV, Mendez A, et al. Metabolic analysis of the asparagine and glutamine dynamics in an industrial Chinese hamster ovary fed-batch process. *Biotechnology and Bioengineering*. 2022;119(3):807-819. doi:https://doi.org/10.1002/bit.27993

212. Agrawal A, Balcı H, Hanspers K, et al. WikiPathways 2024: next generation pathway database. *Nucleic Acids Research*. 2023;52(D1):D679-D689. doi:10.1093/nar/gkad960

213. Templeton N, Dean J, Reddy P, Young JD. Peak antibody production is associated with increased oxidative metabolism in an industrially relevant fed-batch CHO cell culture. *Biotechnology and Bioengineering*. 2013;110(7):2013-2024. doi:https://doi.org/10.1002/bit.24858

214. Duarte TM, Carinhas N, Barreiro LC, Carrondo MJT, Alves PM, Teixeira AP. Metabolic responses of CHO cells to limitation of key amino acids. *Biotechnology and Bioengineering*. 2014;111(10):2095-2106. doi:https://doi.org/10.1002/bit.25266

215. Goudar CT, Piret JM, Konstantinov KB. Estimating cell specific oxygen uptake and carbon dioxide production rates for mammalian cells in perfusion culture. *Biotechnology Progress*. 2011;27(5):1347-1357. doi:https://doi.org/10.1002/btpr.646

216. Anderlei T, Büchs J. Device for sterile online measurement of the oxygen transfer rate in shaking flasks. *Biochemical Engineering Journal*. 2001/03/01/ 2001;7(2):157-162. doi:https://doi.org/10.1016/S1369-703X(00)00116-9

217. Garcia-Ochoa F, Gomez E. Oxygen transfer rate determination: chemical, physical and biological methods. *Encyclopedia of Industrial Biotechnology*. 2010:1-21.

218. Running JA, Bansal K. Oxygen transfer rates in shaken culture vessels from Fernbach flasks to microtiter plates. *Biotechnology and Bioengineering*. 2016;113(8):1729-1735. doi:https://doi.org/10.1002/bit.25938

219. Peter CP, Suzuki Y, Büchs J. Hydromechanical stress in shake flasks: Correlation for the maximum local energy dissipation rate. *Biotechnology and Bioengineering*. 2006;93(6):1164-1176. doi:https://doi.org/10.1002/bit.20827

220. Nienow AW. Scale-up considerations based on studies at the bench scale in stirred bioreactors. *Journal of Chemical Engineering of Japan*. 2009;42(11):789-796. doi:10.1252/jcej.08we317

221. Padawer I, Ling WLW, Bai Y. Case Study: An accelerated 8-day monoclonal antibody production process based on high seeding densities. *Biotechnology Progress*. 2013;29(3):829-832. doi:https://doi.org/10.1002/btpr.1719

222. Brunner M, Fricke J, Kroll P, Herwig C. Investigation of the interactions of critical scale-up parameters (pH, pO(2) and pCO(2)) on CHO batch performance and critical quality attributes. *Bioprocess and biosystems engineering*. 2017;40(2):251-263. doi:10.1007/s00449-016-1693-7

223. Sieblist C, Jenzsch M, Pohlscheidt M. Influence of pluronic F68 on oxygen mass transfer. *Biotechnology Progress*. 2013;29(5):1278-1288. doi:https://doi.org/10.1002/btpr.1770

224. Zakrzewski R, Lee K, Lye GJ. Development of a miniature bioreactor model to study the impact of pH and DOT fluctuations on CHO cell culture performance as a tool to understanding heterogeneity effects at large-scale. *Biotechnology Progress*. 2022;38(4):e3264. doi:https://doi.org/10.1002/btpr.3264

225. Neuss A, Steimann T, Tomas Borges JS, Dinger R, Magnus JB. Scale-up of CHO cell cultures: from 96-well-microtiter plates to stirred tank reactors across three orders of magnitude. *Journal of Biological Engineering*. 2025;19(1):5.

APPENDIX A - EFFECT OF HYDRODYNAMIC CONDITIONS AND FEEDING REGIMENS ON THE PERFORMANCE OF A MONOCLONAL ANTIBODY FOR SCALE-UP OF CHO FED-BATCH CELL CULTURE PRODUCTION

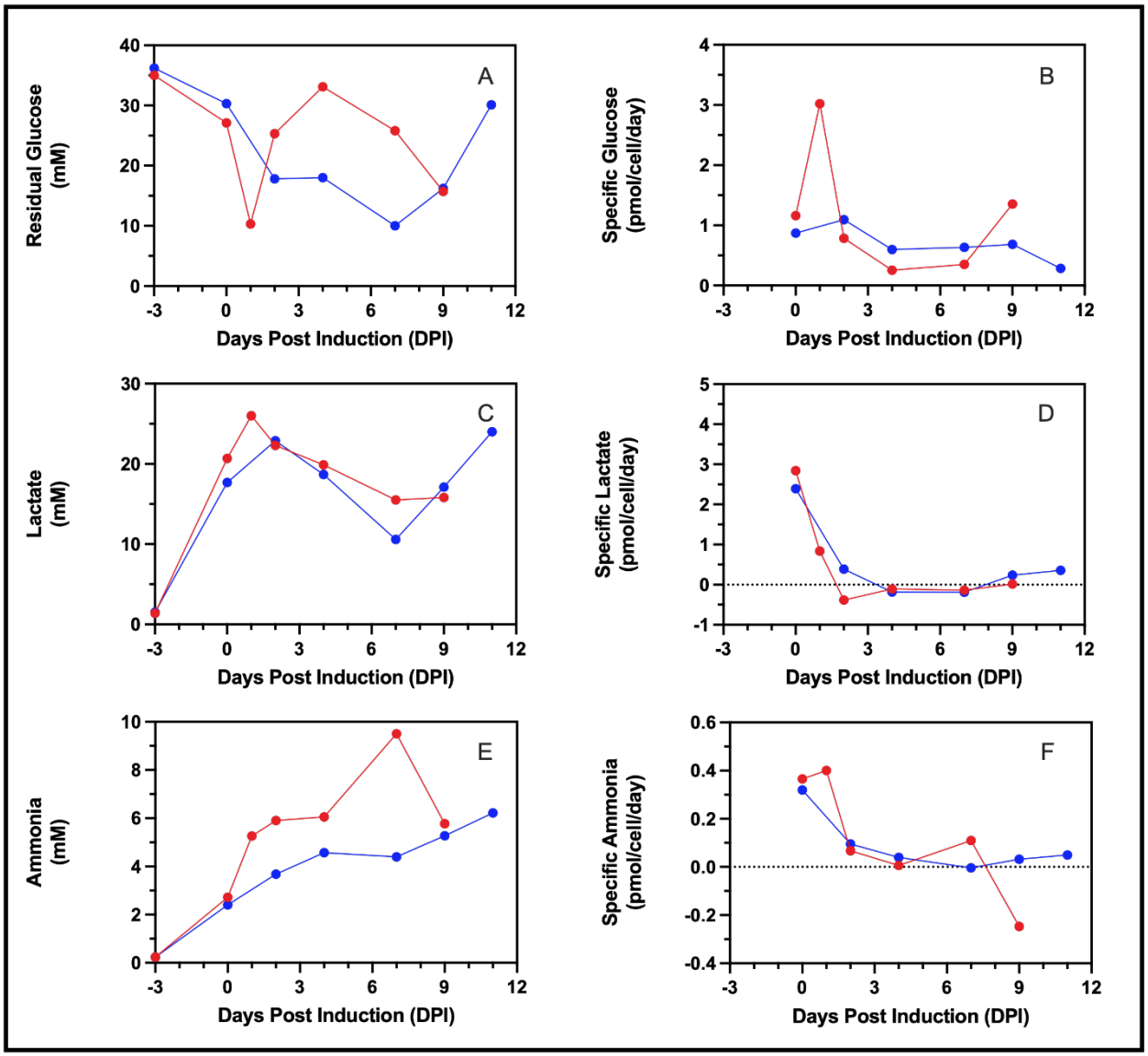

Supplemental Figure A.1: The effect of feeding strategy on the A) residual glucose, B) specific glucose consumption, C) measured lactate, D) specific lactate production E) ammonia concentration, and F) specific ammonia production of 1-L benchtop bioreactor cell cultures. Low feeding strategy (-●- LFS); High feeding strategy (-●- HFS).

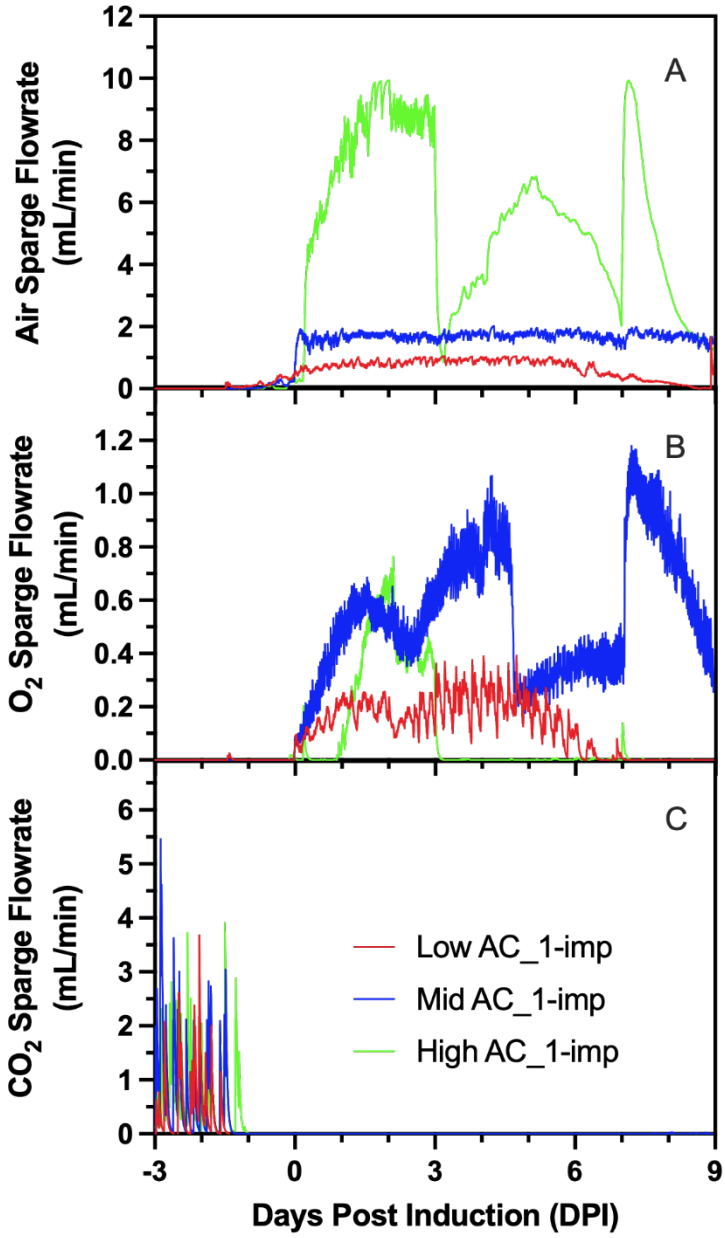

Supplemental Figure A.2: Online sparging data A) air, B) pure oxygen, and C) carbon dioxide for low air cap with 1-impeller (red), mid air cap with 1-impeller (blue), and high air cap with 1-impeller (green) operating parameters.

APPENDIX B - N-1 SEMI-CONTINUOUS TRANSIENT PERFUSION IN SHAKE FLASK FOR ULTRA-HIGH DENSITY SEEDING OF CHO CELL CULTURES IN BENCHTOP BIOREACTORS

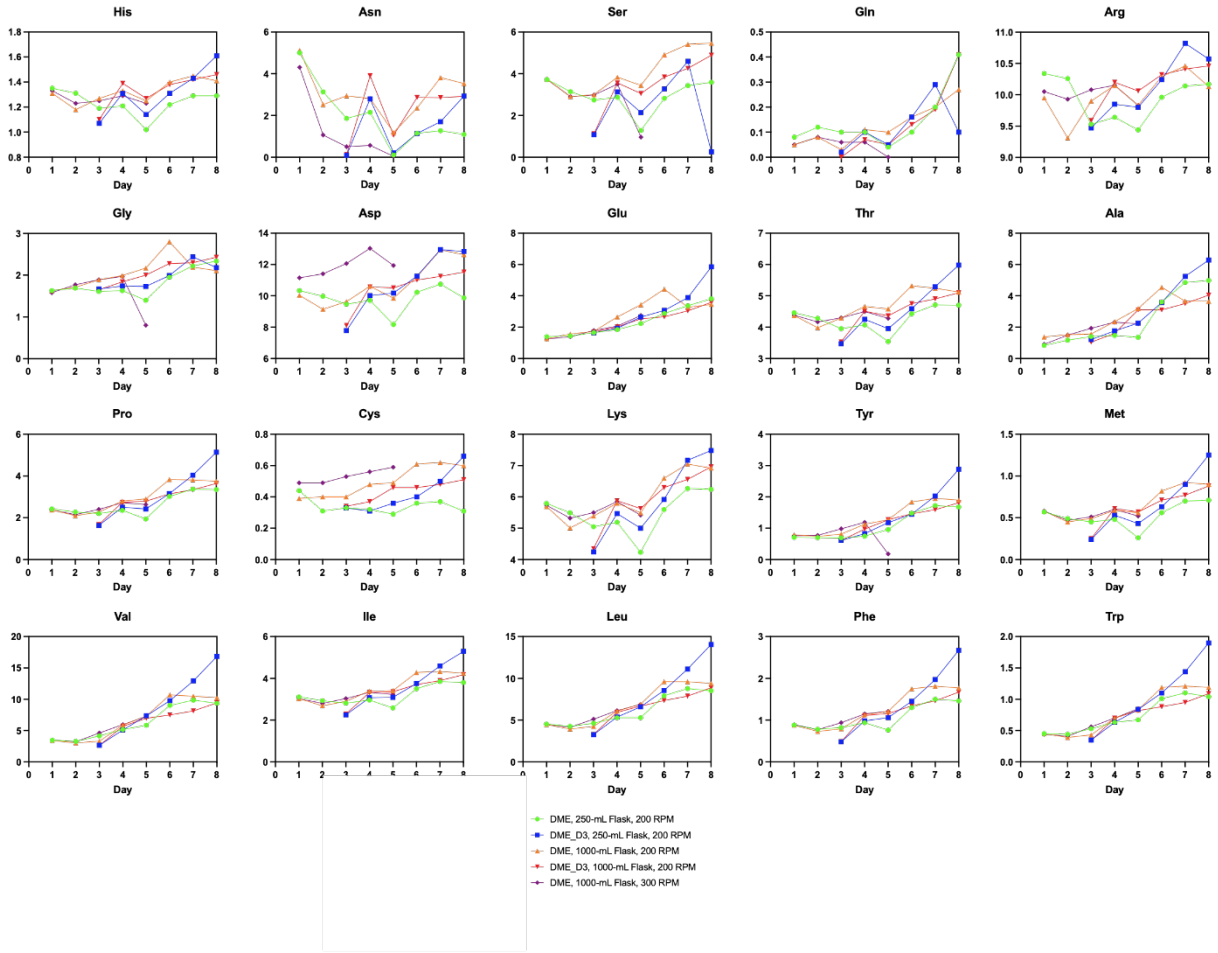

Supplemental Figure B.3: Amino acids measured throughout semi-continuous transient perfusion in shake flasks for daily media exchange (DME) and daily media exchange daily except for days 1 and 2 (DME_D3) media exchange frequency.

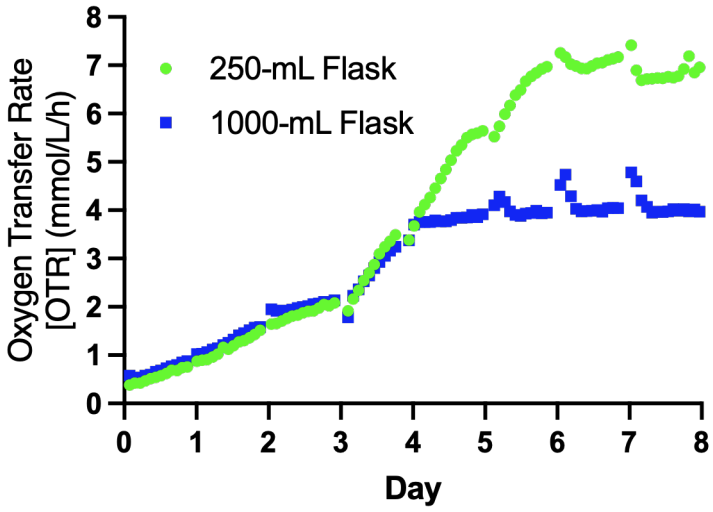

Supplemental Figure B.4: Oxygen transfer rate of semi-continuous transient perfusion cultures in 250-mL and 1000-mL shake flasks with daily media exchange except day 1 and 2 (DME_D3) agitated at 200 RPM.

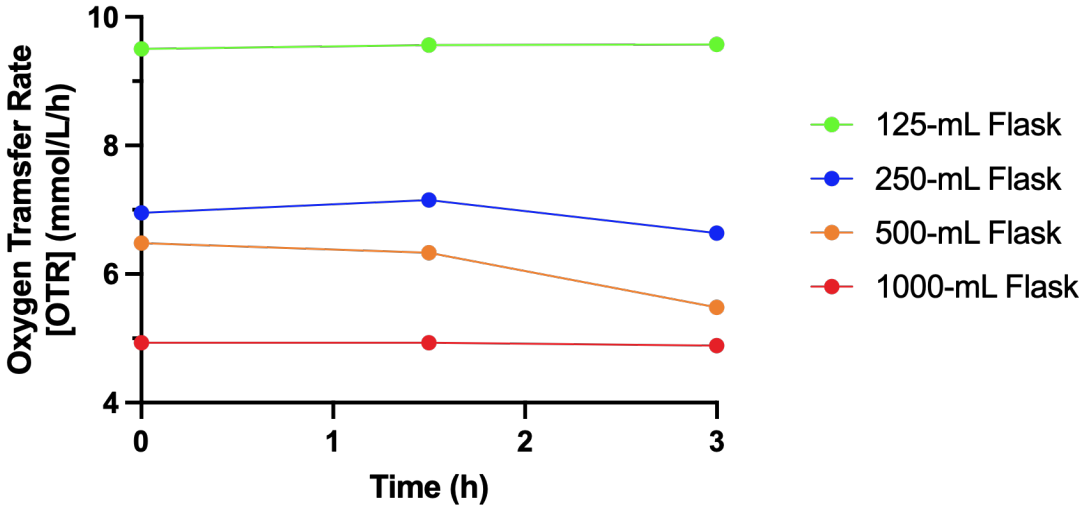

Supplemental Figure B.5: Maximum oxygen transfer rate measured using the sulfite system in 125-mL, 250-mL, 500-mL, and 1000-mL flasks at 20% fill volume agitated at 200 RPM.